ABSTRACT

BOX, GORDON HARLAND. The Structural Character of the Smith River Allochthon and the Lynchburg Group and Implications for the Nature of the Ridgeway Fault, near Pittsville in Southwest Virginia. (Under the direction of James P. Hibbard.)

The Smith River allochthon (SRA) is a regional thrust sheet of metaclastic rocks situated in the southern Appalachians of southwest Virginia. The Ridgeway fault is the boundary between the SRA and the Lynchburg Group, a drift-facies sedimentary cover sequence deposited on the eastern Laurentian (ancient North American) passive margin. The rocks of the SRA and Lynchburg Group differ in biotite and muscovite content, and structural, metamorphic, and intrusive histories. There are conflicting interpretations of the origin of the SRA. A reported Early Cambrian monazite age could represent a tectonothermal event responsible for the metamorphism and structural record that is unique to the SRA. This date, in conjunction with the contrasts between the SRA and Lynchburg Group, has been interpreted as evidence for an exotic origin for the SRA. The SRA may be peri-Gondwanan because an Early Cambrian tectonothermal event at the eastern coast of Laurentia conflicts with the documented drift environment and because similar ages are found in other peri-Gondwanan accreted terranes in the southern Appalachians. However, the SRA and the Lynchburg Group have similar detrital zircon signatures, which suggests that the SRA is peri-Laurentian.

This study strips away the record of each sequential orogenic event to have affected the SRA and the Lynchburg Group, and suggests that Ridgeway fault activity post-dates a main deformation that is shared between the SRA and the Lynchburg Group, and that the foliation resulting from the main deformation on each side of the fault has a common origin. This evidence leads to the conclusion that a tectonothermal event, revealed in the

orientation of planar inclusion trails in garnets and upper amphibolite metamorphic conditions, pre-dates the main deformation in the SRA. This is circumstantial evidence that the Early Cambrian monazite age, the early metamorphic assemblage, and an early foliation all precede the main deformation and therefore may represent the same Early Cambrian event. While detrital zircon data suggest that the SRA is related to peri-Laurentia rather than Gondwana, this study suggests that the SRA does not originate from the eastern passive margin of Laurentia.

THE STRUCTURAL CHARACTER OF THE SMITH RIVER ALLOCHTHON AND THE LYNCHBURG GROUP AND IMPLICATIONS FOR THE NATURE OF THE RIDGEWAY FAULT, NEAR PITTSVILLE IN SOUTHWEST VIRGINIA

by

GORDON HARLAND BOX

A thesis submitted to the Graduate Faculty of
North Carolina State University
in partial fulfillment of the
requirements for the Degree of
Master of Science

MARINE, EARTH AND ATMOSPHERIC SCIENCES

Raleigh

2006

APPROVED BY:

Chair of Advisory Committee

BIOGRAPHY

Born in Ottawa, raised in Brooklyn, I have since enjoyed spending roughly half my life in the southern states. I received a bachelor's degree in geology in 1982 from the University of Tennessee, Knoxville. I worked for several years as a geologist at firms specializing in geotechnical and environmental engineering and am now licensed as a professional geologist in the state of North Carolina. I have also acquired experience in business development and information technology. In 2003, I returned to academia to pursue a master's degree in geology at North Carolina State University. I completed my graduate course work and research requirements in the Spring of 2006. I currently live in Durham, NC.

ACKNOWLEDGEMENTS

First I need to thank my advisor, Jim Hibbard, for his insightful review of my research. I also thank him for his voluminous work over the years, as a result of which this research question arose. My committee members, Kevin Stewart and Skip Stoddard also provided much-appreciated, thought-provoking commentary.

I also benefited from Bill Henika and Bob Tracy, two geologists with extensive experience in the region, whose previous work and advice were invaluable. I am grateful for the support of the National Science Foundation grant number 533389.

I'd also like to acknowledge my fellow graduate students. My conversations with them were invaluable as I accumulated the information necessary to tackle the research question. Thanks to Brad Carter for briefings about his ongoing work and for discussions about the relevant background literature. Thanks to John Allen for sharing his solid sense of structural geology and his valuable feedback on an early draft of the text. Thanks to Jeff Pollock for always cutting to the key issues, and for his technical support. And thanks to Casey Kennedy for his unflagging interest and excellent questions.

This thesis would not have been possible without the support of Betsy Williams, who has provided her editing skills and geologic background and persevered with me through it all.

TABLE OF CONTENTS

LIST OF FIGURES

INTRODUCTION

ROCK UNITS

STRUCTURAL GEOLOGY

METAMORPHISM

APPENDICES

LIST OF ABBREVIATIONS

SRA	Smith River allochthon
Gp.	Group
Fm.	Formation
F.	fault
Mt.	Mountain
Amph	amphibolite
D_r	later deformation
S_r	later foliation
F_r	later folds
M_r	later metamorphism
D_l	late deformation
S_l	late foliation
F_l	late folds
L_i	intersection lineation
M_l	late metamorphism
D_m	main deformation
S_m	main foliation
F_m	main folds
M_m	main metamorphism
L_m	main lineation
D_e	early deformation
S_i	garnet inclusion trails
S_e	early foliation
F_e	early folds
L_i	intersection lineation
L_{i-1}	intersection lineation
M_e	early metamorphism
AB	albite
ALM	almandine
ALS	aluminum-silicate
AN	anorthite
AND	andalusite
BIO	biotite
CD	cordierite
MS	muscovite
OPX	orthopyroxene
PP	pyrope
PYP	pyrophyllite
QZ	quartz
RT	rutile
SA	sapphirine

SIL	sillimanite
ST	staurolite

INTRODUCTION

Purpose of study

The Smith River allochthon (SRA) is a regional thrust sheet composed mainly of metaclastic rocks. The SRA is situated in the Piedmont domain in the southern Appalachians of southwest Virginia (Figures 1 and 2). The SRA is emplaced onto the Lynchburg Group, a drift-facies sedimentary cover sequence deposited on the eastern Laurentian (ancient North American) margin (*e.g.*, Conley, 1985; Wang, 1991). The SRA was first recognized by Conley and Henika (1973) on the basis of lithologic and structural differences from surrounding rocks. They found that rocks on either side of the unexposed contact exhibited a contrasting history of deformation, metamorphism, and plutonic intrusion. Lithodemic units of the SRA are distinguished from the metaclastic rocks of the Lynchburg Group. The SRA rocks are reported to contain evidence of a structural event that predates any structural evidence found in the Lynchburg Group. This structural evidence in the SRA predates the emplacement of the SRA onto the Lynchburg Group (Conley and Henika, 1973). These observations have lead to uncertainty concerning the origin of the SRA, particularly whether the SRA is Laurentian or exotic with respect to Laurentia. A recent geochronological study has revived interest in the affinity of the SRA. Hibbard *et al.* (2003) hypothesized that a *c.* 530 Ma U-Th monazite age reflects the timing of a tectonothermal event in the SRA; they noted that at that time the eastern Laurentian margin was in the drift stage, a time of relative tectonic quiescence. Early Cambrian ages in peri-Gondwanan terranes of the Appalachians (*e.g.*, Hibbard and Samson, 1995; White and

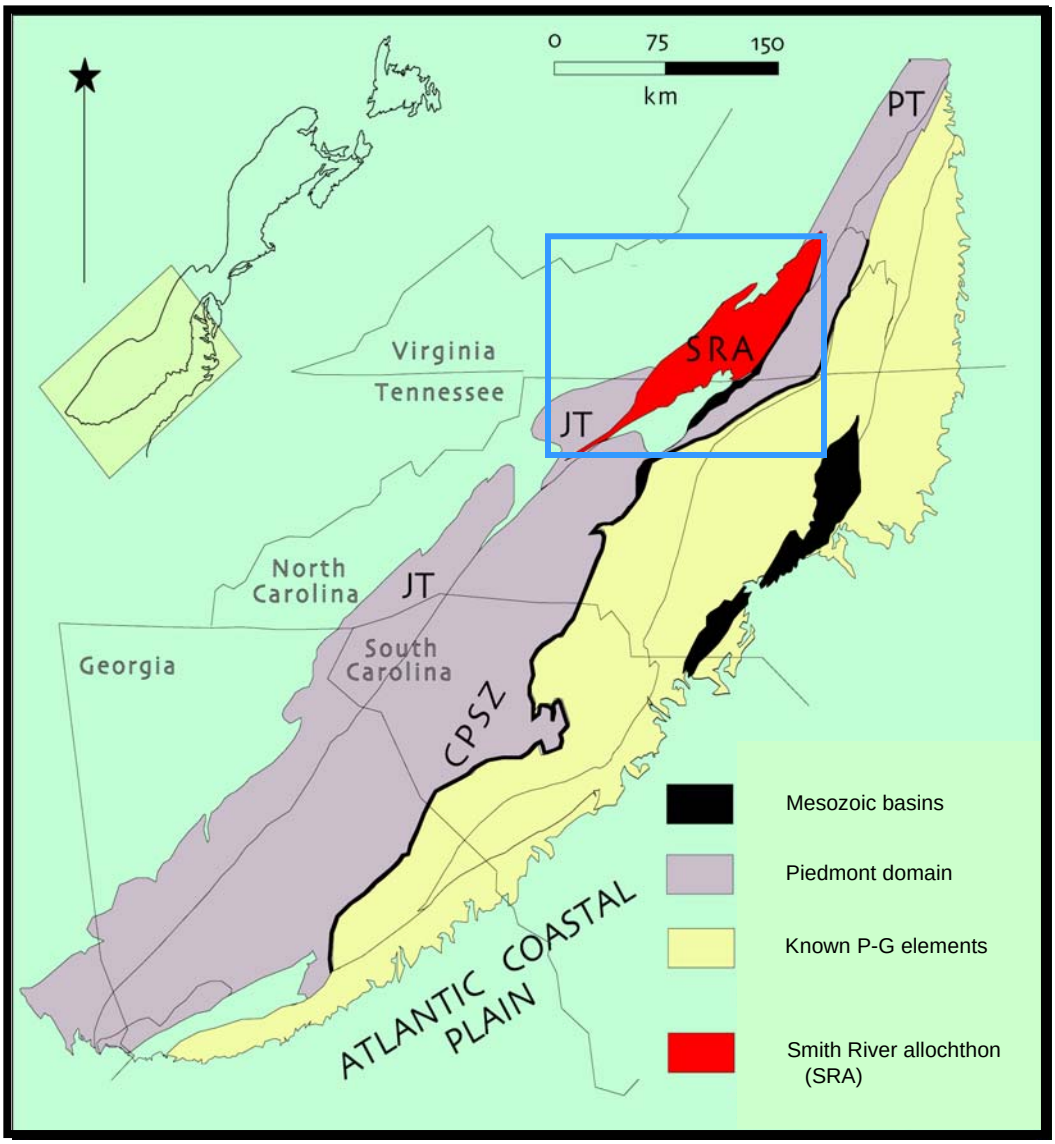

Figure 1: Location map of the Piedmont domain in the central and southern Appalachian orogen. The field within the box outlines the area of Figure 2. Components of the western portion of the Piedmont domain include the Jefferson terrane (JT) and the Potomac terrane (PT). Known peri-Gondwanan (P-G) elements are separated from the Piedmont domain by the central Piedmont shear zone (CPSZ). (after Hibbard *et al*., 2003)

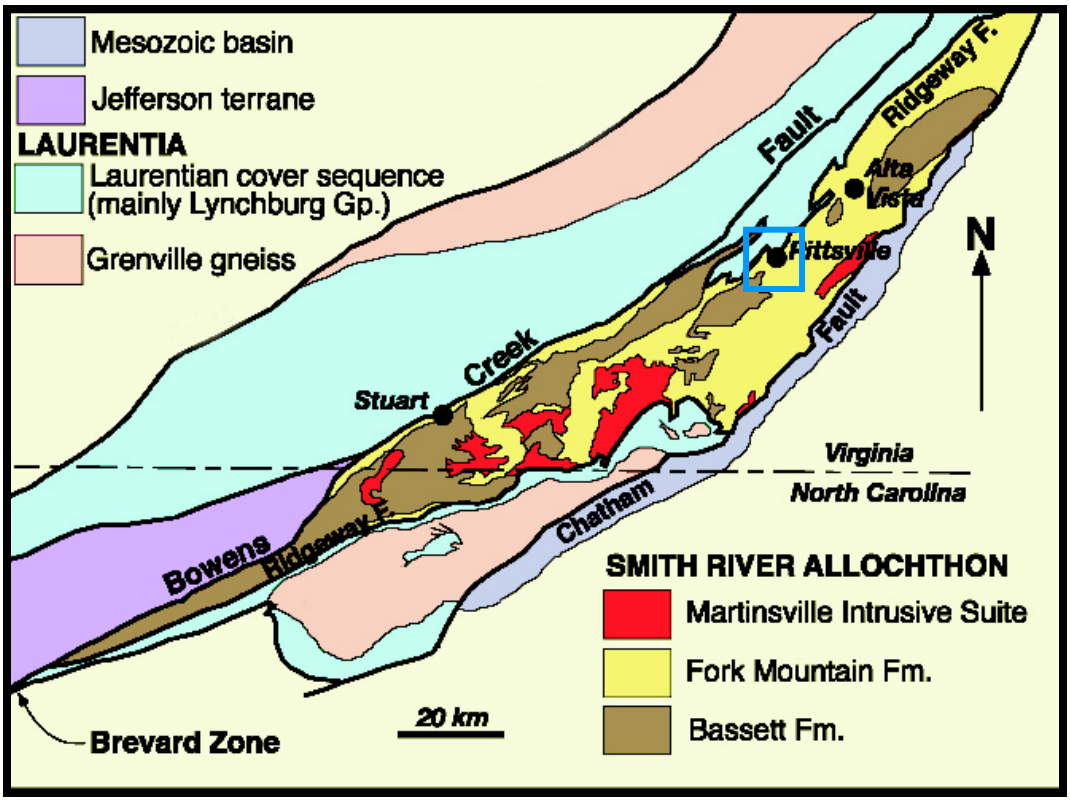

Figure 2: Study area location map. The field within the blue box outlines the study area shown in Figures 3 and 4. The Smith River allochthon (SRA) is bounded by the Ridgeway fault (F.) except where it is truncated by younger faults. The Martinsville intrusive suite (MIS) is truncated by the Ridgeway fault. The SRA is faulted against the Jefferson terrane. The map also shows Grenville basement, the Laurentian drift-facies cover sequence consisting mainly of the Lynchburg Group, and the Mesozoic Dan River basin. Refer to the discussion of regional geology in the Introduction. (after Conley, 1985, Hibbard *et al*., 2003)

Barr, 1996; Dennis and Wright, 1997) led to the hypothesis that the SRA is peri-Gondwanan in origin (Hibbard *et al.,* 2003).

Yet, similarities in detrital zircon signatures in the SRA and the underlying Lynchburg Group suggest that the SRA is peri-Laurentian (Carter *et al.*, 2006). This study examines the SRA and seeks to document the nature of the early deformation that is restricted to the SRA and that may be associated with the Early Cambrian monazite age (Hibbard *et al.*, 2003). It is hoped that clarification of the nature of this early event will elucidate the origin of the SRA.

This study forms a portion of a larger collaborative project undertaken by geochronologists at Virginia Polytechnic Institute and State University, Blacksburg, VA, and geologists at North Carolina State University, Raleigh, NC. The goal of this investigation is to place the deformational events of the SRA into the context of known tectonic events within the southern Appalachians. The ultimate goal of the larger collaborative project is to determine the crustal affinity of the SRA. The nature and timing of deformational events is key to understanding the geologic history of the SRA.

Regional geology

The Piedmont domain (Hibbard *et al.*, 2006) is the middle of three NNE-trending major divisions of the southern Appalachian orogen (Hibbard and Samson, 1995). The domain lies between native Laurentian drift-facies rocks to the west and accreted peri-Gondwanan terranes to the east. The Piedmont domain is separated from the Laurentian drift-facies

cover sequence by a system of faults ranging from the Ordovician Hayesville fault (*e.g.*, Hatcher, 1978) to the Devonian Burnsville fault (*e.g.*, Stewart *et al.*, 1997; Trupe *et al.*, 2003). To the east, the Piedmont domain is bounded by the central Piedmont shear zone (CPSZ), an Alleghanian thrust system. The CPSZ emplaced the peri-Gondwanan elements of Carolinia onto the Piedmont domain (Hibbard *et al.*, 1998; Wortman *et al.*, 1998). In contrast to the terranes of Laurentian and peri-Gondwanan affinity on either side, the origin and affinity of the Piedmont domain terranes is unclear.

The Piedmont domain is divided into eastern and western sections by the Brevard fault zone and equivalent structures to the north. The western Piedmont includes metaclastic rocks with rare metabasalt that may represent eclogite facies metaophiolite (Stewart *et al.*, 1997) and commonly has been interpreted as an accretionary complex (*e.g.*, Stewart *et al.*, 1997; Miller *et al.*, 2006). The eastern section of the Piedmont domain consists of a greater proportion of metaigneous rock than the western section and has been interpreted, in Virginia, as a magmatic arc constructed on some form of continental crust (*e.g.*, Pavlides *et al.*, 1994; Coler *et al.*, 2000a; Coler *et al.*, 2000b).

The SRA is a portion of the western Piedmont domain that extends roughly 250 km from Lynchburg, VA, southwest to ~50 km south of the Virginia-North Carolina border. The SRA has a width of ~50 km (Figure 1). The SRA is faulted against the Potomac terrane (PT) to the northeast and the Jefferson terrane (JT) to the southwest (Figure 1). The structural relation of the PT to the SRA is unknown. The JT structurally underlies the SRA

(Lewis, 1980). To the west, the SRA is faulted against the Lynchburg Group along the unexposed Ridgeway fault (Conley and Henika, 1973).

The SRA is a metaclastic, metaigneous terrane that records a moderate metamorphic grade (greenschist facies) but that also records relict high-grade metamorphism (upper amphibolite facies) (Conley and Henika, 1973; Conley, 1985). The SRA is defined by rock types and structural, metamorphic, and plutonic histories that differ from the Lynchburg Group (Conley and Henika, 1973). The SRA is bounded below by the Ridgeway fault except where that fault is cut by the younger, SE-dipping, dextral-reverse Bowens Creek fault and the brittle, Mesozoic, Chatham fault (Conley and Henika, 1973; Gates, 1987, 1989) (Figure 2). The Lynchburg Group is nonconformable above Grenville basement as observed just to the west of the SRA (Conley, 1985). To the east of the SRA, the Mesozoic Chatham fault juxtaposes the SRA against clastic deposits of the Triassic Dan River Basin.

Previous work

The SRA is allochthonous based on structural relations, rock types, and metamorphic and plutonic histories that are distinct from the Lynchburg Group (Conley and Henika, 1973; Conley *et al.*, 1989). The SRA is interpreted to be a relatively thin (~1-2 km thick) sliver of metamorphic rock that is tectonically emplaced over the Lynchburg Group along the Ridgeway fault (Conley, 1985; Greenberg, 1975). Conley and Henika (1973) and Conley *et al.* (1989) recognized that the SRA consists of the Fork Mountain and Bassett formations. These units are better classified as suites because they are lithodemic units (North

American Commission on Stratigraphic Nomenclature, 2005); however, it is beyond the scope of this study to formally propose such a change. Therefore, their formational status is maintained here following previous work. Other workers do not recognize the SRA as allochthonous, have correlated rocks across the Ridgeway fault, and thus attribute Laurentian affinity to the SRA (Gates, 1997; Glover *et al.*, 1997).

Although accounts of the tectonic histories of the SRA and Lynchburg Group differ, most workers agree on many specific elements of the tectono-metamorphic history of these rocks. A relict upper amphibolite facies metamorphism represents the first tectonothermal event in the SRA (Conley and Henika, 1973; Gates and Speer, 1991) and a set of isoclinal recumbent folds have a penetrative foliation parallel to their axial surfaces that is presumed to have formed during peak metamorphism (Conley, 1985; Gates, 1986, 1987; Gates and Speer, 1991). The two youngest fold generations are upright to moderately inclined folds that deform the penetrative foliation (*e.g.*, Conley, 1985; Gates, 1986, 1987). These two youngest fold generations produce basins and domes in the penetrative foliation likely due to fold interference (*e.g.*, Conley and Henika, 1973), which is interpreted as resulting from transpression with a later component of compression (Gates, 1986, 1987). These youngest folds are interpreted to be Alleghanian (Marr, 1984; Conley, 1985, 1989; Gates, 1986, 1987; Henika, 1997, 2002). Some workers report that while the Lynchburg Group exhibits the youngest Alleghanian structures, it does not exhibit the isoclinal recumbent folds associated with peak metamorphism in the SRA (*e.g.*, Conley, 1989; Gates, 1986, 1987). However, Conley and Henika (1973) and Conley (1985) refer to isoclinal folds in the

Lynchburg Group; Wang (1991) refers to ‘flow folds’ in the Lynchburg Group and has also reported foliation subparallel to primary bedding (S_0), which might indicate isoclinal folding.

The peak upper amphibolite facies metamorphism in the SRA is strongly suggested to predate emplacement of the SRA because it is not shared with the adjacent Lynchburg Group, which has attained a maximum of greenschist facies metamorphism in the study area (Conley and Henika, 1973). Peak metamorphism also precedes emplacement of the Martinsville intrusive suite (MIS) and its localized contact metamorphic hornfels, which is confined to the SRA and sheared and truncated by the Ridgeway fault (Henika, 1971; Conley and Henika, 1973; Conley, 1985). Many workers (*e.g.*, Horton *et al.*, 1989; Wang, 1991; Gates, 1997) consider peak metamorphism in the SRA to be Ordovician, based on an age from Rb-Sr biotite-whole-rock analysis of pelite (Odom and Russell, 1975). ^{238}U-^{206}Pb analysis of a staurolite rim from a pelitic schist also results in an Ordovician age (*c.* 489 Ma) (Lanzirotti and Hanson, 1997). A similar U-Th monazite age (*c*. 486 Ma) was also obtained by Hibbard *et al.*, 2003.

Peak metamorphism in the Lynchburg Group attained greenschist facies, in the study area, while southwest of the study area it attained middle amphibolite facies in rocks that are structurally lower than those exposed in the study area (*e.g.*, Conley and Henika, 1973; Conley, 1985; Wang, 1991). The age of Lynchburg Group rocks is constrained by *c.* 1.0 Ga basement and the *c.* 564 Ma overlying Catoctin Formation (Aleinikoff *et al.*, 1995). Monazite is not observed in the Lynchburg Group (Tracy, pers. com. 2005), so monazite

ages have not been obtained from those rocks for comparison to those obtained from the SRA.

The Martinsville intrusive suite (MIS) forms concordant to discordant masses that intrude the metaclastic and amphibolite rocks of the SRA. The MIS intruded the SRA following peak metamorphism (Conley and Henika, 1973; Conley, 1985). The MIS is truncated by the Ridgeway fault and absent in the Lynchburg Group (Conley, 1985; Conley and Henika, 1995; Henika *et al.*, 1996). The MIS is composed of the cogenetic Rich Acres norite and Leatherwood granite (Conley and Henika, 1973; Conley, 1985). Deformation of the MIS has been reported in proximity to the Ridgeway fault (Rankin, 1975). The ages of the MIS are *c.* 430 Ma for the Rich Acres norite and *c.* 445 Ma for the Leatherwood granite, based on SHRIMP U-Pb ages of zircon (Wilson, 2001). This age corresponds reasonably closely to a U-Pb monazite age determination of *c.* 433 Ma for the contact aureole of the MIS gabbro (Tracy *et al.*, 2001). Thus, SRA rocks are presumed to be Late Ordovician or older, because they are intruded by the MIS. The SRA was, therefore, emplaced along the Ridgeway fault after the Late Ordovician and before the Carboniferous (Conley, 1978). The Carboniferous upper limit of emplacement is based on the young, upright structures that are shared by both the SRA and the Lynchburg Group and are interpreted to be Alleghanian (*e.g.*, Conley, 1985; Gates, 1986, 1987). The lower limit is based on the Ordovician intrusion of the MIS, which is confined to the SRA.

Recent U-Th monazite microprobe ages from the schists of the Fork Mountain Formation are *c.* 530 Ma and *c.* 486 Ma (Hibbard *et al.*, 2003). The Ordovician monazite age (*c.* 486

Ma) is broadly consistent with Taconic events. However, the Early Cambrian monazite age (*c.* 530 Ma) appears to preclude contemporaneous tectonothermal events (presumed to be responsible for the monazite age (Kohn and Malloy, 2004)) from having occurred at the eastern Laurentian passive margin that had been established by this time (Hibbard and Samson, 1995; Hibbard *et al.*, 2005). Hibbard *et al.* (2003) hypothesized that the SRA may be exotic with respect to Laurentia. However, similarities between the detrital zircon signatures in the SRA and in the underlying Lynchburg Group (Carter *et al.*, 2006), and metamafic geochemistry in each unit (Carter, 2006) suggest that the SRA is peri-Laurentian.

Study area location

The study area is located in the southwest Virginia Piedmont, and contains the small community of Pittsville to the east of Leesville Lake (Figure 2). Frequent areal repetition of SRA and Lynchburg Group rocks occur here in a relatively small area as a result of folding and subsequent erosion and provide ample opportunity for multiple transects of the shallow, low-angle Ridgeway fault that separates them (Greenberg, 1975; Marr, 1984; Conley, 1985; Henika, 1997, 2002). The resulting multiple exposures of the Ridgeway fault permit comparison of the structural and metamorphic character of SRA and Lynchburg Group rocks, and permit contrast of the character of these rocks with respect to distance from the Ridgeway fault.

In the study area, the SRA consists dominantly of medium- to coarse-grained, aluminous, schist of the Fork Mountain Formation, which typically weathers to clayey soil (Marr, 1984). The Lynchburg Group is finer-grained and more siliceous than the Fork Mountain Formation and typically weathers readily to sandy loam, which is found in many valleys in the study area (Marr, 1984). The Lynchburg Group is more granular and porous and less aluminous than the SRA. The SRA typically forms higher topographic areas than the Lynchburg Group due to its higher structural position and relatively impermeable, weather-resistant character.

The study area is ~97 km^2 and is contained within the boundaries of the Leesville and Pittsville quadrangles (Figures 3 and 4). The northern edge of the study area, in the Leesville quadrangle, is ~3.5 km south of Leesville Dam. The southern edge is ~1 km north of Virginia Route 40 (~36^o 57’ 30”). The study area is bounded by the eastern edge of the Leesville and Pittsville quadrangles (~79^o 22' 30"), which passes through the intersection of Interstate 29 and Virginia Route 40. The western edge is bounded dominantly by Leesville Lake and the Pigg River. The highest reported point in the area is 1086 ft at Farmers Mountain; the lowest reported area is Leesville Lake, with a normal pool elevation of 604 ft (US Department of the Interior, 1966, 1982).

Methods

Structural mapping of the SRA and the Lynchburg Group was conducted at two different scales in the study area. 1:24,000-scale structural mapping was performed across the study

Figure 3: Geologic study area map including cross section locations N-N', C-C', and S-S'. The study area is delineated into three transects that each cross the Ridgeway fault (northern, central, and southern) and a central domain that exhibits consistent structural character. The central domain is oriented perpendicular to the NNE-SSW-trend of the hinge of a macroscale, upright fold train and appears to be constrained to this fold train (refer to the discussion in Structural Geology). The central domain is further subdivided into subdomains that consist of outcrop(s) at each location (designated by Loc##) or groups of locations that lie within the same part of a limb or hinge of the macroscale fold train. The central subdomains consist of (from west to east): Loc11, 12, and 17; Loc09 and 10; Loc18; Loc08; and Loc05. An additional subdomain located at "The Wall" outcrop is delineated and enlarged in the inset and consists of Loc02, 06, 07, and 13. Refer to Figure 4 for a guide to geologic symbols. The map consists of portions of the Leesville and Pittsville 7.5' quadrangles north and south of latitude 37 degrees respectively.

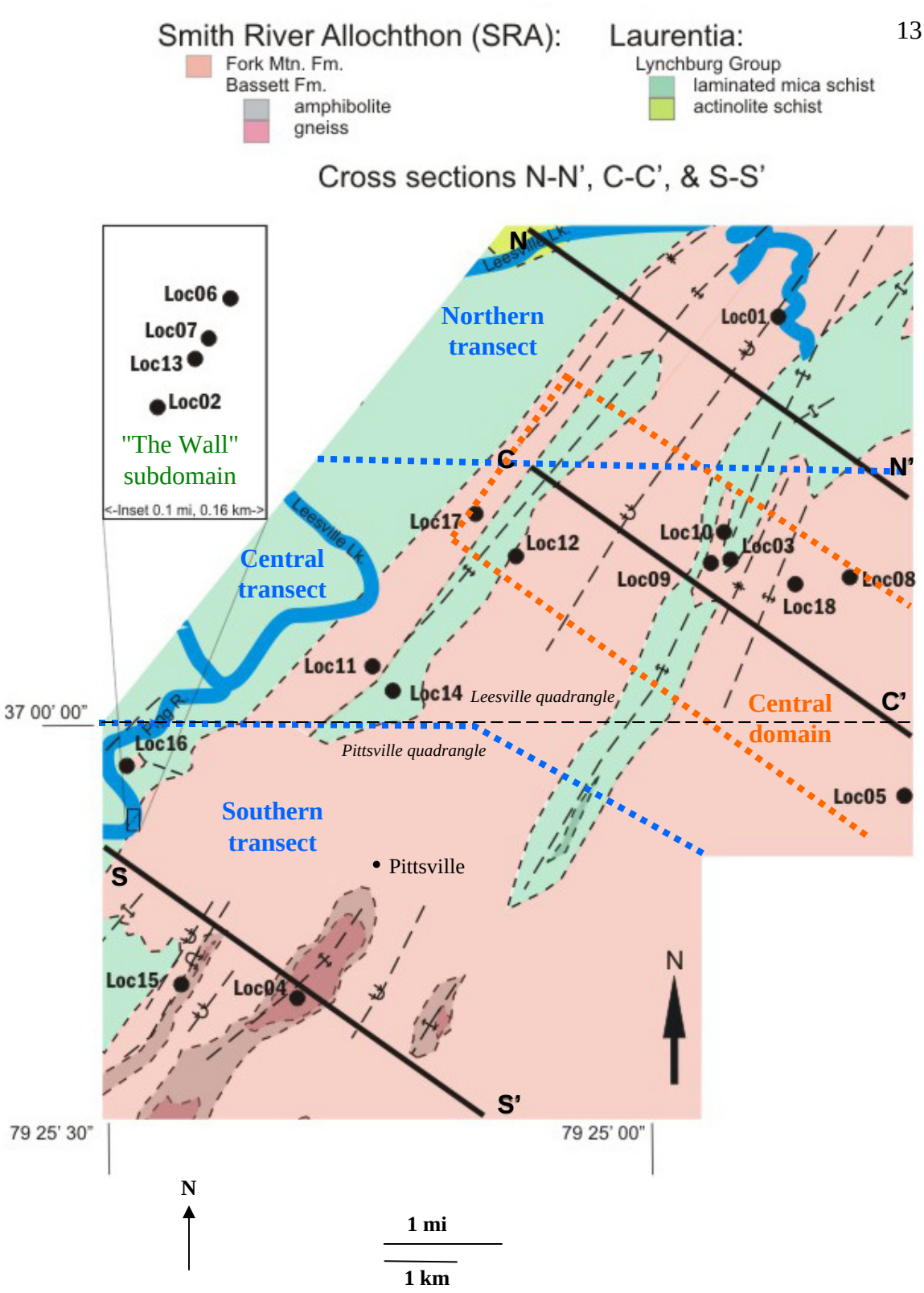
Smith River Allochthon (SRA):
Fork Mtn. Fm.
Bassett Fm.
amphibolite
gneiss
Laurentia:
Lynchburg Group
laminated mica schist
actinolite schist
Cross sections N-N', C-C', & S-S'
Loc06
Loc07
Loc13
Loc02
"The Wall" subdomain
<-Inset 0.1 mi, 0.16 km->
Leesville Lk.
Northern transect
Central transect
Southern transect
N
N'
C
C'
S
S'
Loc01
Loc17
Loc12
Loc10
Loc03
Loc09
Loc08
Loc18
Loc11
Loc14
Leesville quadrangle
Pittsville quadrangle
Central domain
Loc16
Loc05
Pittsville
Loc15
Loc04
37 00' 00"
79 25' 30"
79 25' 00"
N
1 mi
1 km

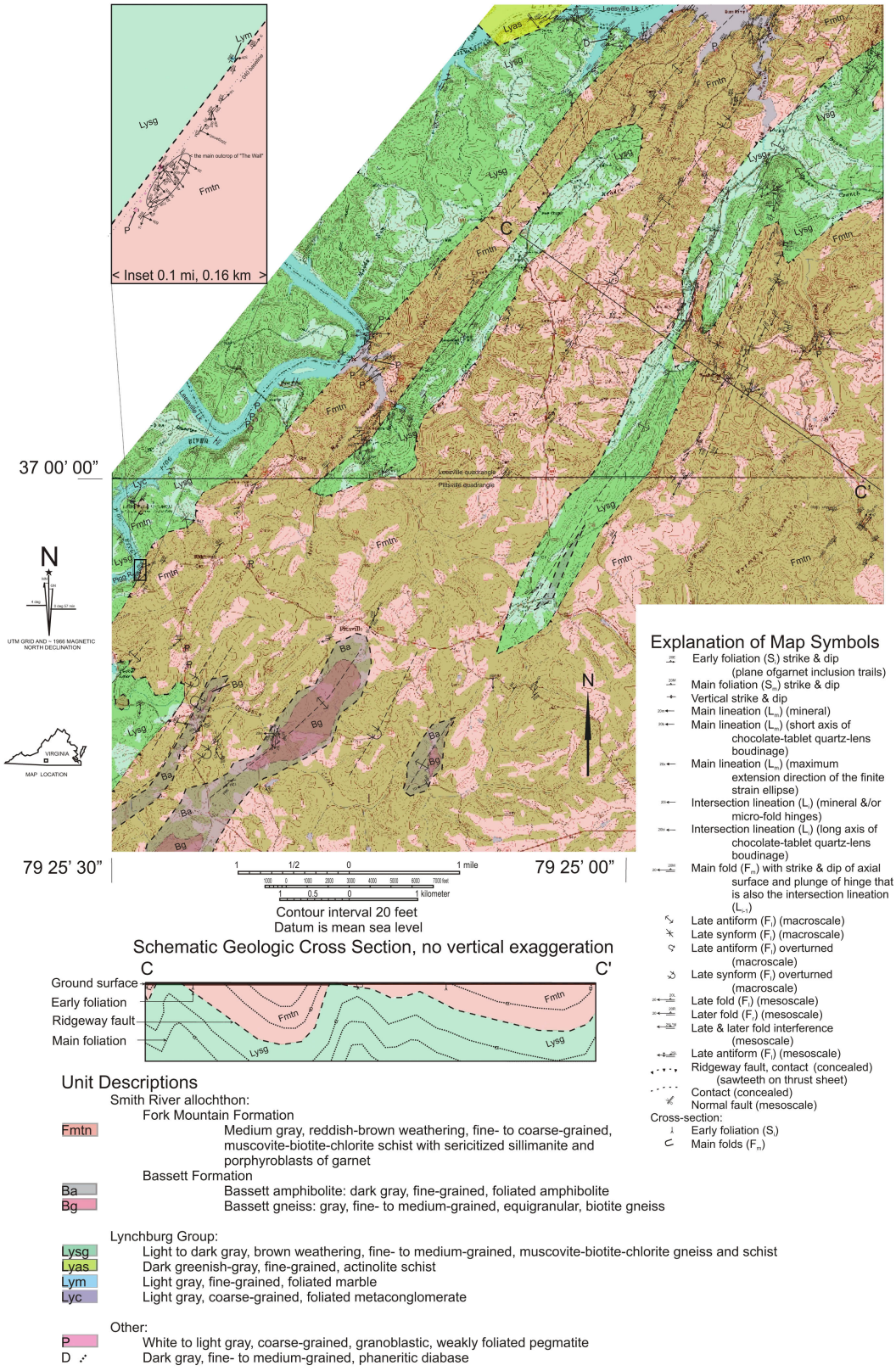

Figure 4: Geologic map of the area of Pittsville, Virginia, portions of Leesville and Pittsville USGS 7.5' quadrangles, geology by Gordon Box 2004-2006. Refer to Appendix 1 for 1:24,000 version of geologic map.

area. In addition, more detailed mapping was performed at one large outcrop in close proximity to the Ridgeway fault facilitated by a baseline (azimuth ~040) subparallel to strike of the penetrative foliation, in order to determine the relative structural levels within that outcrop. 1:24,000-scale mapping was assisted by visiting outcrops previously recorded and mapped by Marr (1984) and Henika (1997, pers. com. 2005).

The study area is weathered and covered by soil and vegetation. Limited outcrop is available in stream beds and drainage ditches. Generous outcrop along Leesville Lake results from steep, water-inundated banks. Lithologic, structural, and mineralogic data and ~175 oriented samples were collected from ~500 outcrops. From these samples, ~80 oriented thin-sections were prepared for petrographic analysis. Two thin-sections were generally prepared at orthogonal orientations from selected samples, producing thin-sections perpendicular to the penetrative foliation and parallel to the penetrative lineation as well as perpendicular to the foliation and perpendicular to the lineation.

Orientation data are reported according to the right-hand rule and are plotted onto lower hemispheric projection, equal area stereonets. Poles to planes are plotted on stereonets rather than planar surfaces. Data were plotted, and best-fit great circles and Kamb contours were calculated, using software made available by Allmendinger (2003).

ROCK UNITS

Introduction

To evaluate the significance of the Ridgeway fault and to contrast the history of the Smith River allochthon (SRA) with that of the Lynchburg Group, it is vital to recognize the rock units involved. Both the SRA and the Lynchburg Group are predominantly metaclastic sedimentary rocks, but the Lynchburg Group preserves primary structures, whereas primary structures have been obliterated in the SRA. The Lynchburg Group represents a sedimentary drift-facies cover sequence (*e.g.*, Conley, 1985; Henika *et al.*, 1996; Henika, 1997). The SRA consists of two lithodemic units, the Fork Mountain and Bassett formations. The Fork Mountain Formation lies structurally above the Bassett Formation, but the stratigraphic sequence is unknown. The broad distribution of the SRA and Lynchburg Group rocks is controlled by the geometry of the Ridgeway fault because the SRA lies structurally above, and the Lynchburg Group lies structurally below the fault. Regional definition, description specific to the study area, and known age constraints of rock units follow. Mineralogical constituents are petrographically estimated.

Lynchburg Group

Lynchburg Group rocks were first described and named as the Lynchburg Formation by Jonas (1927). They were later raised to the group status by Furcron (1969). The Lynchburg Group predominantly comprises fine-grained, interlayered, biotite paragneiss, micaceous schist, and quartzite, metasiltstone, graphitic schist, with minor metaconglomerate, and

marble (Marr, 1984; Conley, 1985; Berquist, 1988). Local graded bedding lies subparallel to schistosity (*e.g.*, Conley, 1985; Wang, 1991). The protoliths of the Lynchburg Group are interpreted to represent the fine-grained, drift-facies cover sequence of the Laurentian margin (*e.g.*, Conley, 1981; Marr, 1984; Conley, 1985; Berquist, 1988; Wang, 1991). Metabasalts analyzed in the Lynchburg Group away from the study area are similar in composition to ocean floor basalt (Conley, 1985).

The Lynchburg Group is exposed over ~30 km^2 of the study area (Figures 3 and 4). It is exposed in the NW part of the study area and two NNE-trending irregular oval areas in the central part of the study area. Eroded antiforms control the exposure of the Lynchburg Group, which otherwise lies below the SRA. Outcrop of the Lynchburg Group is limited because it is readily weathered to loam. The Lynchburg Group appears to be in tectonic contact with the SRA. The Ridgeway fault, the mutual contact of the SRA and the Lynchburg Group, is unexposed in the study area. The Ridgeway fault is further discussed below (refer to the discussion of the Ridgeway fault in Structural Geology).

In the study area, the Lynchburg Group predominantly includes quartz-rich, micaceous schist, and also includes rare metaconglomerate and foliated marble in the western part of the southern transect, and dark greenish-gray, fine-grained, actinolite schist in the western part of the northern transect. In hand-sample, micaceous schist is hard and resistant to parting (Figure 5). Micaceous schist consists dominantly of light to dark gray, brown-weathering, fine- to medium-grained (<0.1 to ~1.4 mm), muscovite-biotite-chlorite schist (Figure 5). These rocks contain ~70-90% quartz, ~10-30% mica and chlorite, and rare

Figure 5: Typical quartz-rich, micaceous and chlorite-rich schist of the Lynchburg Group at Loc03. This quartz-rich schist shows bedding subparallel to schistosity (top photograph) and a high proportion of foliated quartz and is light to dark gray, brown-weathering, fine- to medium-grained, muscovite-biotite-chlorite schist with a seriate, interlobate metamorphic texture consisting dominantly of elongated, aligned quartz grains and micaceous and chlorite-rich layers consisting of foliated, interlocking or isolated, equigranular, subhedral grains (bottom photomicrograph; field of view 1.2 mm). Refer to the discussion in Rock Units. (Sample is not oriented.)

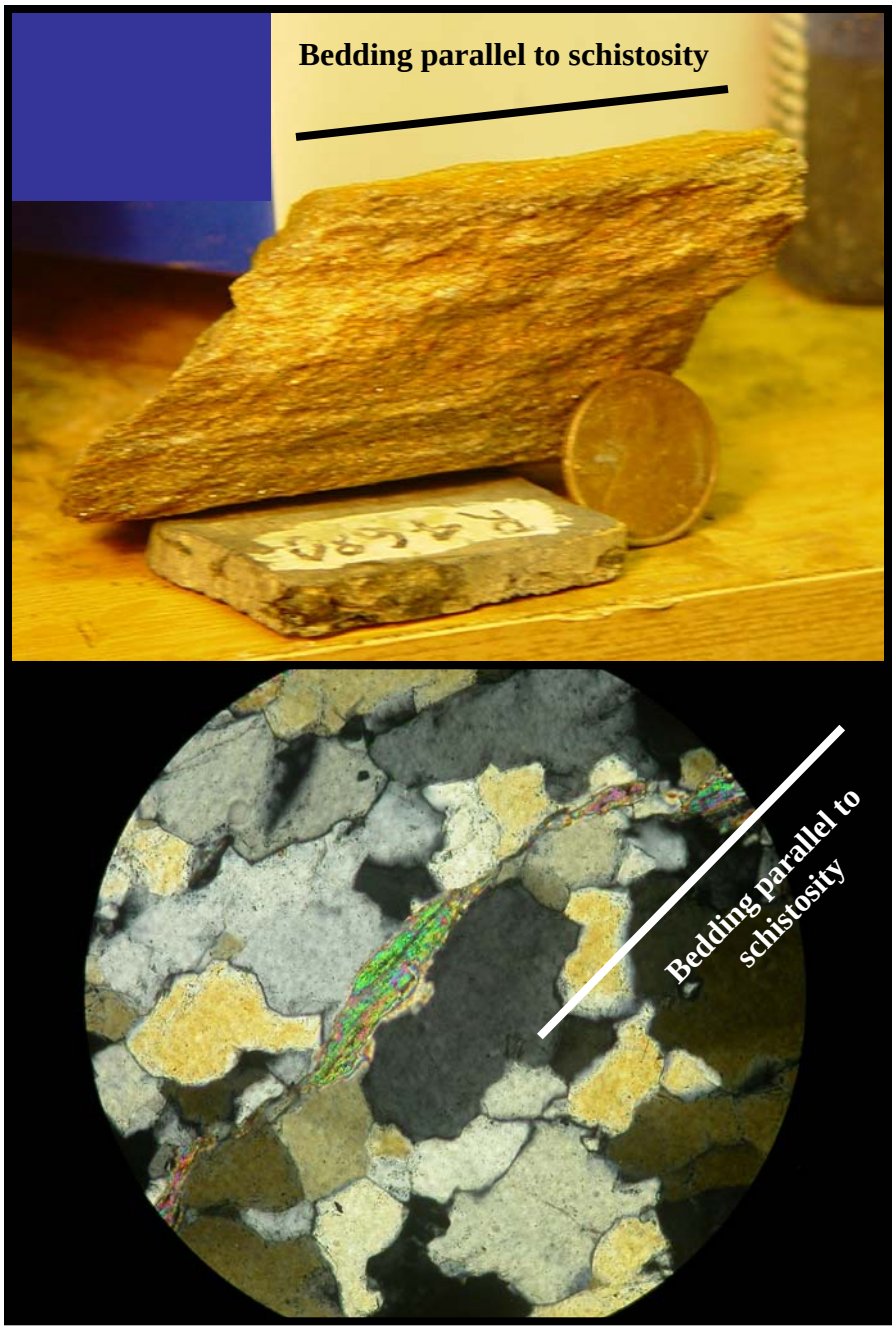
Bedding parallel to schistosity
Bedding parallel to schistosity

plagioclase feldspar (<5%), epidote, ilmenite, and magnetite. The fine-grained schists have a seriate, interlobate metamorphic texture consisting dominantly of elongated, aligned quartz grains. Micaceous layers consist of foliated, interlocking or isolated, equigranular, subhedral grains. Metaconglomerate is gray, foliated, coarse-grained, clastic quartz with rare feldspar. Marble is gray, foliated, fine-grained calcite with amphibole (likely calcic) and minor quartz. Actinolite schist consists of dark greenish-gray amphibole with chlorite.

The Lynchburg Group was considered to be late Precambrian by Brown (1958). The age of the Lynchburg Group is between *c.* 1.0 Ga and *c.* 564 Ma (Figure 6), as constrained by the Grenville basement rocks below and the overlying Catoctin Formation (Aleinikoff *et al.*, 1995). Metasedimentary rocks exhibit detrital zircon ages of *c.* 0.9-1.4 Ga (Carter *et al.*, 2006). This age range is consistent with detritus originating from Grenville-aged source rocks and accumulating during the Early Cambrian drift stage of the eastern Laurentian margin (*e.g.*, Hibbard and Samson, 1995; Kohn and Malloy, 2004; Hibbard *et al.*, 2005).

Smith River allochthon (SRA)

SRA rock units, which include the predominantly metaclastic sedimentary rocks of the Fork Mountain Formation and metabasaltic rocks of the Bassett Formations, were first described and named by Conley and Henika (1973). The rocks of the SRA are considered by some workers to be distinct from, and unrelated to, the Lynchburg Group (*e.g.*, Conley and Henika, 1973; Rankin, 1975; Conley *et al.*, 1989). However, other workers have correlated rocks in the SRA with those of the Lynchburg Group (*e.g.*, Gates, 1987, 1997; Glover,

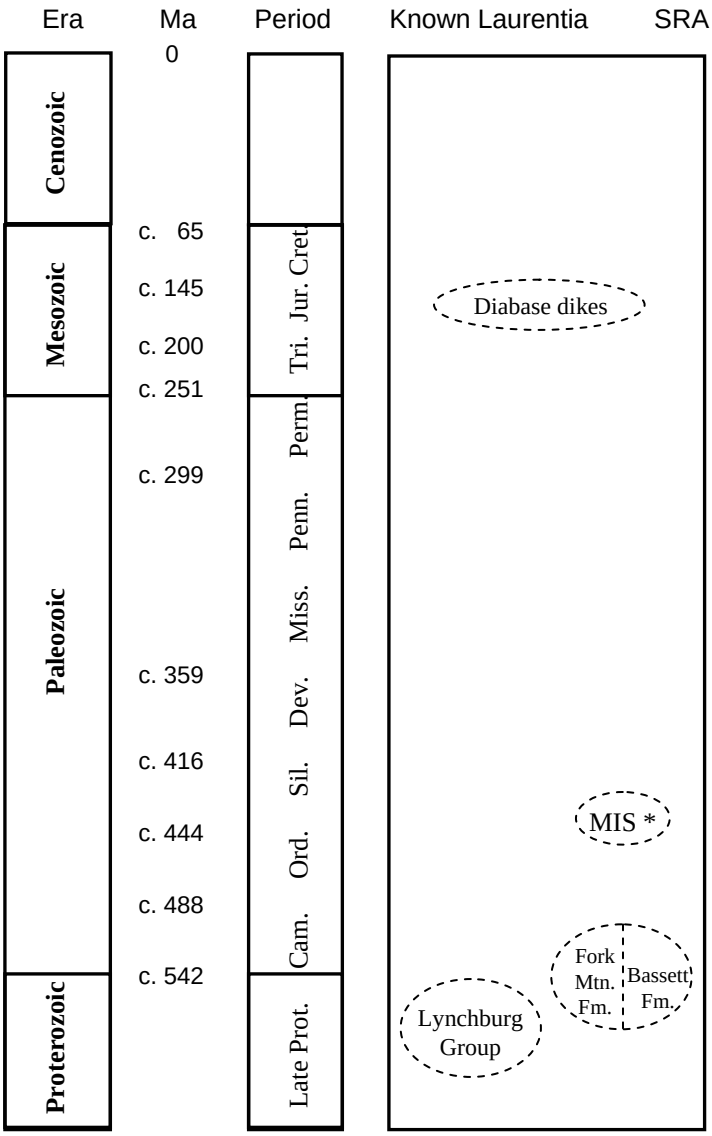

Figure 6: Chronologic sequence of rock types in the area of Pittsville, Virginia. * The Martinsville igneous suite (MIS) is not observed in the study area.

1989; Glover *et al.*, 1997). For the purposes of the study we will consider them to be separate.

The Fork Mountain Formation structurally overlies the Bassett Formation. Their contact appears be conformable, gradational, and to intertongue over short distances (*e.g.*, Conley and Toewe, 1968; Henika, 1971; Conley and Henika, 1973; Marr, 1984; Conley, 1985). In contrast to the Lynchburg Group, the SRA exhibits multiple phases of metamorphism and primary structures have been obliterated. The Fork Mountain Formation is the predominant unit in the study area and is thus the first described.

Fork Mountain Formation

Regionally, the Fork Mountain Formation contains biotite paragneiss and highly aluminous micaceous schist that interfinger laterally with each other (Henika, 1971; Conley and Henika, 1973; Marr, 1984; Conley *et al.*, 1989). The unit also contains subordinate calc-silicate quartzite and granofels, schistose and gneissic amphibolite, diamictite, and rare marble (Marr, 1984). Diamictite with clasts of quartzite, calc-silicate quartzite, and biotite gneiss compares favorably to precursor mélanges in the Potomac terrane (Rankin, 1975; Horton *et al.*, 1989). The Potomac terrane lies in fault contact with the SRA to the north, and holds a position in the Piedmont similar to that of the SRA, also emplaced onto the cover sequence of the Laurentian margin.

The Fork Mountain Formation is exposed over ~64 km^2 of the study area (Figure 3 and 4). NNE-trending synforms preserve the Fork Mountain Formation, which lies above the

folded Ridgeway fault. The Fork Mountain Formation is exposed at the ground surface except where NNE-trending irregular oval fensters expose the Lynchburg Group, or where the Bassett Formation, at the base of the SRA thrust sheet, is exposed by antiforms. Outcrop of the Fork Mountain Formation is limited because it readily weathers to regolith and clayey soil. Near the Ridgeway fault, the Fork Mountain Formation looks like the Lynchburg Group in outcrop. At microscale, these rocks are discerned from the Lynchburg Group based on metamorphic character (as described in following chapters). The distribution of the Fork Mountain Formation has been modified from the published accounts of Marr (1984) and Henika (1997, 2002) as a result of reclassification of some outcrops. The Ridgeway fault trace has also been revised, and the study area is thus underlain by a greater area of Fork Mountain Formation rocks than had been anticipated based on previous mapping.

The Fork Mountain Formation appears to be in tectonic contact with the Lynchburg Group along the Ridgeway fault, although the fault and therefore the contact, is unexposed in the study area. Previous work considers the fault trace to be exposed at “The Wall” outcrop (Figures 3 and 4) (Marr, 1984; Henika, 1997, 2002, pers. com. 2005). However, petrographic evidence has led to classification of all rocks as Fork Mountain Formation at “The Wall” outcrop, as well as rocks to the north at Loc11 and Loc12 (Figure 3). The presence of fine-grained Fork Mountain Formation rocks close to the Ridgeway fault suggests that grain-size reduction in response to a strain gradient may be associated with Ridgeway fault activity.

In the study area, the Fork Mountain Formation is predominantly a highly aluminous micaceous schist. In close fault proximity structurally lower in the Fork Mountain Formation, these schists are more siliceous and finer-grained than rocks that are structurally higher in the Fork Mountain Formation. In hand-sample, Fork Mountain Formation schists are generally highly weathered, pliable and fissile (Figure 7). In thin-section, the Fork Mountain Formation schist is composed of medium gray, reddish-brown weathering, fine- to coarse-grained (<0.1 mm to ~1.4 mm), muscovite-biotite-chlorite schist (Figure 7) with sericitized sillimanite (~10-20%) (the presence of sillimanite fibrolite is verified by microprobe analyses (Carter, 2006)). The Fork Mountain Formation also includes garnet porphyroblasts (<1 to ~2 mm diameter), chloritoid, staurolite, plagioclase feldspar, tourmaline, epidote, ilmenite, magnetite, monazite, and apatite. Mica and chlorite concentration ranges from ~30% (in closest proximity to the Ridgeway fault) to ~60%.

At microscale, micaceous and chlorite-rich layers alternate with quartz-rich layers. Micaceous and chlorite-rich layers consist of foliated, interlocking, equigranular, subhedral grains. The quartz in these rocks has weakly foliated, seriate (~0.025 to 1.5 mm in diameter), interlobate metamorphic texture. Quartz content ranges from ~5-50% generally, and up to ~70% in the closest proximity to the Ridgeway fault. Petrographic estimates of quartz content are consistent with whole rock analyses performed on samples near the study area (~45 to 70%) (Carter, pers. com. 2006). Microprobe work performed on samples near the study area yield plagioclase feldspar $An_{\sim 22\text{-}25}$ (Carter, 2006).

Figure 7: Typical Fork Mountain Formation schist with rare compositional layering at Loc09. Fork Mountain Formation schist is medium gray, reddish-brown weathering, fine- to coarse-grained, muscovite-biotite-chlorite schist with sericitized sillimanite and garnet porphyroblasts. Micaceous and chlorite-rich layers consist of foliated, interlocking, equigranular, subhedral grains and alternate with quartz-rich layers. Compositional layers consist of quartz-rich layers (~3-4 mm thick) that appear to alternate with micaceous and chlorite-rich layers (top photograph). The quartz has a weakly foliated, seriate, interlobate metamorphic texture (width of field of view bottom of photomicrograph is 5.0 mm). Refer to the discussion in Rock Units.

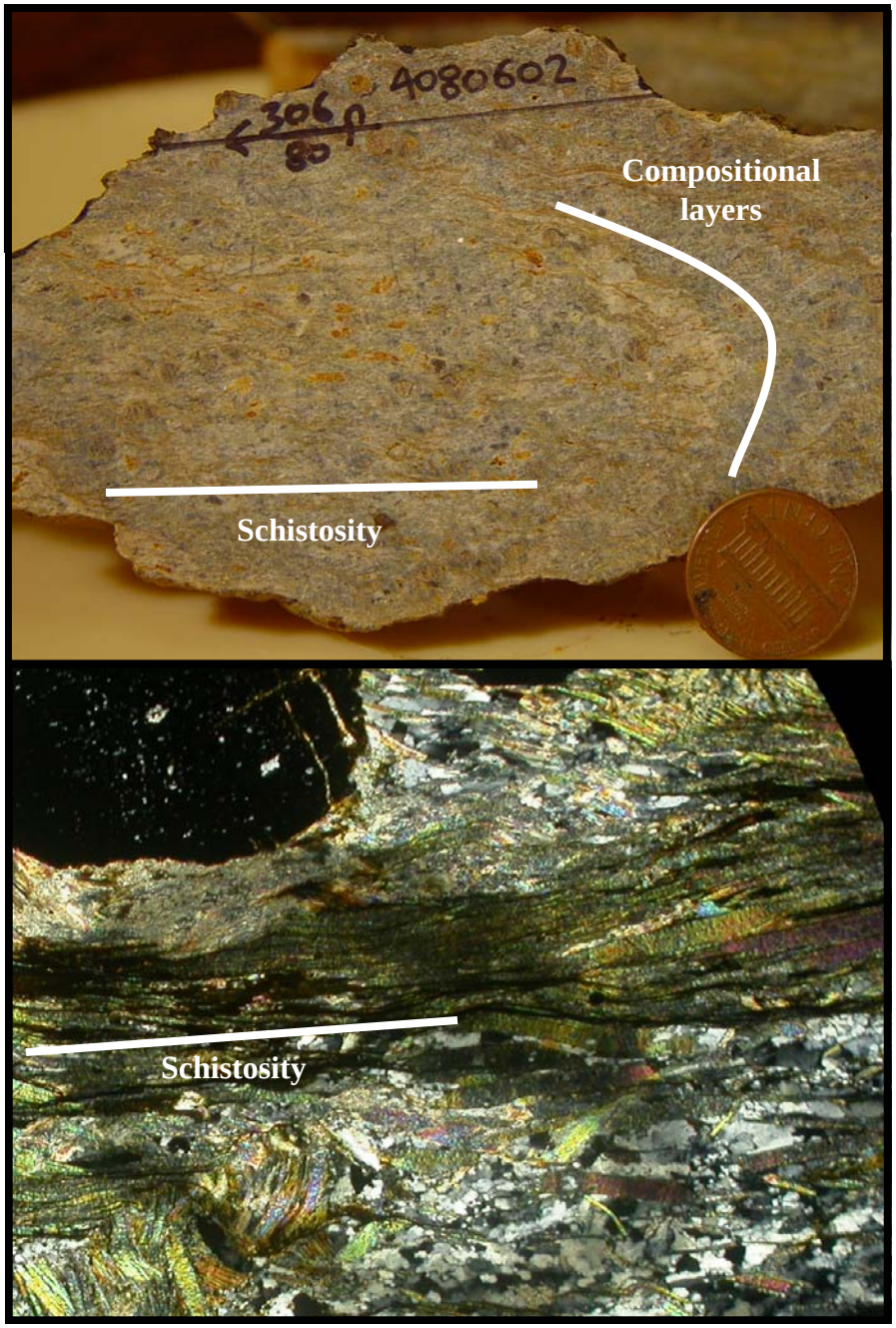
4080602
306
80
Compositional layers
Schistosity
Schistosity

Compositional layers and quartz lenses are also present in the Fork Mountain Formation. Compositional layers are rarely observed because they are only distinguishable where they lie perpendicular to the main foliation at isoclinal recumbent fold hinges (Loc05, 05, 09, and 10). Compositional layers consist of quartz-rich layers (~3-4 mm thick) that appear to alternate with micaceous and chlorite-rich layers. Compositional layers may represent relict schistosity or gneissic banding. The minerals that comprise compositional layering are difficult to discern with confidence, but they appear to include biotite, muscovite, chlorite, and quartz. In close proximity to the Ridgeway fault, many quartz lenses are also present in the Fork Mountain Formation. Quartz lenses near the fault range in dimension from microns to decimeters and are concordant with the main foliation.

The Fork Mountain Formation predates the Late Ordovician (*c.* 445 Ma) age of the Martinsville intrusive suite (MIS), which intrudes the SRA beyond the limits of the study area (Wilson, 2001) (Figure 6). The Fork Mountain Formation presumably also predates the *c.* 530 Ma age of monazite contained therein (Hibbard *et al.*, 2003).

Bassett Formation

The Bassett Formation consists of the Bassett gneiss and the Bassett amphibolite. The Bassett gneiss is a biotite paragneiss with local quartzite (Conley and Henika, 1973). The Bassett Formation appears to have a conformable contact that is gradational and intertongues over short distances with the Fork Mountain Formation that structurally overlies it (*e.g.*, Conley and Toewe, 1968; Henika, 1971; Conley and Henika, 1973; Marr,

1984; Conley, 1985). The discussion of the Bassett Formation is limited because the exposure in the study area is limited.

Regionally, the Bassett gneiss occurs sporadically as concordant discontinuous lenses (Marr, 1984). Biotite produces gneissic banding between quartz-rich layers. Quartz and feldspar layers and quartz and epidote layers occur sporadically throughout the unit (Marr, 1984). The Bassett amphibolite is cross-cut locally by ptygmatically folded feldspar and quartz dikes and pegmatites (Marr, 1984). Major and trace element analysis suggests that the amphibolite may represent continental rift basalts (Conley, 1981; Achaibar and Misra, 1984; Carter, 2006).

The Bassett Formation is locally exposed in the southern portion of the study area in plunging antiforms that expose the lower SRA (Figure 3 and 4); there, the extent of exposure of the Bassett Formation is ~3 km^2.

The contact between the Bassett and Fork Mountain formations is unexposed in the study area. The Bassett gneiss is the structurally lowest subunit and is cross-cut by, and interlayered with, the Bassett amphibolite, beyond the study area (Henika, 1971; Box *et. al.*, 2006; Carter, 2006) (Figure 8). In the study area, the Bassett gneiss is a gray, fine- to medium-grained, equigranular biotite gneiss with quartz, plagioclase feldspar, epidote, ilmenite. The Bassett amphibolite is a dark gray, fine-grained amphibolite with biotite, plagioclase feldspar, quartz, and epidote. Like the Fork Mountain Formation, the Bassett

Formation predates the *c.* 445 Ma emplacement age of the Late Ordovician Martinsville intrusive suite (MIS) (Wilson, 2001) (Figure 6).

Pegmatite

Pegmatite dikes and irregular masses are sparsely distributed in the Fork Mountain Formation throughout the study area (Figure 4). They clearly intrude the Fork Mountain Formation in the study area and may be discordant with both the Lynchburg Group and the Ridgeway fault. They range in thickness from centimeters to meters. Pegmatite bodies can not be correlated between outcrops due to their discontinuous nature. Pegmatites consist of white to light gray, coarse-grained, granoblastic quartz, plagioclase, potassium feldspar, and muscovite. They are weakly deformed and exhibit a weak foliation.

Diabase dike

Mafic diabase dikes are widespread in the region. These intrusions are not deformed by the events that deformed the SRA and Lynchburg Group. Only one diabase dike is observed in the study area (Figure 4). The orientation of the diabase dike within the study area (~035) is consistent with the generally northerly trend of other dikes mapped in the region (Marr, 1984; Henika, 1997, 2002). This dike is sub-vertical and cross-cuts the foliation of the Fork Mountain Formation at a high angle. The diabase dike is dark gray, fine- to medium-grained, phaneritic, and appears to be consistent with similar dikes characterized by Conley (1985) as dark gray, generally ophitic, comprising ~50% calcic plagioclase feldspar ($An_{\sim 56}$) and ~30% augite as well as magnetite and olivine. The dike exhibits spheroidal weathering

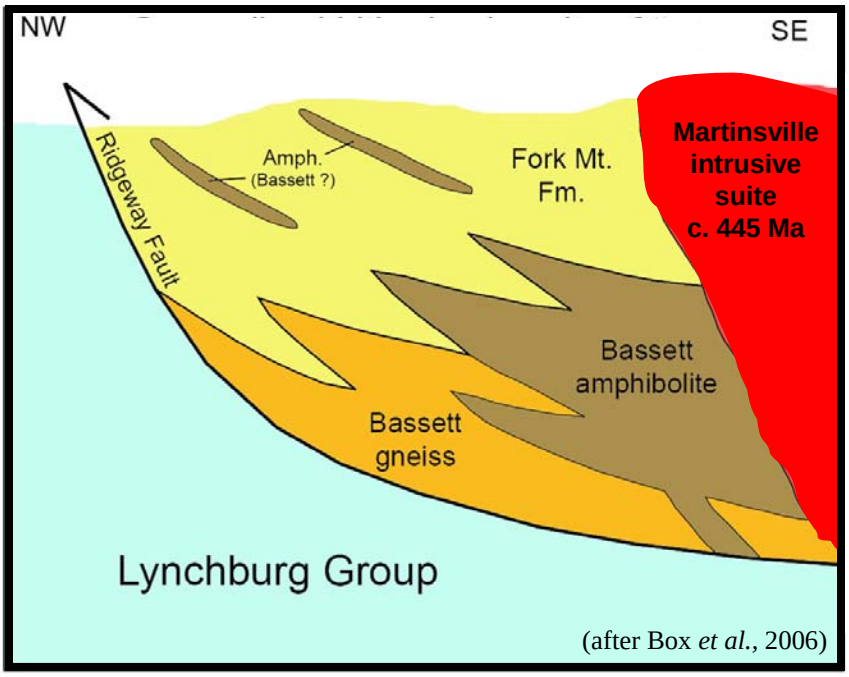

Figure 8: Generalized relationships of the main lithodemic units of the Smith River allochthon (note: neither pegmatite nor diabase are represented).

and weathers to reddish-orange saprolite. This dike is consistent with other dikes mapped in the region that are related to Mesozoic extension (Marr, 1984; Henika, 1997, 2002). Paleomagnetic and isotopic data suggest an early Jurassic age (*c.* 200 Ma) for these dikes (Ragland, 1991) (Figure 6).

STRUCTURAL GEOLOGY

Introduction

Major orogenic events in the SRA that are shared with the Lynchburg Group must be discerned in order to allow any unshared earlier structures to be distinguished. Differences in structure, fabric, cross-cutting and overprinting relationships of fabric, geometric style and orientation, and metamorphic mineral assemblages distinguish these deformational events. In this analysis, younger structures are progressively stripped away in order to recognize the more obscure, and possibly strongly modified, strain record of the early deformation. Therefore, the structural analysis progresses from the youngest to the oldest structures.

The study area is divided into three transects (northern, central, and southern), each of which crosses the Ridgeway fault (Figure 3). Within the central transect a WNW-ESE-trending central corridor is delimited as a domain that exhibits consistent structural character (Figure 3). The central domain is oriented perpendicular to the NNE-SSW-trend of the hinge of a macroscale, upright fold train and appears to be constrained to this fold train. The central domain is further subdivided into subdomains that consist of outcrop(s) that lie within the same part of a limb or hinge of the macroscale fold train. Subdomains are not delineated on Figure 3; instead, they are referred to by their constituent location number(s) (*i.e.*, LocX, Y). The large outcrop referred to as “The Wall” (Loc02, 06, 07, and 13) (Marr, 1984; Henika, pers. com. 2005) defines an additional subdomain in close

proximity to the trace of the Ridgeway fault in the southern transect (Figures 3 and 4). These subdomains permit isolation of portions of structures (*e.g.*, fold limbs and hinges, and rocks near the Ridgeway fault), and thus provide structural control for further analysis including interpretative cross sections (Figures 3, 4 and 9).

Rocks in the study area exhibit evidence of up to four deformational events. The SRA and Lynchburg Group appear to share three of these events. The three events that are shared are referred to, from the youngest to the oldest, as: 1) the later deformation (D_r), 2) the late deformation (D_l), and 3) the main deformation (D_m). The SRA also contains evidence for an early deformation (D_e) that is unshared with the Lynchburg Group, thus making it impractical to assign numbers to the events because the starting points differ.

Later (D_r) and late (D_l) deformations

Observation of the later (D_r) and the late (D_l) deformations

Late folds (F_l) deform the preexisting main foliation (S_m). The late deformation (D_l) is characterized by asymmetric, non-cylindrical, alternately and gently plunging, upright to moderately inclined, open folds (F_l) with NNE-SSW-trending hinges and axial surfaces. Some F_l are overturned and all axial surfaces appear to dip toward the SE (Figure 9).

Later deformation folds (F_r) appear to overprint F_l, however it is difficult to confidently assess the superposition of F_r over F_l, thus the relative timing of D_r and D_l is difficult to assess and F_l/F_r may represent at single generation of plunging folds. Furthermore, it is possible that mesoscale F_r, observed only near the Ridgeway fault trace (at “The Wall”

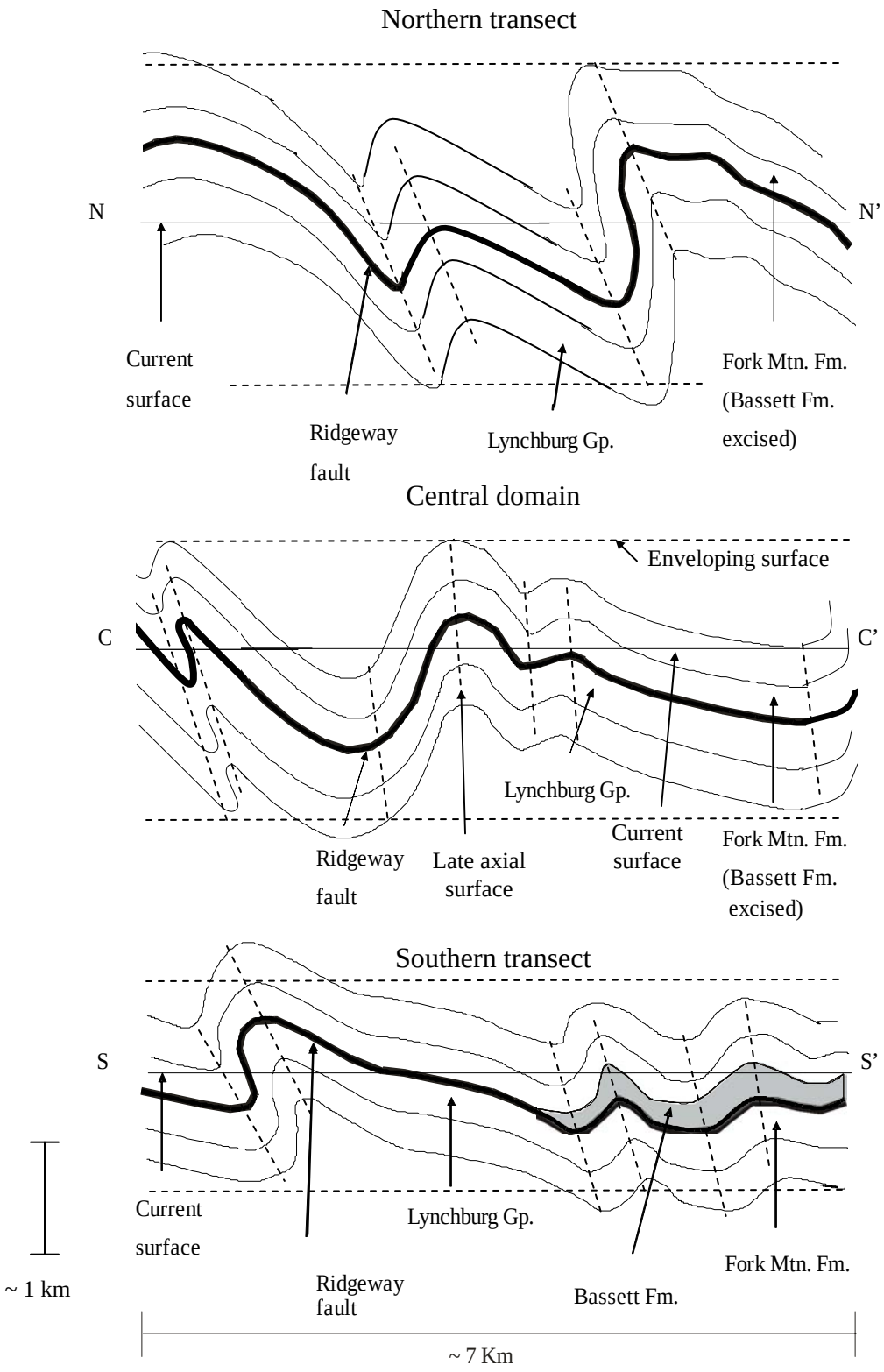

Figure 9 A: Cross sections of the study area. Interpretive cross sections of late folds (F_l) of the main foliation at N-N' in northern transect , C-C' in central domain, and S-S' in southern transect as in Figure 3 and 4. Plane of view is oriented WNW (left)-ESE (right).

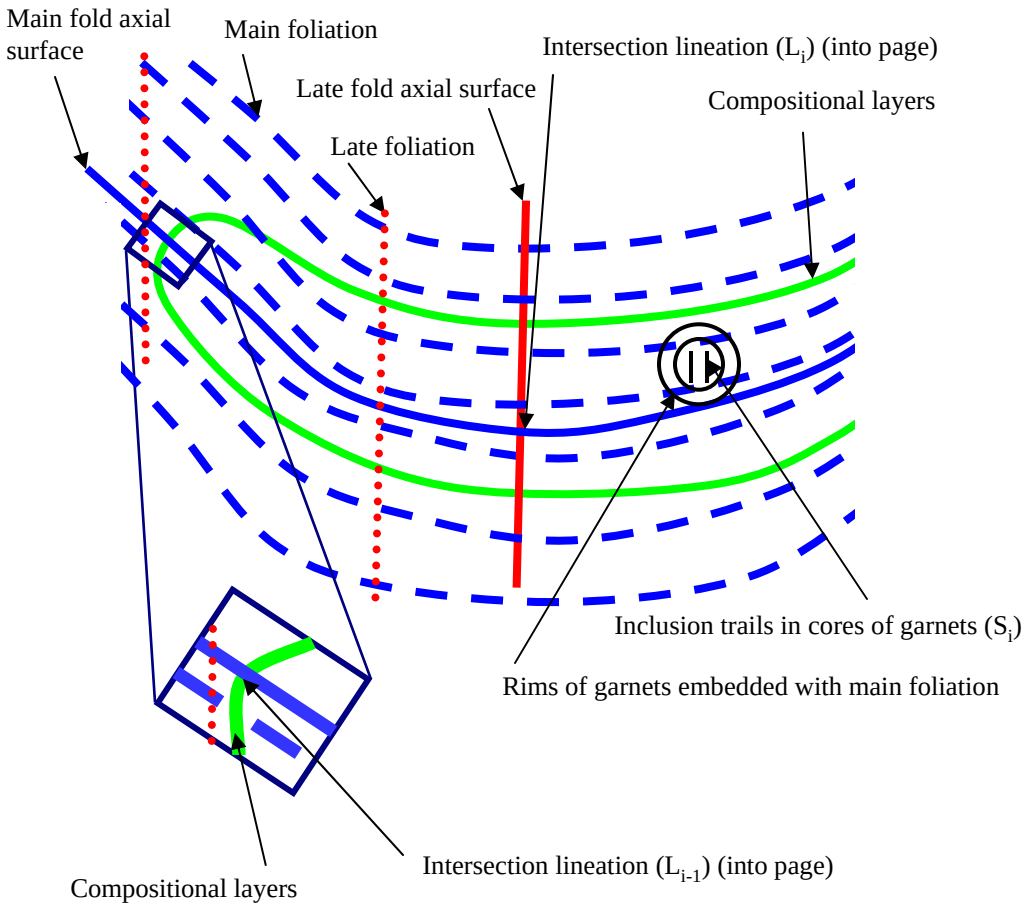

Figure 9 B: Cross sections of the study area. Schematic cross section of structure showing axial surfaces and foliations of the main and late folds, compositional layers, intersection lineation (into page), and garnet with inclusion trails in the cores and embedded main foliation minerals in the rims (diameter of garnets and thickness of compositional layers up to ~4 mm).

outcrop, Figure 3), may represent fault-related folding (*e.g.*, van der Pluijm and Marshak, 1997). Mesoscale F_r may also be present away from the fault, but may be unobserved because they are more easily seen at the largest outcrop in the study area, which is coincidentally near the Ridgeway fault trace. However, individual mesoscale F_r observed at "The Wall" are consistent with the rough orientation of a possible second macroscale fold generation (F_r) that could be responsible for producing macroscale NNE-SSW-trending elongated domes and basins by Type-1 (Ramsay, 1967) interference of these two obliquely oriented folds. Evidence for strike-slip movement along the Ridgeway fault, however, is not observed in the study area.

The geometry of the macroscale F_r is difficult to assess but appears to consist of generally E-trending open folds. Later folds (F_r) appear to be asymmetric, non-cylindrical, subhorizontal to moderately plunging, roughly E-trending, upright to moderately inclined, open to closed folds with axial surfaces that dip south to southeast (Figures 3, and 4). A penetrative foliation parallel to the axial surfaces of F_r is not observed. Trends of F_r hinges range from ~055, 00 to ~170, 40 (Figures 10 and 11) with axial surfaces that dip ~45^o to the SE as observed in three-dimensional outcrop at "The Wall". Rare fragmented quartz grains exhibit brittle failure (*i.e.*, cataclastic deformation) in F_l fold hinges. Stereoplots of the poles to the main foliation (S_m) that is folded by F_l deviate from a great circle (Figures 12 and 13). This deviation of orientations from a great circle on the stereoplot corresponds with the alternate plunging of antiforms and synforms in the region.

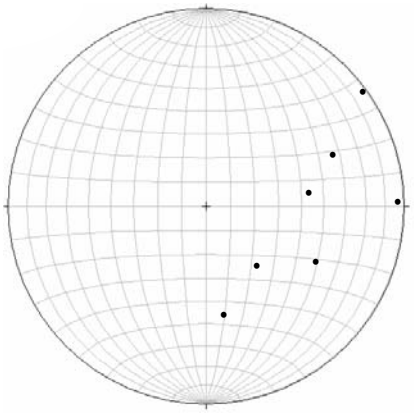

n = 7
Rose outer circle = 14%

Figure 10: Equal area, lower hemisphere, stereoplot of the minor later fold (F_r) hinges in the southern transect (SRA).

Figure 11: Tight later fold in the Fork Mountain Formation at Loc02. This closed, tight fold has a moderately plunging hinge oriented ~140 (into page), 55 and an ESE-trending, moderately inclined axial surface that dips toward the south oriented at ~140, 45 (purple). The folded main foliation is shown in blue. The plane of view is ~020 (left), 85.

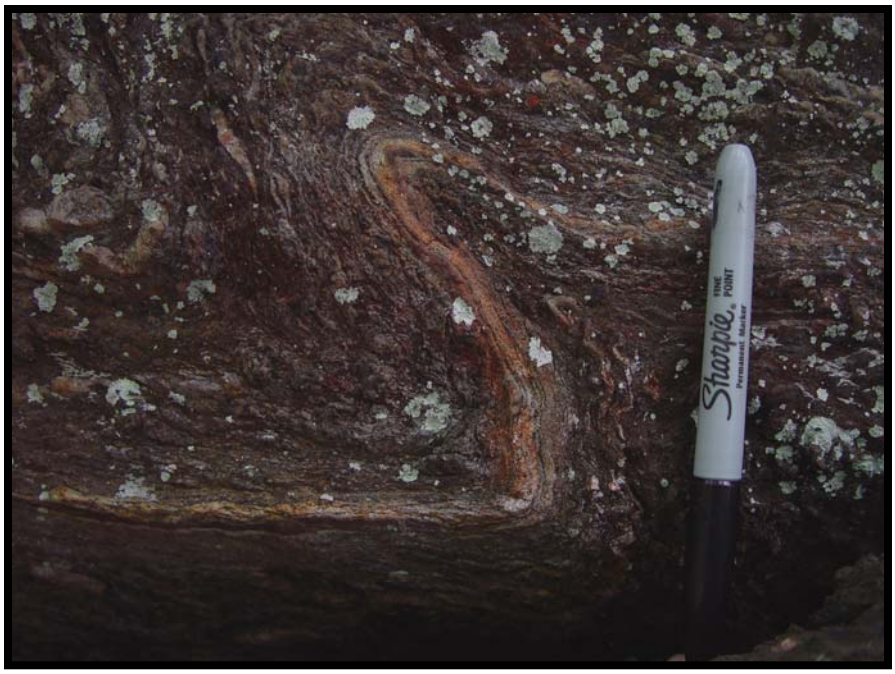
Sharpie
FINE POINT
Permanent Marker

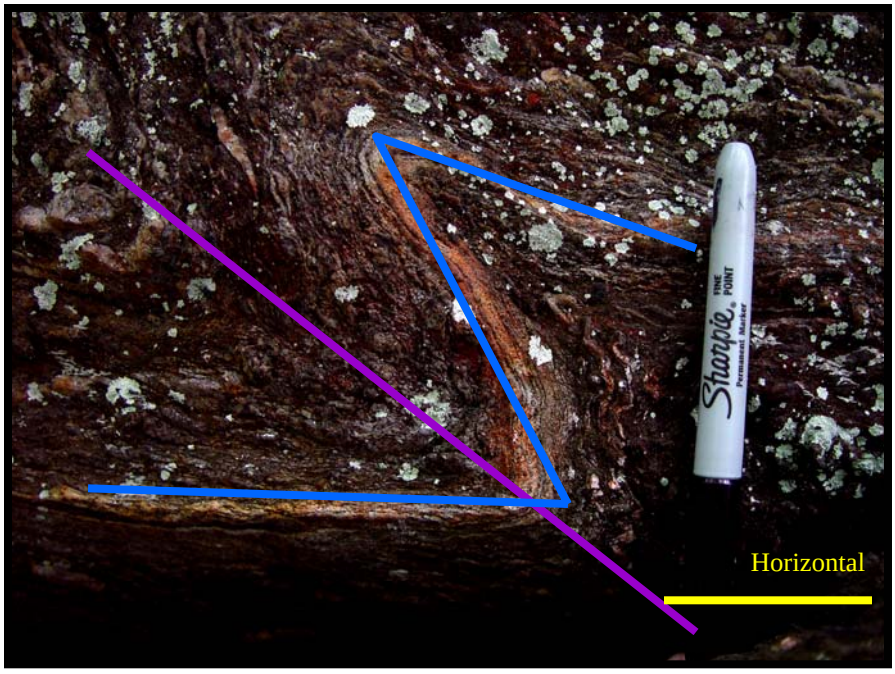
Sharpie
FINE POINT
Permanent Marker
Horizontal

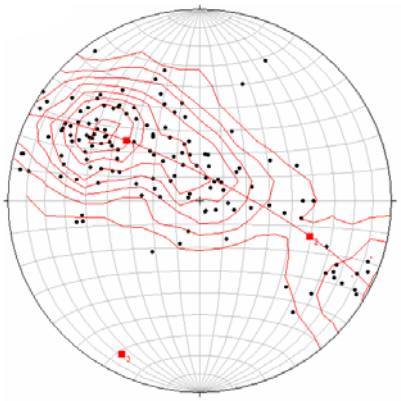

n = 147
Kamb contour interval
(c) = 2 sigma
Pole to best-fit great circle
(a) = 207, 11

Figure 12: Equal area, lower hemisphere, stereoplot of poles to planes of the main foliation in the SRA and the Lynchburg Group in the study area. Refer to Appendices 2, 3, and 4 for stereoplots of individual transects and rock types.

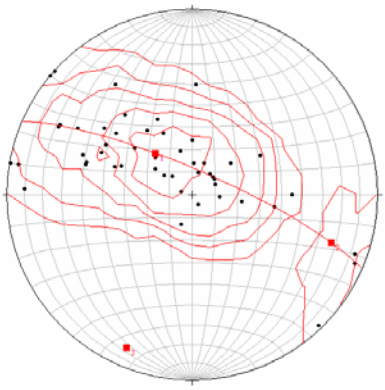

n = 52
Kamb contour interval
(c) = 2 sigma
Pole to best-fit great circle
(a) = 204, 11

A-Sm across central domain

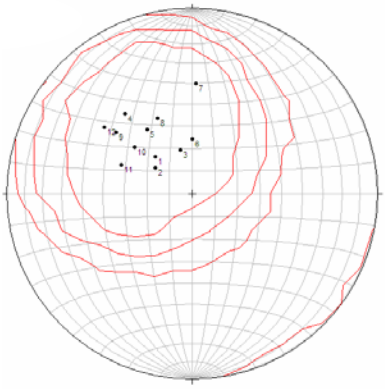

n = 12
c = 2

B-Subdomain of Loc11, 12, and 17

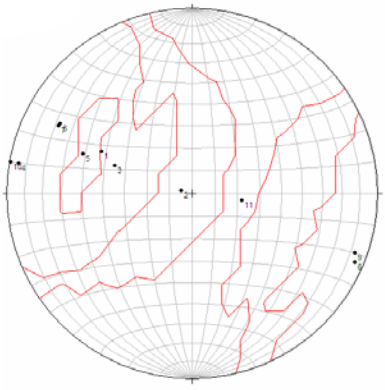

n = 11
c = 2

C-Subdomain of Loc09, 10

Figure 13 A, B, C: Equal area, lower hemisphere, stereoplot of poles to planes of the main foliation in the central domain (SRA).

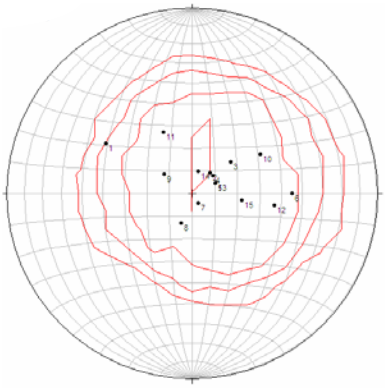

n = 15
Kamb contour interval
(c) = 2 sigma

D-Subdomain of Loc18

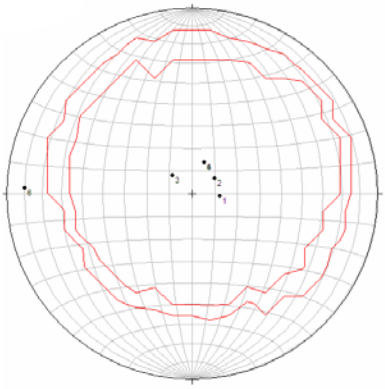

n = 6
c = 2
*Note suborthogonal outlier (left) that is field evidence for another foliation generation

E-Subdomain of Loc08

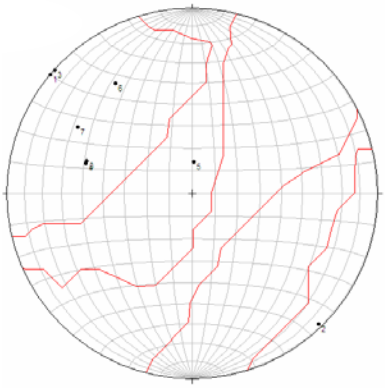

n = 8
c = 2

F-Subdomain of Loc05 (incorporates two data points from Marr, 1984 (093,14 and 030, 61)

Figure 13 D, E, F: Equal area, lower hemisphere, stereoplot of poles to planes of the main foliation in the central domain (SRA).

F_l exhibits a moderately penetrative late foliation (S_l) that weakly overprints the main foliation and is defined by biotite, muscovite, quartz, and sericitized sillimanite mats. Minerals of preexisting assemblages may have been transposed to produce S_l. Quartz with undulose extinction and euhedral garnet devoid of strain caps or shadows may also be associated with D_l.

Several mesoscale, NE-trending, upright, gentle F_l folds are directly observed in outcrop along the northern transect (Figure 14). The trend of the hinge and plunge of an example of a SE-dipping, overturned F_l synform in the Fork Mountain Formation is ~031, 00 and the orientation of the axial surface is ~031, 60 (Figure 15). In this example at Loc01, the main foliation (S_m) is partially transposed into S_l as the micaceous and chlorite-rich layers and sericitized sillimanite mats that define the main foliation (S_m) are partially realigned (Figure 15 B). In another example, a Lynchburg Group sample from near a late antiform (F_l) shows the moderately penetrative late foliation (S_l) weakly overprinting S_m (Figure 16). S_l appears to lie subparallel to the axial surface of the late antiform (F_l).

A third example of F_l includes coaxial Type-3 (Ramsay, 1967) folding of F_m by F_l in a float block at Loc05 (Figure 17). The relation between main and late events is identified by the prominence of the main foliation. The 010, subhorizontal trend and plunge of the fold hinges correspond with the ~010, 00 apparent orientation of fold hinges in an *in situ* pavement outcrop in the nearby creek bed suggesting that the float block is in its original orientation.

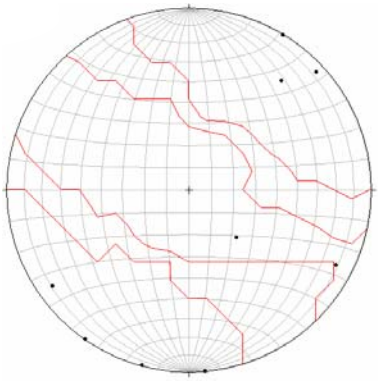

n = 9
Kamb contour interval
(c) = 2 sigma
Rose outer circle = 22%

A-SRA and Lynchburg Group

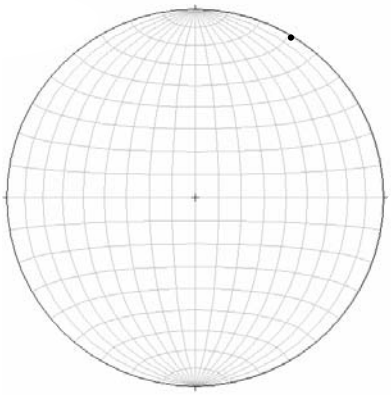

n = 1
Rose outer circle = 100%

B-SRA

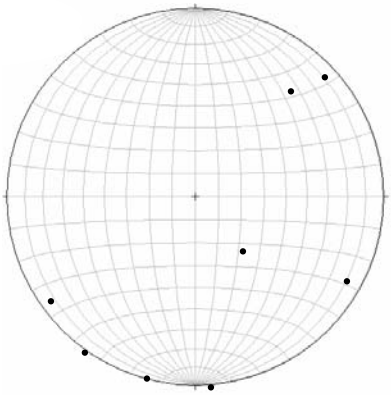

n = 8
Rose outer circle = 25%

C-Lynchburg Gp

Figure 14: Equal area, lower hemisphere, stereoplot of the mesoscale late fold hinges in the northern transect.

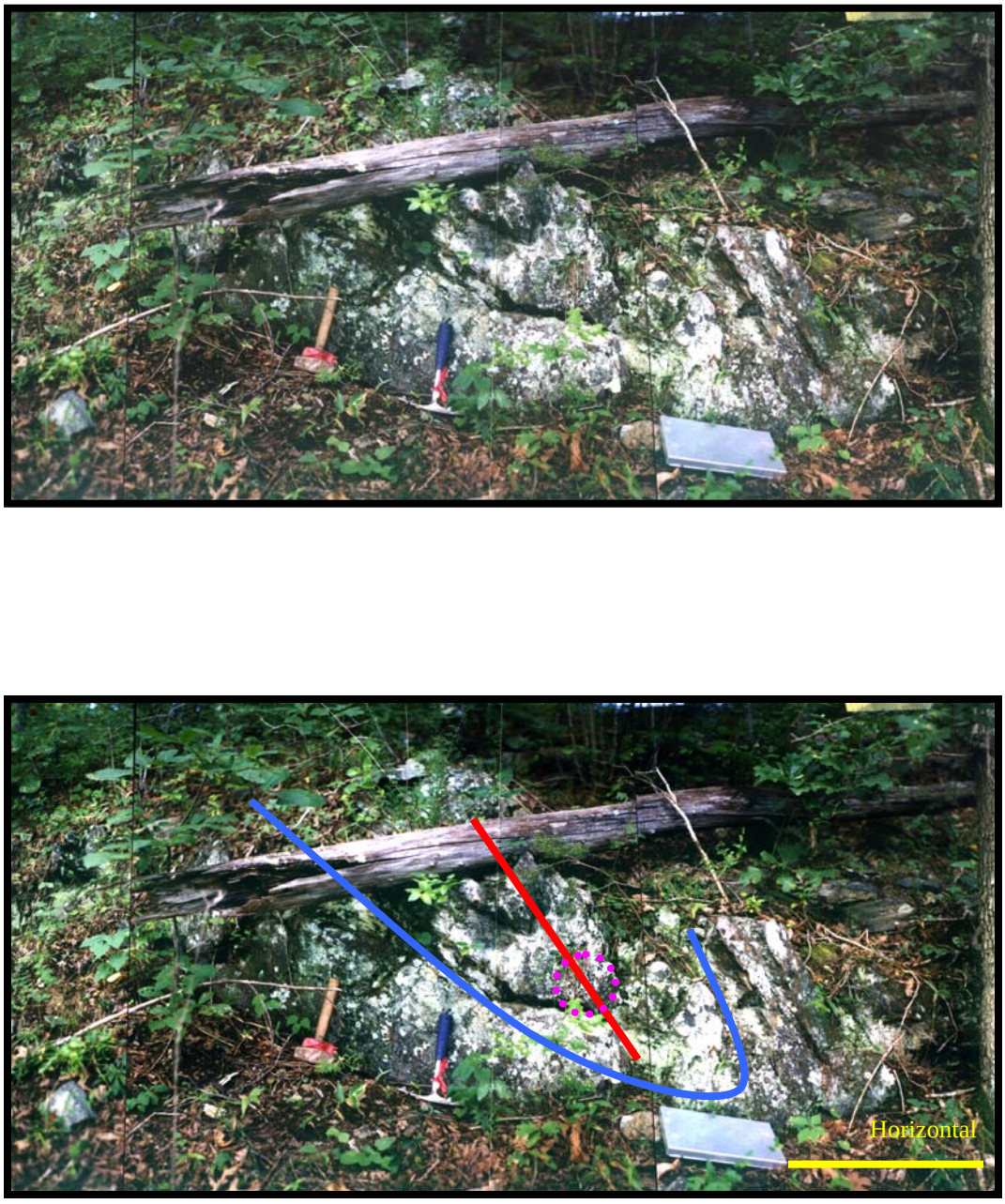

Figure 15 A: Late synform in the Fork Mountain Formation at Loc01. This open synform has a subhorizontally plunging hinge oriented ~031 (into page), ~00 and moderately inclined axial surface dipping ESE oriented ~031 (into page), ~60 (red). The folded main foliation is shown in blue. The dotted fuchsia circle indicates the sample location (Figure 15 B, C). The plane of view is oriented ~120 (right), 90.

Figure 15 B: Late synform in the Fork Mountain Formation at Loc01. The moderately penetrative foliation is oriented ~031 (into page), ~60 (red) subparallel to the approximate axial surface (see previous photograph). The approximate location of the main foliation is marked in dark blue. The plane of view is ~137 (right), ~90 (photo at slight angle) subperpendicular to the late fold hinge that is oriented ~031 (into page), 00. The digits marking the ruler in the photo are centimeters (cm). The thin-section is photographed where it originated from in the hand sample. The dotted light-blue circle is the location of the following thin-section photomicrograph (Figure 15 C).


Horizontal

Figure 15 C: Late synform in the Fork Mountain Formation at Loc01. The moderately penetrative foliation parallel to the axial surface of the late fold is oriented ~031 (into page), subvertical (red). The difference between the dip in the late foliation plane in each photo is due to the unevenness of the plane. The late foliation is defined by biotite and aligned sericitized sillimanite mats. The main foliation is subhorizontal (dark blue). The early foliation, as represented by inclusion trails in garnet, is marked in green. The plane of view is ~137 (right), 90. The field of view is 10 mm, subperpendicular to the late fold hinge that is oriented 031 (out of page), 00. (cross-polarized light)

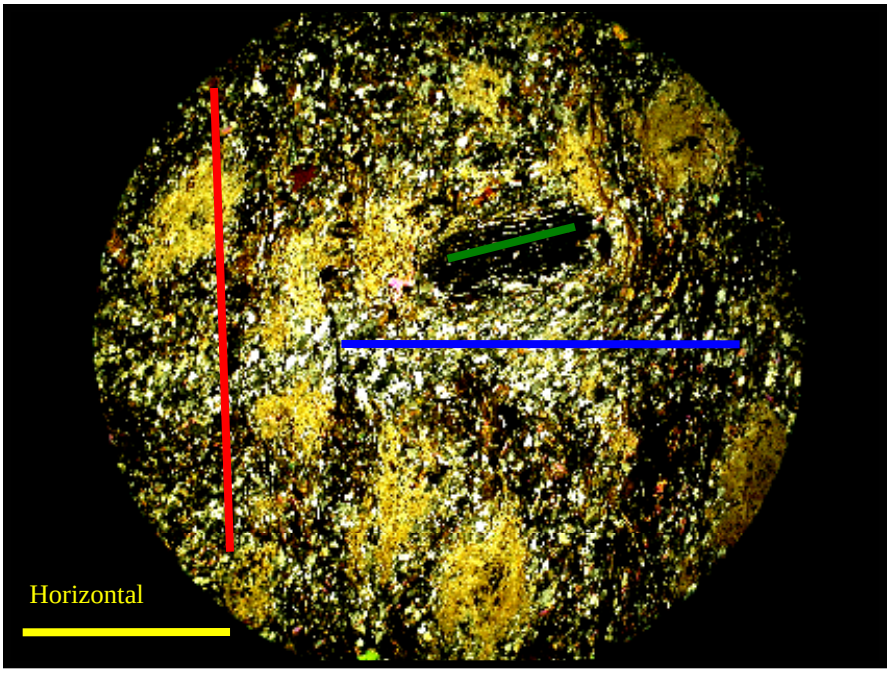
Horizontal

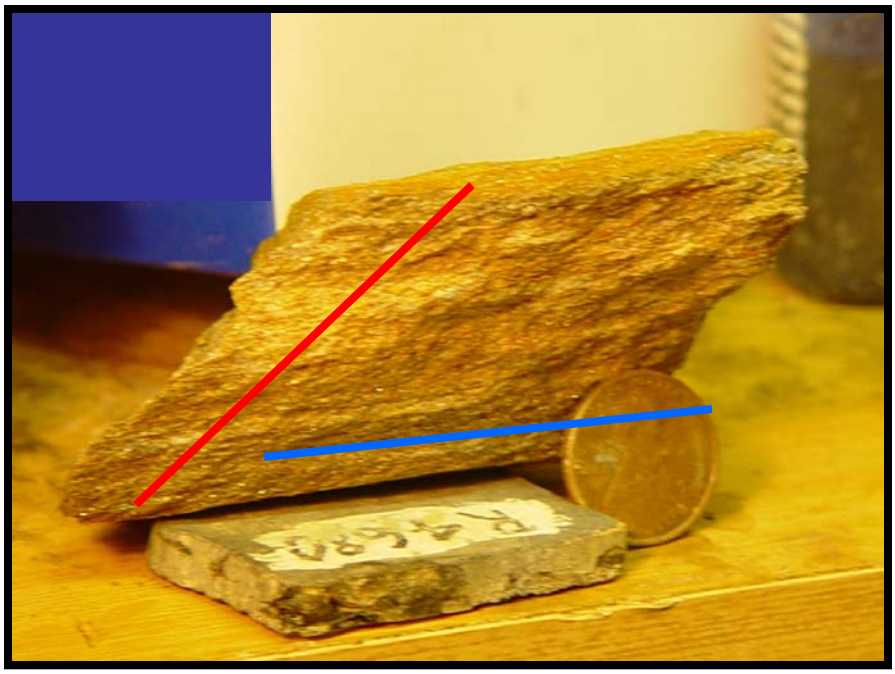

Figure 16: Main and late foliations in the Lynchburg Group at Loc03. The main foliation is marked in blue and is parallel to bedding in this sample. The non-penetrative foliation parallel to the late axial surface is marked in red. The sample is not oriented.

Figure 17: Refolded (Type-3) folds in the Bassett gneiss. Late deformation of main folds in the Bassett gneiss at Loc04. The main fold hinge (blue) and the late fold hinge (red) (into page), subhorizontal plunge. The sample is float but appears to be in its original orientation because the hinge of the main fold in the float (~010, subhorizontal plunge) are confirmed by apparent orientations of main fold hinges (~010) in a nearby creek pavement outcrop. The early foliation is marked in green. The plane of view is ~E-W nearly perpendicular to the main and late fold hinges.

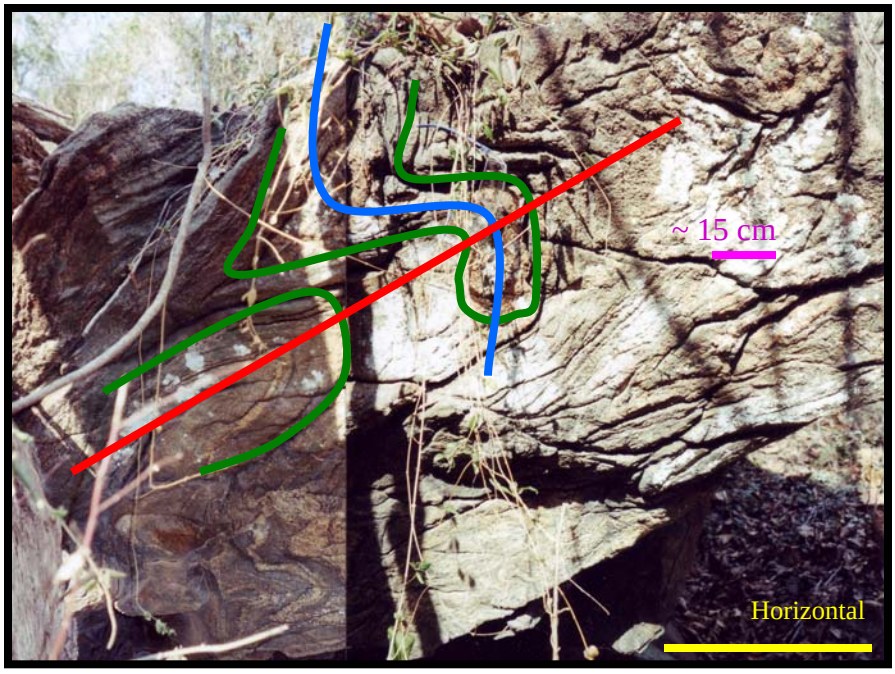
~ 15 cm
Horizontal

The F_l hinges are determined from best-fit great circles on stereoplots. The trends of F_l hinges across the study area and central domain are shown on Figures 12, 13, 14, and 18 and Appendices 1, 2, and 3. These F_l hinge orientations, generated from mesoscale data on stereoplots, are consistent with previous mapping in the study area (Marr, 1984; Henika, 1997, 2002). Stereoplots of the central subdomains exhibit specific segments of a late synform and antiform fold train (Figure 9). Mesoscale fold data from the central domain, and the macroscale alternation of exposures of the different rock types, provide data for interpretation of macroscale late fold hinges (Figure 3 and 4) and interpretative cross sections (Figure 9).

Interpretation of the later (D_r) and late (D_l) deformations

D_l is associated with a moderately penetrative foliation parallel to the late axial surface (S_l) that is defined by a mineral assemblage comprising biotite, muscovite, quartz, sericitized sillimanite mats, and possibly garnet. Cataclastic deformation of quartz observed in two later fold (F_r) hinges indicates that some brittle deformation of quartz occurred in tight fold hinges. Temperatures characteristic of brittle quartz deformation are typically $<350^o$ C (*e.g.*, Passchier and Trouw, 1996; van der Pluijm and Marshak, 1997). Low-temperature deformation ($<350^o$ C) is consistent with the presence of a relatively low-grade metamorphic mineral assemblage.

F_l and F_r share a similar style of deformation (*e.g.*, asymmetric, non-cylindrical, upright to moderately inclined, open to closed folds). Despite the differing trends of their hinges, these

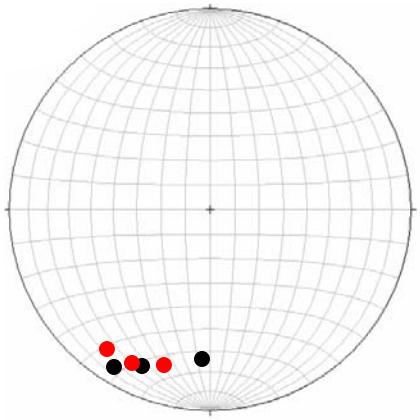

n = 6
Rose outer circle = 33%

Figure 18: Equal area, lower hemisphere, stereoplot of late fold (F_l) hinges as derived from poles to best-fit great circles of deformed main foliation orientation in each transect. The orientations of the SRA and the Lynchburg Group in the three transects are shown in red and black respectively.

similarities imply that D_l and D_r occurred under similar conditions, either contemporaneously, or sequentially or both, in a transpressional environment as interpreted by Gates (1986, 1987). Simultaneous occurrence of D_l and D_r would permit a single tectonic transport direction (Gates, 1986).

Previous workers associate these folds with Alleghanian deformation (Marr, 1984; Conley, 1985, 1989; Gates, 1986, 1987; Henika, 1997, 2002). Gates (1986) attributed the deformation responsible for late upright domes and basins (*i.e.*, D_l and D_r) in the Altavista, VA area to the Alleghanian based on a comparison of regional shear zones.

Observation of the intersection lineation (L_i and L_{i-1})

A regionally pervasive, penetrative NNE-SSW-trending intersection lineation (L_i) is observed on the surface of the main foliation (S_m). L_i orientations in each transect are shown on Figure 19 and Appendices 4, 5, and 6. L_i is defined by the alignment of muscovite and chlorite streaks in both the SRA and the Lynchburg Group. In the SRA, L_i is also defined by micro-fold hinges of muscovite (~1 cm between hinges) and by the alignment of quartz rods, sericitized sillimanite mats, and less common tourmaline. L_i occurs in weathered Fork Mountain Formation as rock “pencils” (~5 cm by ~1 cm) or elongate fragments. In general, S-and-C fabric can not be confidently identified on the plane perpendicular to S_m and parallel to L_i.

L_i orientations are subparallel to the hinges of late folds (F_l) (Figures 14 and 18). L_i appears to result from the intersection S_m*S_l (Figure 9 B). L_i appears to be a product of the late

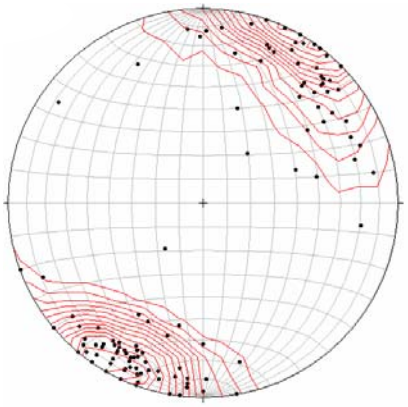

n = 127
Kamb contour interval
(c) = 2 sigma

Figure 19: Equal area, lower hemisphere, stereoplot of the intersection lineation in the SRA and the Lynchburg Group in the study area. Refer to Appendices 5, 6 and 7 for stereoplots of individual transects and rock types.

deformation, wherein the penetrative main foliation (S_m) and the moderately penetrative foliation parallel to the late axial surface (S_l) intersect (S_m*S_l = L_i). The orientations of L_i in the Lynchburg Group are indistinguishable from L_i in the SRA (Appendices 5, 6, and 7). The consistent orientation of L_i in rocks on both sides of the Ridgeway fault strongly supports the interpretation that L_i was created by the intersection of the main foliation and the moderately penetrative late foliation because it is created an event shared by the SRA and the Lynchburg Group (S_m*S_l) (*i.e.*, $L_{i\ SRA} = L_{i\ Lynchburg\ Group}$). An example of this is observed at a late synform (F_l) where S_l and S_m are each evident (Figure 15 B).

Locally in the SRA, a second intersection lineation (L_{i-1}) lies parallel to the intersection of S_m and the compositional layers that are folded by isoclinal recumbent main folds (F_m) (compositional layering*S_m) (Loc05, 08, 09, and 10) (Figures 3, 4, 9 B, 20 and 21). Thus, L_{i-1} is parallel to the intersection of the compositional layering and main foliations. The orientations of the local L_{i-1} are indistinguishable from the pervasive L_i observed throughout the SRA.

Interpretation of the intersection lineation (L_i and L_{i-1})

Foliation created by strain in an initial orientation that has a subsequent strain superimposed at a different orientation can accumulate as an intersection lineation that appears to be a product of lengthening (Ramsay, 1967). Thus, L_i may be an accumulation of strain from multiple events.

Figure 20: Main fold and relict compositional layering in the Fork Mountain Formation at Loc05. This upright, isoclinal fold (F_m) has a moderately plunging, NE-trending, hinge oriented at ~032 (out of page), 30. The subvertical, NE-trending axial surface is oriented at ~032 (out of page), 90 (blue). The folded compositional layering is shown in green. S-and-Z, parasitic micro-folded grains of mica (white) appear to confirm the presence of a fold hinge. S_e*S_m defines the intersection lineation (L_{i-1}) oriented at ~032 (out of page), subvertical dip. The plane of view is ~138 (left), 50, nearly perpendicular to the main fold hinge.

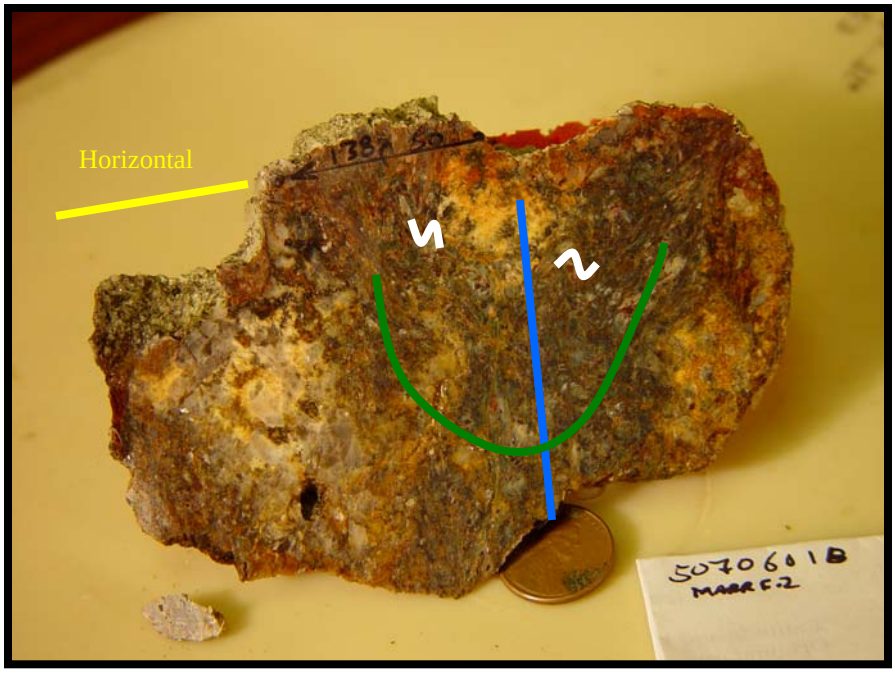
Horizontal
u
2

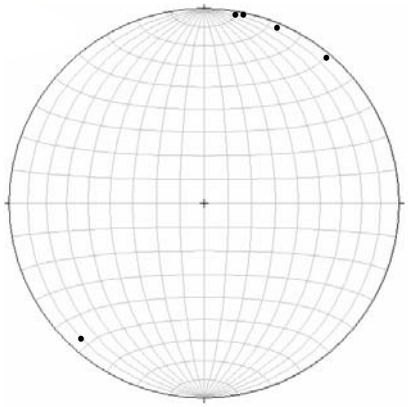

n = 5
Rose outer circle = 40%

Main fold (Fm) hinges

Figure 21: Equal area, lower hemisphere, stereoplot of main fold hinges that are also the intersection lineation (L_{i-1}) in the central domain (SRA) including Loc04 in southern transect (SRA).

Main deformation (D_m)

Observation of the main deformation (D_m)

The predominant structural feature in the study area is a continuous, penetrative foliation (S_m) that is parallel to the axial surface of isoclinal recumbent main folds (F_m) in the SRA, subparallel to bedding (S_0) in the Lynchburg Group, and subparallel to the surface of the Ridgeway fault. This foliation is deformed by the late deformation (D_l). Analysis of its orientation contributes to an understanding of the orientation of S_m before D_l. The orientation of S_m in the SRA is indistinguishable from that in the Lynchburg Group (Appendix 2B, 3B, 4B (SRA) *vs.* Appendix 2C, 3C, 4C (Lynchburg Group), Figure 18). The enveloping surface to the folds that affect the Ridgeway fault is subhorizontal, suggesting that S_m was originally subhorizontal (Figure 9). Thus, unfolding of the late (F_l) and later (F_r) folds would theoretically restore S_m to subhorizontal. A subhorizontal orientation of S_m strongly implies that S_m on each side of the Ridgeway fault had the same initial orientation and therefore, that S_m represents a single deformation.

The metamorphism that is responsible for S_m is referred to as M_m. However, the Ridgeway fault emplaces higher-grade onto lower-grade metamorphic rocks. S_m is defined in the SRA by a lower amphibolite facies metamorphic mineral assemblage (M_m), while S_m is defined in the Lynchburg Group by a greenschist facies metamorphic mineral assemblage (M_m) in the study area. Because S_m is continuous across the fault, S_m on both sides of the fault appears to be generated by the main metamorphic event (D_m).

The micro-fabric of the quartz component defining S_m in the matrix of the Fork Mountain Formation and in the Lynchburg Group is seriate to equigranular, with interlobate grain boundaries. Undulose extinction is present in quartz, particularly in the larger grains of the seriate grain size distribution (*e.g.*, Figure 22). Grain boundary migration in quartz is exhibited in both Lynchburg Group and SRA rocks (Figure 22). Quartz grain sizes range from ~0.025 to 1.5 mm. The aspect ratio of quartz grains is ~2:1:1 in the Lynchburg Group and ~1.5:1:1 in the Fork Mountain Formation.

The micro-fabric of S_m in the Fork Mountain Formation consists of a schistosity that is also a continuous cleavage (Powell, 1979). S_m comprises ~50% foliated micaceous and chlorite-rich layers and ~50% foliated quartz-rich layers. The micaceous and chlorite-rich layers consist of interlocking subhedral, tabular grains of mica and chlorite that define an approximately planar S_m that is uneven at meso- and microscale. The distance between micaceous and chlorite-rich layers ranges from ~1-2 mm. The transitions between micaceous and chlorite-rich layers and quartz-rich layers are gradational. As in the SRA, the micro-fabric of S_m in the Lynchburg Group consists of a schistosity that is also a continuous cleavage. In the Lynchburg Group, S_m comprises ~80% quartz-rich layers and ~20% micaceous and chlorite-rich layers that define an approximately planar S_m that is uneven at microscale. The micaceous and chlorite-rich layers consist of interlocking to isolated subhedral, tabular grains of mica and chlorite. The distance between micaceous and chlorite-rich layers ranges from ~0.05-0.75 mm. The transitions between micaceous and chlorite-rich and quartz-rich layers are gradational.

Figure 22: Grain boundary migration in quartz in the Fork Mountain Formation at Loc06. Embayment of quartz by quartz (red) suggests grain boundary migration. Also evident is seriate grain size distribution of quartz. The main foliation is oriented ~030, 50 (blue). The plane of view is ~210 (right), 40. The field of view is 2.5 mm, subparallel to the intersection lineation ~205 (right), 20. (cross-polarized light)

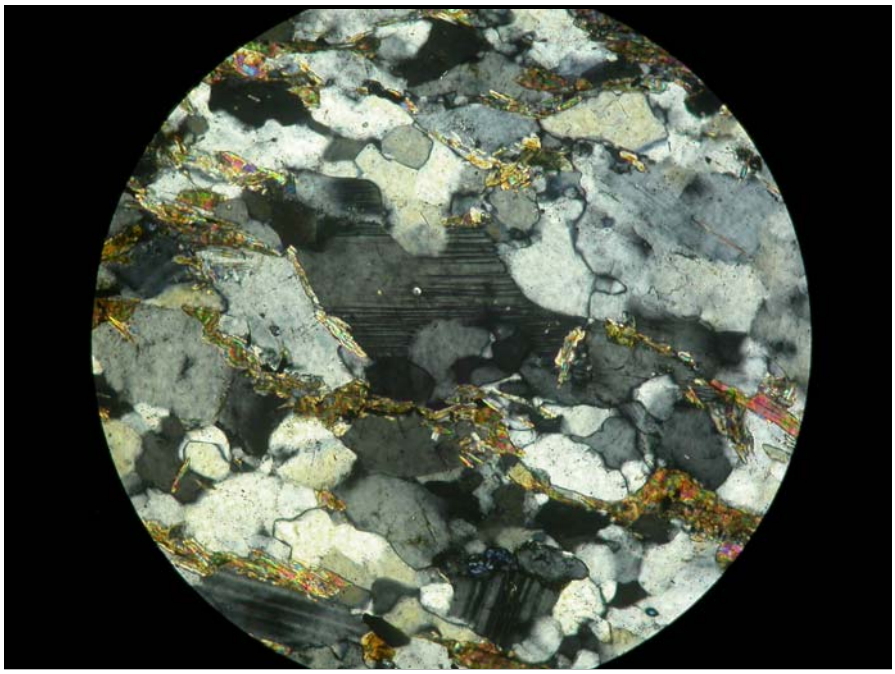

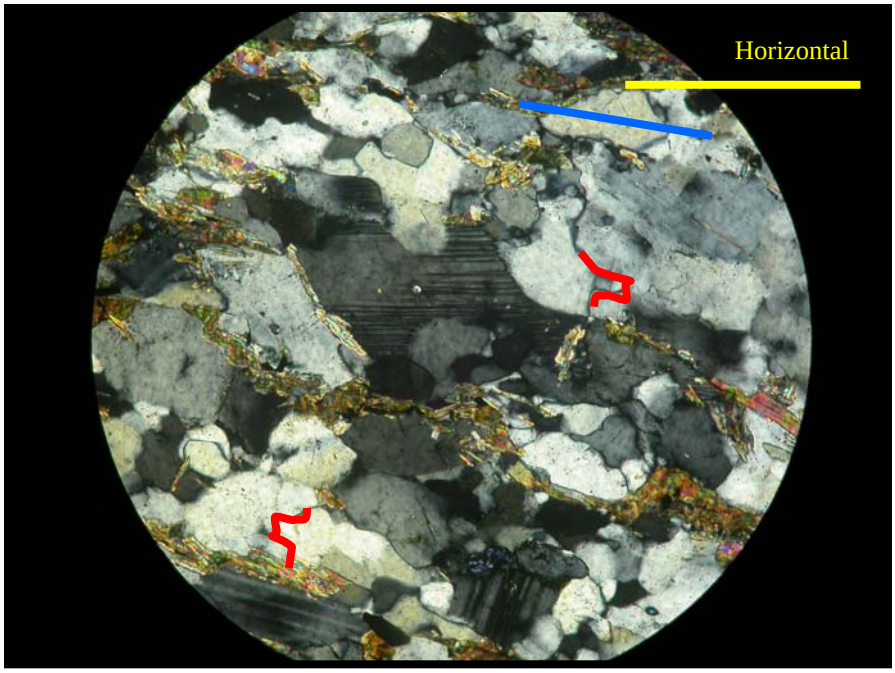
Horizontal

Near the Ridgeway fault, the distance between micaceous and chlorite-rich layers of S_m in the Fork Mountain Formation is reduced to <1 mm and the micaceous and chlorite-rich layers are more smooth and more closely approximate a plane, especially in discrete zones. The transitions between micaceous and chlorite-rich layers and quartz-rich layers are also more discrete than further from the fault. Outcrops of Lynchburg Group rocks were not found in contact with Fork Mountain Formation rocks. Lynchburg Group rocks in close proximity to the Ridgeway fault consist of subunits that are observed only at single outcrops within the study area (*i.e.*, marble and conglomerate). Therefore, comparison between similar Lynchburg Group rocks at contrasting distances from the fault was not possible in the study area.

The Fork Mountain Formation is more micaceous than the Lynchburg Group. Quartz-rich layers in the Lynchburg Group are more intensely foliated than quartz-rich layers in the Fork Mountain Formation. In contrast to the Lynchburg Group, the SRA is porphyroblastic and exhibits evidence of an early relict upper amphibolite facies metamorphic mineral assemblage (M_e). The more pelitic composition and complex metamorphic history of the SRA results in more diverse mineralogy than the Lynchburg Group. This diverse mineralogy introduces differences in fabric due to the differing competencies and habits of the minerals that are only present in the SRA. Otherwise, with respect to similar minerals (*e.g.*, mica, chlorite, and quartz) the SRA and Lynchburg Group exhibit similar micro-fabric (Figures 5 and 7).

The main foliation (S_m) is parallel to the axial surface of the main folds (F_m) that are present in the SRA. F_m hinges are gently to moderately plunging and both F_m hinges and axial surfaces are NNE-trending (Figure 21). F_m are isoclinal and upright to recumbent depending on position on F_l. F_m are rarely observed in the SRA because they are highly attenuated and difficult to recognize; however, five outcrops (Loc04, 05, 08, 09, 10) in the central domain and the southern transect do contain relict F_m in the Fork Mountain and Bassett formations. F_m are also present (Loc04, 05) where they are coaxially folded by F_l, generating Type-3 fold interference (Ramsay, 1967). The trends of F_m hinges are consistently near parallel to each other (Figure 20). S-and-Z parasitic micro-folds of mica are present on either side of F_m axial surfaces (***e.g.,*** Figure 20). The orientation and style of F_m have been described in previous work (***e.g.***, Conley and Henika, 1973; Marr, 1984; Gates, 1987).

Compositional layers are observed only where they lie perpendicular to S_m in F_m hinges. Compositional layers consist of quartz-rich layers (~3-4 mm thick) that appear to alternate with micaceous and chlorite-rich layers. Compositional layers are difficult to recognize because they are sparse and highly transposed into S_m (Figure 7). The prominent main foliation (S_m) is also observed in the Lynchburg Group and is subparallel to bedding (S_0) where S_0 is evident, but F_m folds are not observed in the Lynchburg Group in the study area. However, foliation subparallel to S_0 might indicate isoclinal folding.

Interpretation of the main deformation (D_m)

Evidence for crystal plastic deformation of quartz in both the SRA and Lynchburg Group that has produced small grains of quartz through grain-size reduction suggests that deformation was ductile with respect to quartz; in other words, at a temperature >350^{o} C (*e.g.*, van der Pluijm and Marshak, 1997). The presence of large mineral grains at the upper range of the seriate distribution suggest that these grains experienced less grain-size reduction and are relict with respect to, and thus, predate the main deformation (D_m).

It appears that compositional layering predates the main deformation (D_m), because compositional layering is observed to be deformed by D_m in the SRA. Although difficult to recognize, the compositional layers appear to be schistose and/or gneissic layers of the same composition as the SRA host rock. The relation of compositional layering to the relict, early upper amphibolite facies metamorphism (M_e) is unclear. It is possible that compositional layering represents bedding remnants (S_0). However, M_e also predates D_m and it would be consistent for any layering associated with such high-grade metamorphism to reflect a metamorphic texture and structural fabric. Circumstantial evidence suggests that because the early metamorphic assemblage (M_e), a possible early foliation, and the Early Cambrian monazite age each precede the main deformation they may represent the same Early Cambrian event.

Conley and Henika (1973) and Conley (1985) refer to first-generation isoclinal folds in the Lynchburg Group. Wang (1991) has reported foliation subparallel to primary bedding (S_0)

throughout the Lynchburg Group and also refers to first generation "flow folds" in the Lynchburg Group. The relation of S_m to these reported folds is unclear because they are not observed in the study area. S_m would be parallel to the axial surfaces of these folds if they are the same fold generation as the isoclinal, recumbent folds observed in the SRA in the present study area. Thus, it is possible that no folding associated with the main deformation occurred in the Lynchburg Group in the study area, or that folding also occurred in the Lynchburg Group but has either been unobserved or that any folded layers have been fully transposed into S_m. Alternatively, isoclinal recumbent folding may be a less pervasive mode of deformation in the Lynchburg Group rocks. It would be consistent with the shared nature of the main deformation to have isoclinal folds in both the SRA and the Lynchburg Group.

Observation of the main lineation (L_m)

A main lineation (L_m) trends WNW-ESE (Figure 23) (Loc04, 15, 16, 02, 06, 07, and 13). L_m is more rarely observed than L_i. L_m is observed in three forms that share subparallel orientation and a component of elongation. L_m consists of: 1) a main lineation defined by aligned clusters of mica and chlorite, boudinaged tourmaline and garnet, and elongated, aligned quartz (Figure 23 B), 2) a main lineation defined by elongated quartz-lens boudinage (Figure 23 C), and 3) a maximum elongation direction of a prolate strain ellipse in a Lynchburg Group conglomerate (Figure 23 D). The minerals defining these lineations are consistent with the main metamorphic mineral assemblage (M_m) that defines S_m. These three indications of L_m lie on S_m (Loc04, 15, 07, 16). L_m is oriented perpendicular to the late fold hinges (F_l), and folded by D_l.

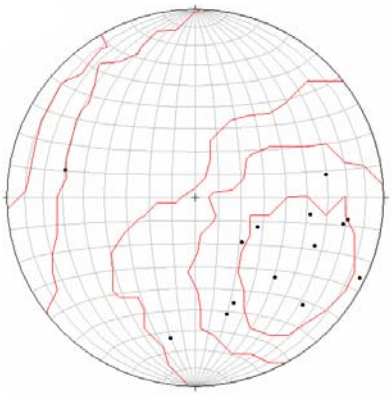

n = 13
Kamb contour interval
(c) = 2 sigma
Rose outer circle = 21%

A-SRA and Lynchburg Group, all types of stretching main lineations

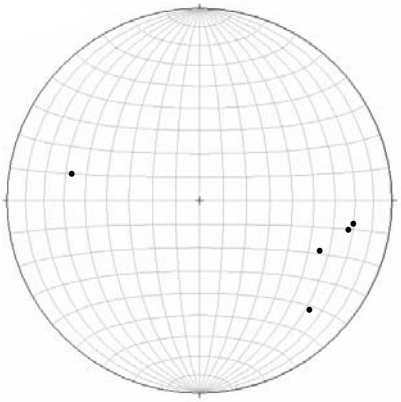

n = 5
Rose outer circle = 20%

B-SRA stretching main mineral lineation

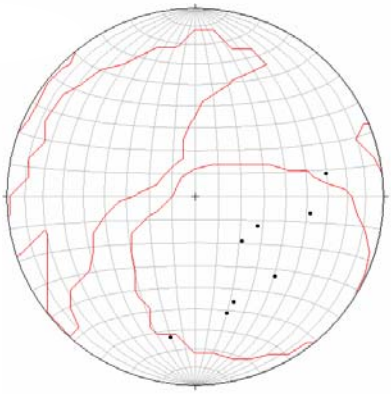

n = 8
c = 2
Rose outer circle = 25%

C-SRA stretching quartz lens boudinage main lineation

Figure 23 A, B, C: Equal area, lower hemisphere, stereoplot of the stretching main lineation in southern transect.

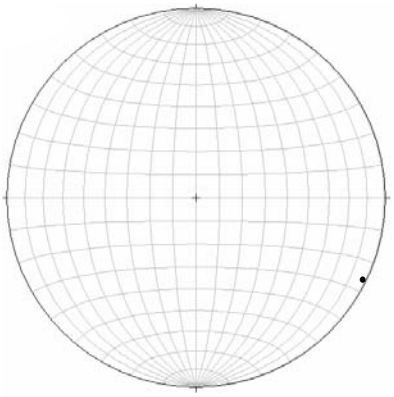

n = 1
Rose outer circle = 100%

D-Stretching main lineation, maximum extension direction of prolate strain ellipse in conglomerate and supporting main lineation in Lynchburg Group

Figure 23 D: Equal area, lower hemisphere, stereoplot of the stretching main lineation in southern transect.

L_m is only observed structurally close to the Ridgeway fault (<0.5 km) and is present in both the SRA and the Lynchburg Group. Boudinaged tourmaline crystals lie parallel to a prominent mineral lineation defined by mica and chlorite in the Fork Mountain Formation (Figure 24). Boudinaged cataclastic garnet lies parallel to L_m (Figure 25). Boudinaged quartz lenses, pervasive outcrop-wide at "The Wall", exhibit deformation by subgrain rotation (Figure 26). These quartz lenses are revealed to be sigma-clasts when viewed in a surface parallel to L_m and perpendicular to S_m (Figure 27).

The maximum elongation direction of a prolate strain ellipse parallel to L_m is revealed by R_f-Φ strain analysis performed on deformed quartz clasts in one conglomerate sample (*e.g.*, Ramsay and Huber, 1983; Lisle, 1985). The conglomerate sample is mapped as Lynchburg Group (Marr, 1984; Henika, 2002, pers. com. 2005) and is located on a late fold limb in close proximity to the Ridgeway fault (Loc16). The orientation of the main foliation (S_m) at Loc16 is 110, 30. The sample location was chosen because it is the only conglomerate in the study area (Loc16, Figure 3) and the constituent clasts form convenient strain markers.

The objective of the analysis is to determine the orientation of the maximum principal axis of strain of the finite strain ellipsoid (X), the strain shape (K), and the strain intensity (D). Principal axes of strain are designated as: X-direction, parallel to the maximum extension direction; Y-direction, the intermediate stretch axis; and Z-direction, the minimum axis of stretch. Principal planes of finite strain are designated as: XY, XZ, and YZ. The ellipticity and orientations were measured for ~40 quartz clasts in the XY and XZ principal planes of the sample. The ratio of X:Y (Rs_{XY}) and of X:Z (Rs_{XZ}) are found by statistical methods

Figure 24: Stretching main lineation as exhibited by tourmaline boudinage (in white ellipse) along the main foliation in the Fork Mountain Formation at Loc15. The main foliation is oriented ~025, 22 (blue). The plane of view is ~280 (right), 65, nearly parallel to the stretching lineation ~098 (left), 20. (flatbed scan of thin-section)

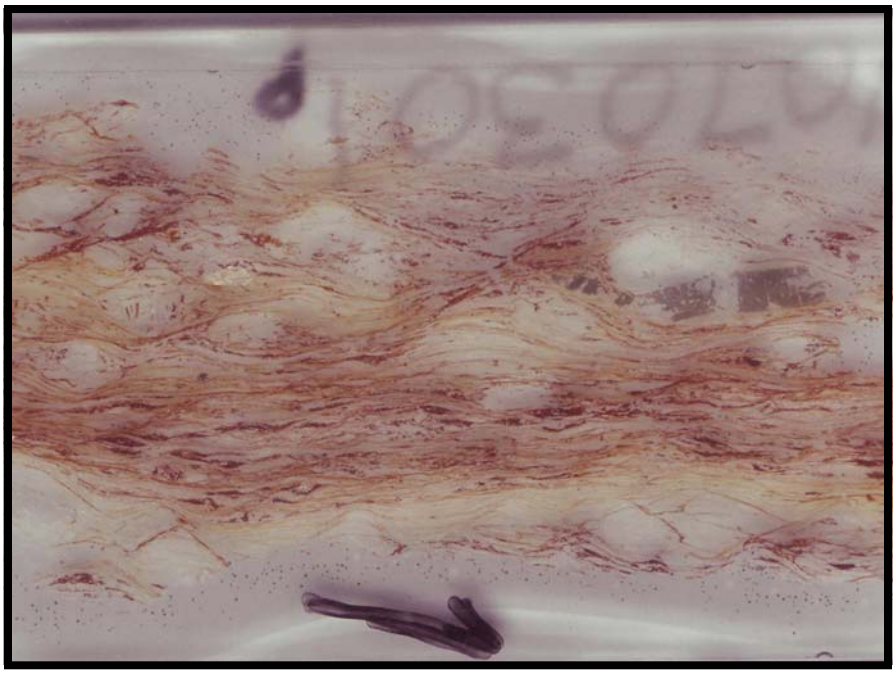

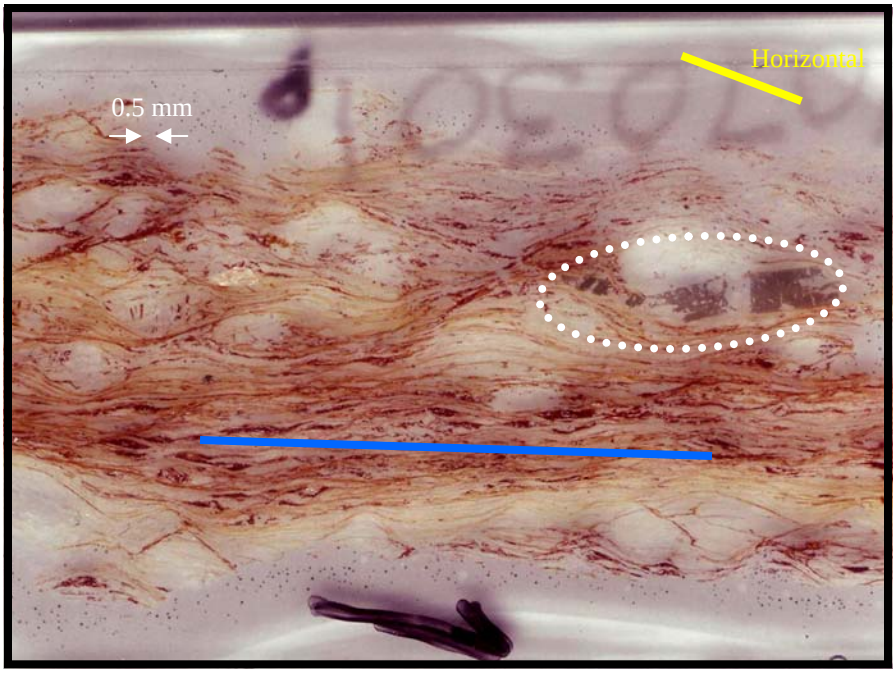
Horizontal
0.5 mm

Figure 25: Cataclastic garnet in fine-grained matrix in Fork Mountain Formation mylonite. The main foliation is oriented ~035, 32 (blue). Cataclastic garnet boudinage is oriented subparallel to the WNW-trending stretching main lineation (in white ellipse). The intersection lineation (S_l*S_m) is oriented ~188 (into page), 34. The plane of view is 293 (right), 87. The field of view is 10 mm. (plane polarized light)

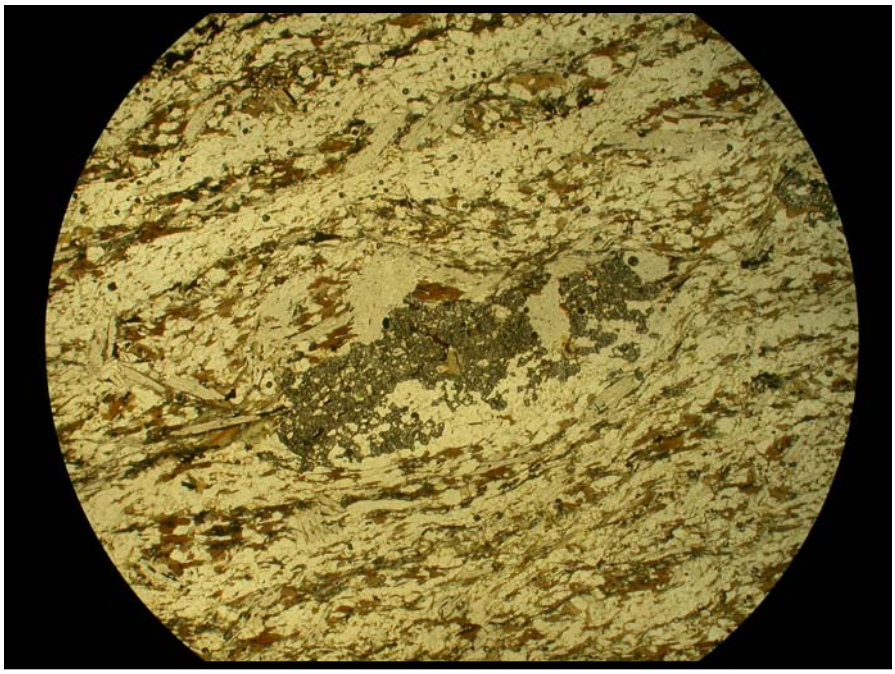

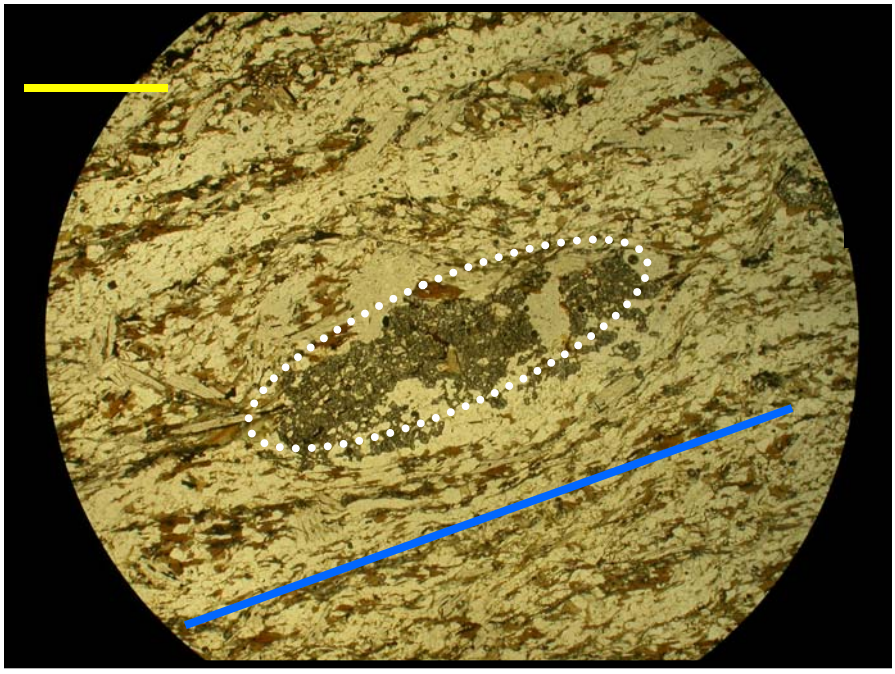

Figure 26: Mortar texture indicating subgrain rotation in quartz lens in the Fork Mountain Formation at Loc07 (in red ellipse). The main foliation is oriented ~035, 45 (blue). The intersection lineation is oriented ~204 (out of page), 18. The plane of view is ~133 (right), 65. The field of view is 10 mm. (cross-polarized light)

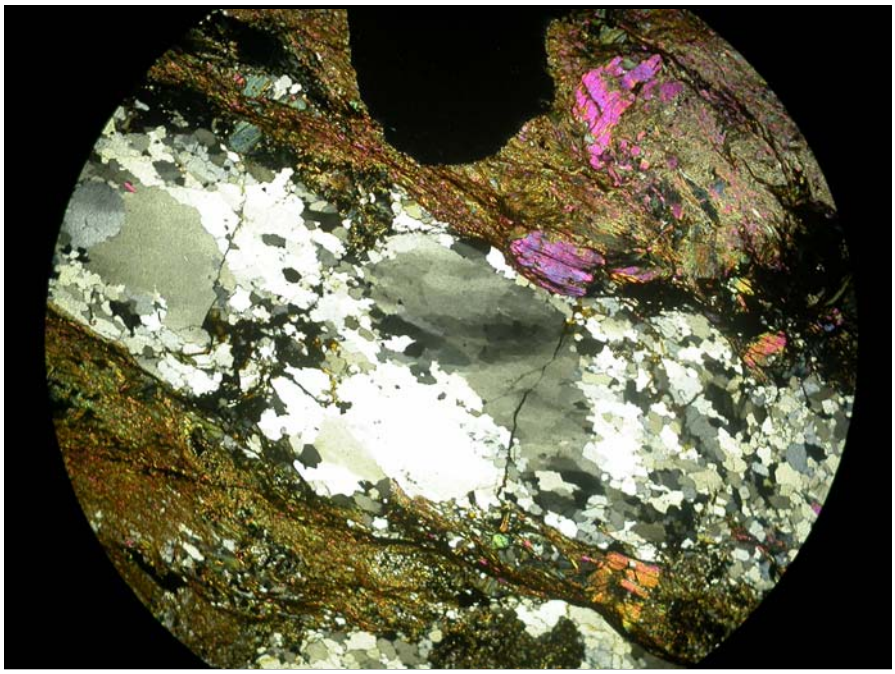

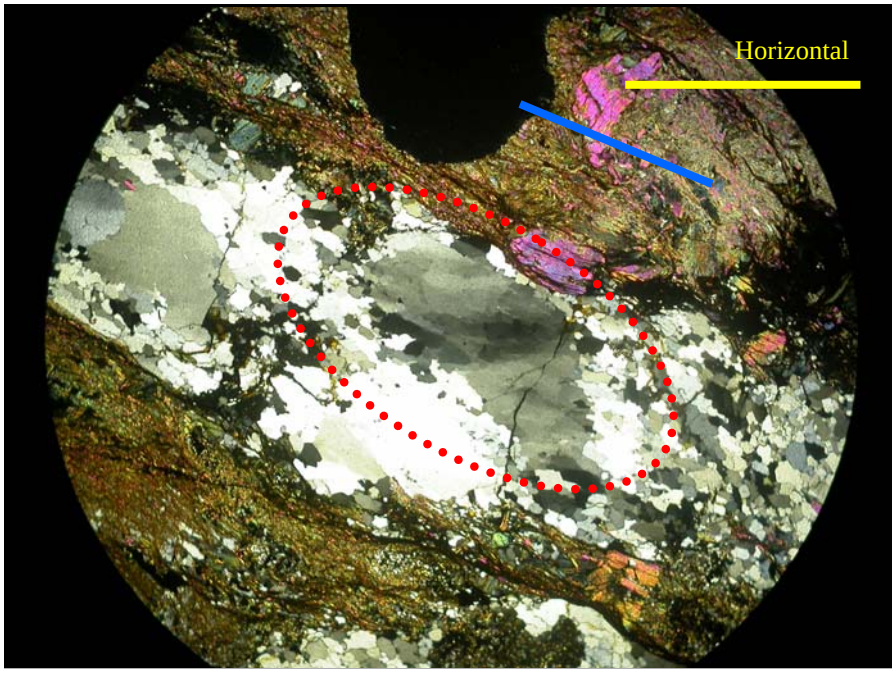
Horizontal

Figure 27: Top-(SRA)-to-WNW shear sense exhibited by sigma-clasts of quartz lenses in the Fork Mountain Formation at Loc07 (red). WNW toward left. The main foliation is oriented ~035, 45 (blue). The main stretching lineation is oriented ~160 (right), 40. The intersection lineation is oriented ~204 (out of page), 18. The plane of view is ~133 (right), 65 nearly parallel to the main lineation.

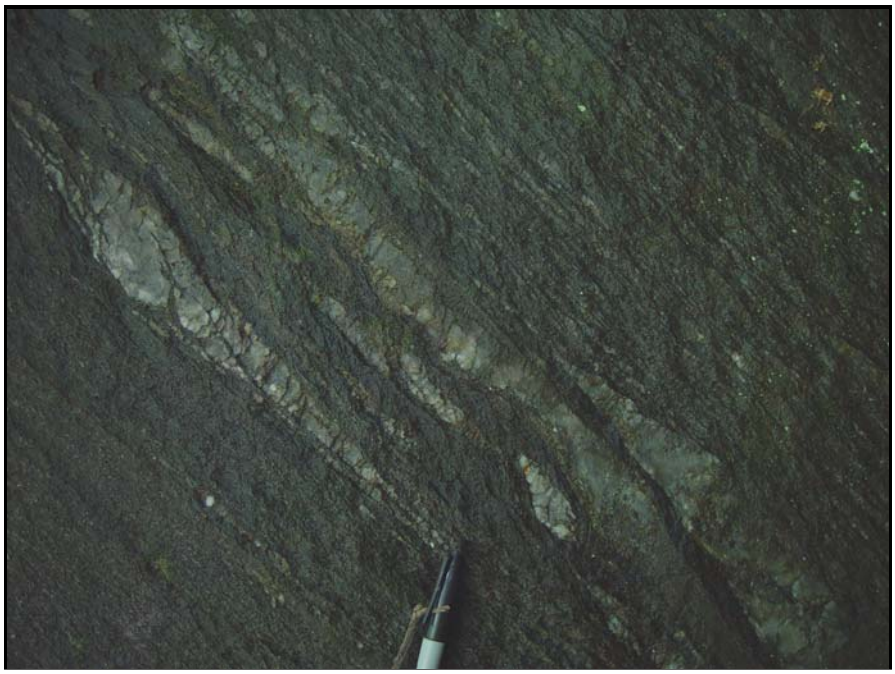

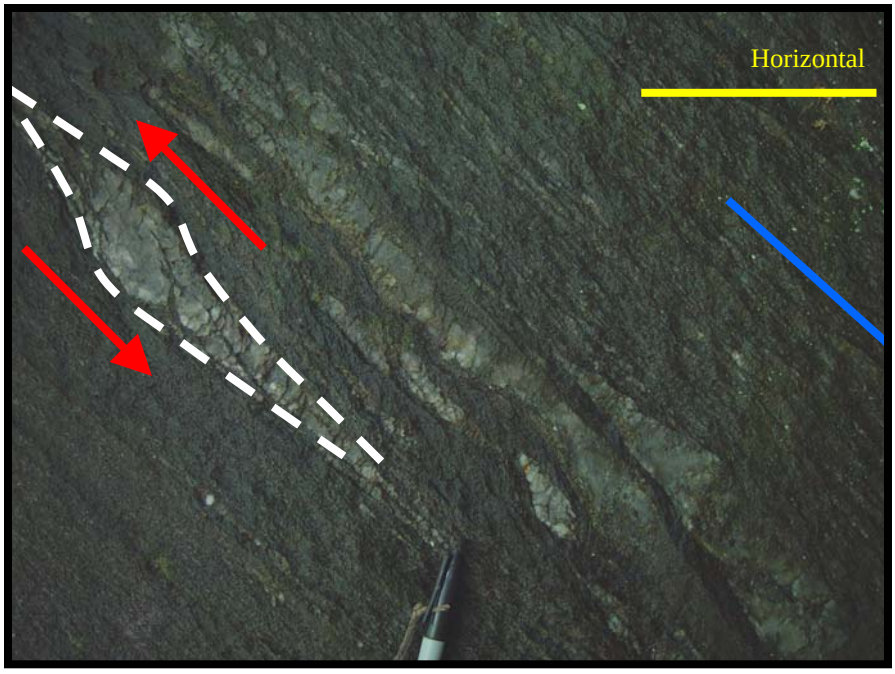
Horizontal

(*e.g.*, Ramsay and Huber, 1983; Lisle, 1985), while the ratio of Y:Z (Rs_{YZ}) is determined by calculation. This analysis assumes that long axes of quartz clasts are initially randomly oriented throughout a sample, and that rocks are homogeneously deformed (*i.e.*, there is no contrast in competencies between clasts and matrix). R_f-Φ strain analysis reveals that the maximum extension direction (X-axis) of the strain ellipse is ESE-trending (~116 degrees with subhorizontal plunge). The resulting data are: $Rs_{XY} = 1.9$; $Rs_{XZ} = 2.8$; $Rs_{YZ} = 1.5$, $K = Ln[(X:Y)/(Y:Z)] = 1.56$. The resulting ellipsoid is apparently slightly prolate, however, the position of plotted data in the prolate rather than oblate field is also dependent on volume change which is unknown in this case (Figure 28). The moderate value of Rs_{XZ} suggests that this rock has not been intensely attenuated or strained (strain intensity $(D) = \{[Ln (X/Y)]^2 + [Ln (Y/Z)]^2\}^{0.5} = 0.76$). The symmetry of the distribution of the data are $I\text{-}sym_{XY} = 0.74$, $I\text{-}sym_{YX} = 0.87$. These relatively high I-sym values appear to confirm the lack of an initial preferred orientation (Ramsay, 1967), which implies that the Lynchburg Group clasts were initially randomly oriented, thus likely not deformed previous to the deformations responsible for the strain ellipse. One analytical result is insufficient to characterize regional strain; however, the orientation of the maximum extension direction of the finite strain ellipsoid is consistent with other observations of L_m. Furthermore, the suggestion that only moderate strain occurred at Loc16, near the Ridgeway fault, implies that high strain is limited to even closer proximity to the Ridgeway fault. However, it is possible that L_m may have been more pronounced before the accumulation of flattening strain from subsequent deformations.

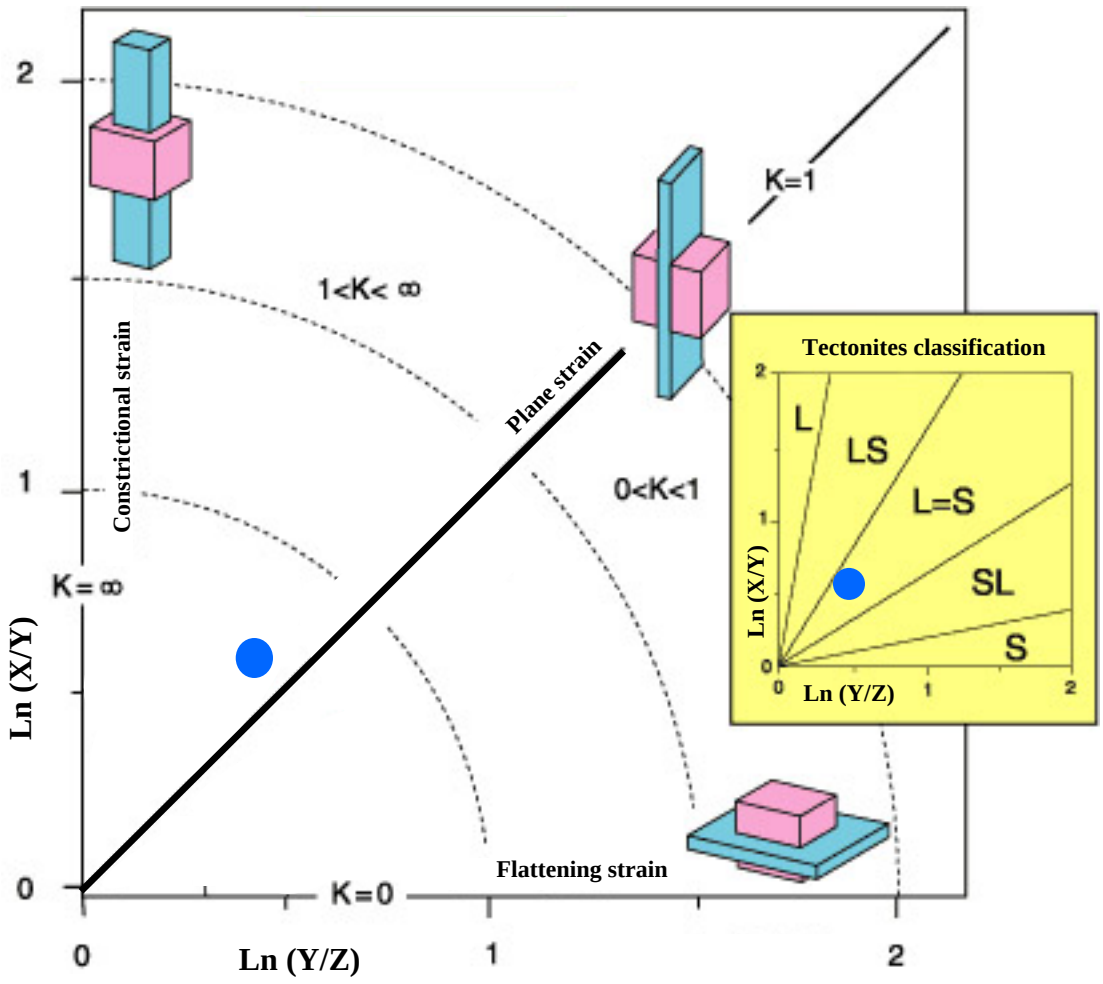

● Ln (X/Y) = Ln 1.9 = 0.64 and Ln (Y/Z) = Ln 1.5 = 0.41

K = 1.56 = Ln (X/Y)/(Y/Z) = Strain shape

D = 0.76 = $\{[\text{Ln } (X/Y)]^2 + [\text{Ln } (Y/Z)]^2\}^{0.5}$ = Strain intensity

Figure 28: Flinn diagram with data plotted from strain analysis of conglomerate at Loc16. (Figure after Flinn, 1962 modified by Ramsay, 1967, after University of Sydney, School of Geosciences, 2006)

Interpretation of the main lineation (L_m)

L_m is interpreted to indicate stretching because of boudinaged tourmaline, garnet, and quartz lenses, as well as the strain ellipse. L_m predates the late deformation (D_l) because it is folded by F_l. L_m lies only on S_m, suggesting that it is related to Dm. Observations of top-(SRA)-to-WNW shear sense parallel to L_m are consistent with shear sense in other regions of the SRA (Allen, pers. com. 2005; Carter, 2006). L_m is interpreted to be a stretching lineation associated with tectonic transport during the main deformation.

Early deformation (D_e)

Observation of the early deformation (D_e)

Compositional layers in SRA rocks comprise alternating micaceous and quartz-rich layers that are folded by F_m as observed at meso- and microscale. Compositional layers are most easily discernible from S_m where they lie perpendicular to S_m in main fold (F_m) hinges. The mineral assemblage that defines the layers is difficult to identify with confidence, however, it appears to include biotite, muscovite, and quartz. Micas are dominantly transposed into S_m even where compositional layers wrap around F_m hinges. These micas are tightly folded, locally kinked, and generally do not cross the plane of S_m. Sericitized sillimanite mats generally lie parallel to S_m (*e.g.*, Figure 29) rather than fold around F_m fold hinges.

Some grains of mica that are isolated in the matrix of SRA rocks and located away from identifiable folded compositional layers are oriented with their long dimensions and/or

Figure 29: Main foliation with parallel sillimanite mats and early foliation as exhibited by inclusion trails in garnet in the Fork Mountain Formation at Loc11. Inclusion trails in garnet (S_i) are oriented (~206, 42) (green) as determined graphically from the apparent dip in orthogonal thin-sections. The main foliation is oriented ~075, 42 (blue) and includes transposed sericitized sillimanite mats (in white ellipse). The plane of view is ~195 (right), 75. The field of view is 2.5 mm, subparallel to the intersection lineation ~205 (right), 35. (cross-polarized light)

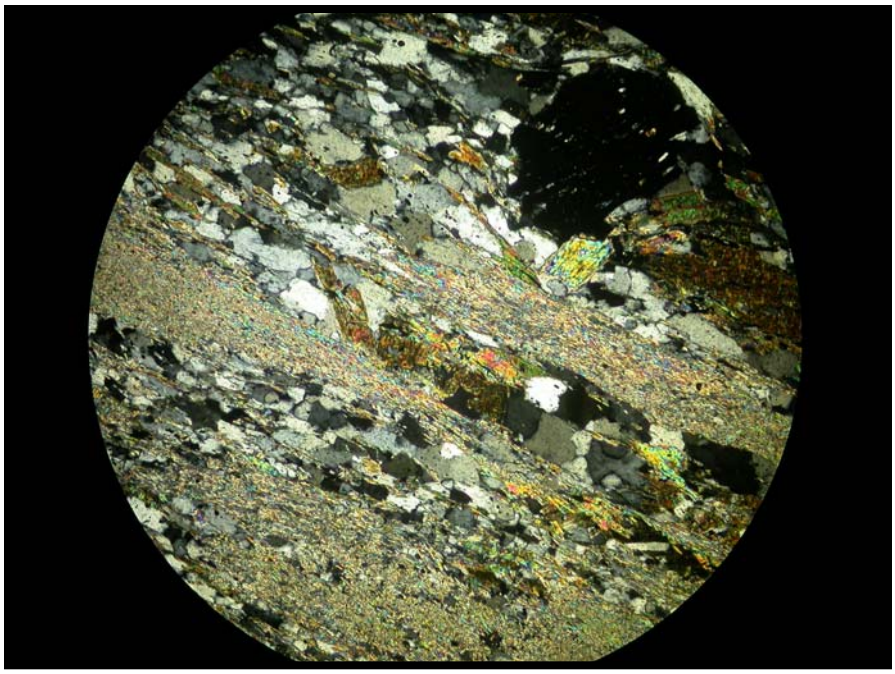

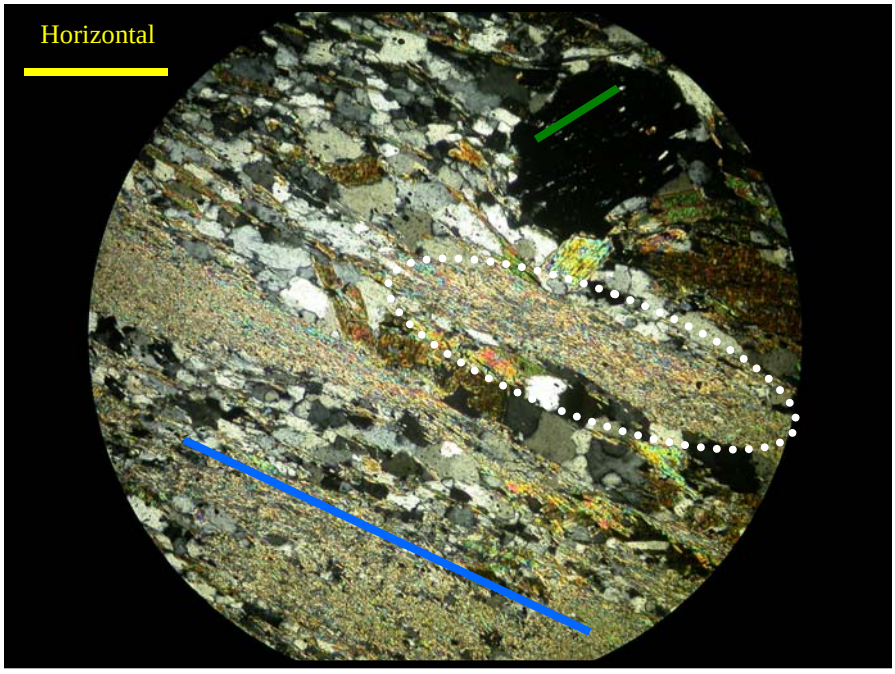
Horizontal

basal cleavage oblique to S_m (Figure 30 A). Some of these grains of mica are poikiloblastic and have poorly defined, ragged edges. These grains of mica are difficult to attribute to a particular generation because they are not aligned with S_m or associated with folded compositional layers that predate D_m. These isolated relict grains of mica, oblique to S_m, may predate D_m if they are overprinted by S_m. However, if overprinting relationships are unclear, it may not be possible to distinguish them from the moderately penetrative late foliation (S_l) or from pseudomorphs of preceding minerals. Isolated grains of mica that are overprinted by the S_m may represent differing degrees of transposition into S_m of compositional layering that is folded by F_m (Howard, 2001). Thus, some isolated, overprinted grains of mica may also represent a relict, early foliation (S_e) that predates D_m.

Inclusion trails (S_i) are present in garnet in the schist of the Fork Mountain Formation. S_i appear to consist predominantly of biotite and elongate quartz, however, petrographic assessment is limited by the small grain size (<0.01 mm). Orientations of S_i are mapped across the central domain in the Fork Mountain Formation. Inclusion trails are consistently nearly coplanar within outcrops, subdomains, and across the central domain (*i.e.*, non-sigmoidal, non-random, and nearly parallel to each other) (Figures 29 and 30). The orientation of the plane of S_i at central subdomains is reconstructed geometrically by plotting the apparent, two-dimensional orientations recorded in orthogonally oriented thin-sections onto stereonets (Figure 30). The orientations of S_i across the central domain define NNE-trending planes that lie at a high angle to S_m (Figures 30 and 4). Containment within garnet distinguishes S_i planes from the nearly parallel S_l, which lies parallel to the axial

Figure 30 A: Inclusion trails in garnets (S_i) – Possible relict mica of early foliation (fuchsia) oblique to and overprinted by the main foliation (S_m) (blue) in the Fork Mountain Formation at Loc09. The main foliation is 015, 05 (blue). The early foliation (fuchsia) is oblique to S_m and subparallel to inclusion trails in the core of garnet (green). Garnet has strain caps and shadows. The plane of view is ~036 (right), subvertical. (width of field of view ~5.0 mm), subparallel to the intersection lineation ~025 (right), 01. (cross-polarized light)

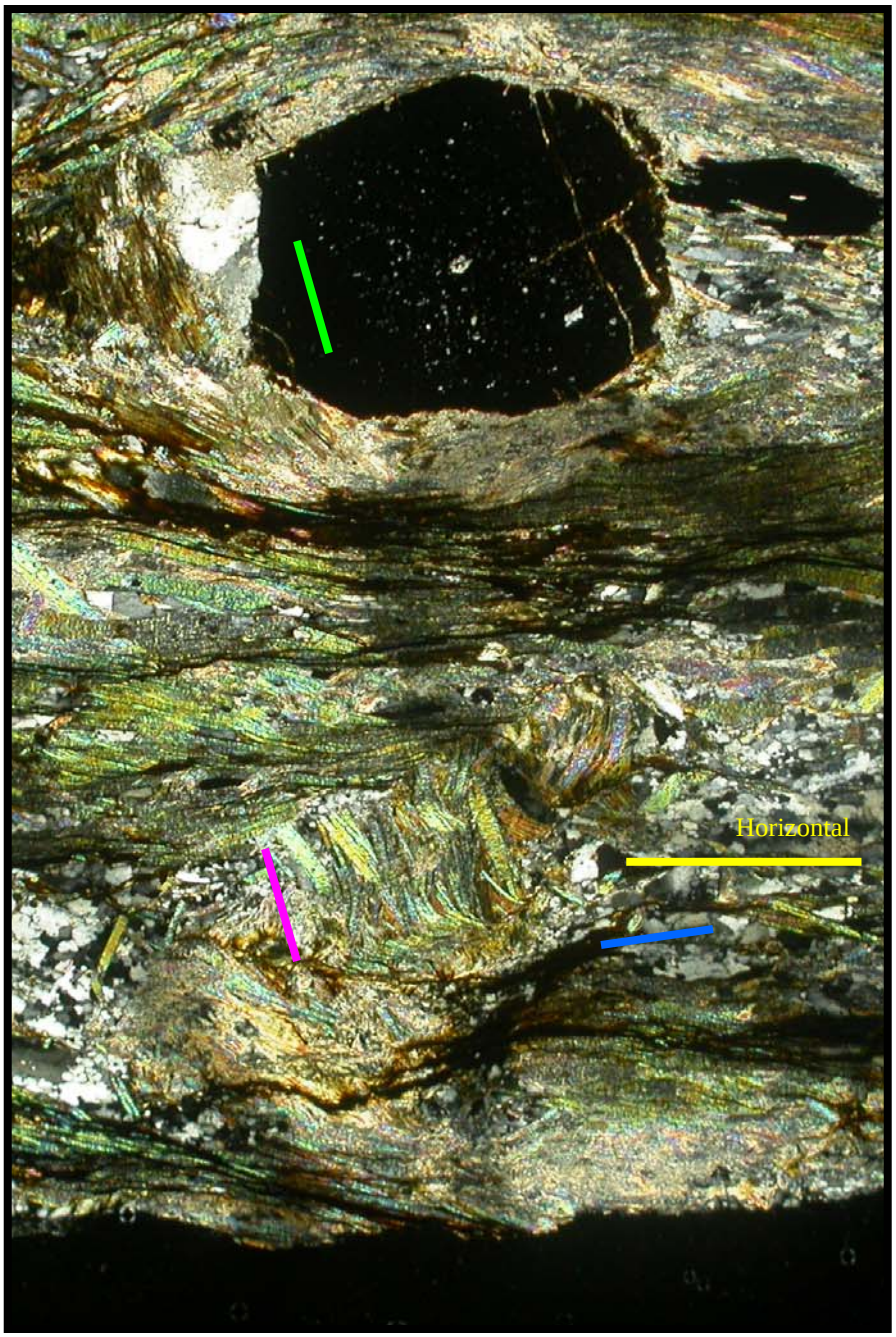
Horizontal

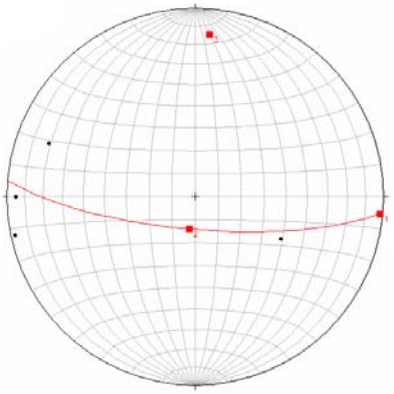

n = 4
Pole to best-fit great circle
(a) = 005, 14

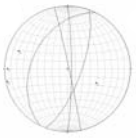

B-S_i current orientation

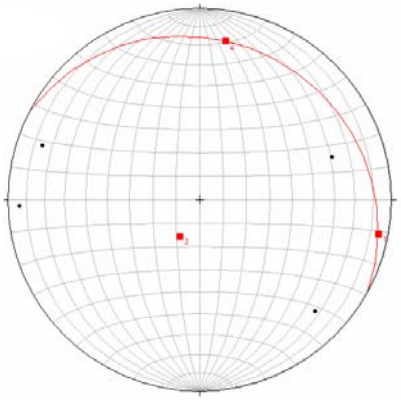

n = 4
a = 009, 17

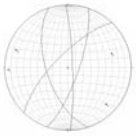

C-S_i orientation altered as the main foliation (S_m) is geometrically restored to the horizontal presumed to predate D_m

Figure 30 B, C: Inclusion trails in garnets (Si) - Equal area, lower hemisphere, stereoplot of poles to planes of the early foliation (S_e) as defined by inclusion trails (S_i) in multiple garnets at each location represented by the four data points (above) in the central domain (SRA).

surfaces of late generation folds (F_l). Many garnets that contain S_i have strain caps and strain shadows constructed of S_m grains of mica. In rocks proximal to the Ridgeway fault, garnet grains show evidence of cataclastic fragmentation and redistribution (Figure 25). Thus, in fault proximity, the planes upon which S_i lie are either obliterated or are inconsistent with those of other S_i.

Some rims of garnets are partially embedded with sigmoidal grains of quartz and mica that extend from the rim of the garnet out into the rock matrix (Figure 31). These inclusions integrate with S_m in the matrix and appear to represent a continuum between the rim of the garnet and the matrix. Thus, the garnet rims appear to record progressively transposed orientations of the inclusions as simultaneously engulfment by garnet.

Interpretation of the early deformation (D_e)

It is difficult to be confident that biotite is present in compositional layering because biotite appears to be compatible with both main and early metamorphism and overprinting relationships are difficult to establish. However, the definition of compositional layering, in part, by biotite suggests attainment of at least greenschist facies metamorphism by the event responsible for the layering. This compositional layering may represent bedding remnants (S_0). However, these compositional layers may instead represent a relict, early foliation (S_e) (*i.e.*, schistose or gneissic layering) that predates D_m.

Sericitized sillimanite mats appear to be sufficiently mobile to adjust relatively easily to new, even weak, foliations. It is therefore consistent with the ease of mobility that a record

Figure 31: Partial transposition into the main foliation of a sigmoidal grain of biotite in a rim of a garnet in the Fork Mountain Formation at Loc11 (in green square). The main foliation is oriented ~075, 42 (blue). The early foliation is oriented ~206, 42 (green line) as preserved by inclusion trails in garnet. The plane of view is 195 (right), 75. The field of view is 2.5 mm subparallel to the intersection lineation, which is oriented ~205 (right), 35. (plane polarized light)

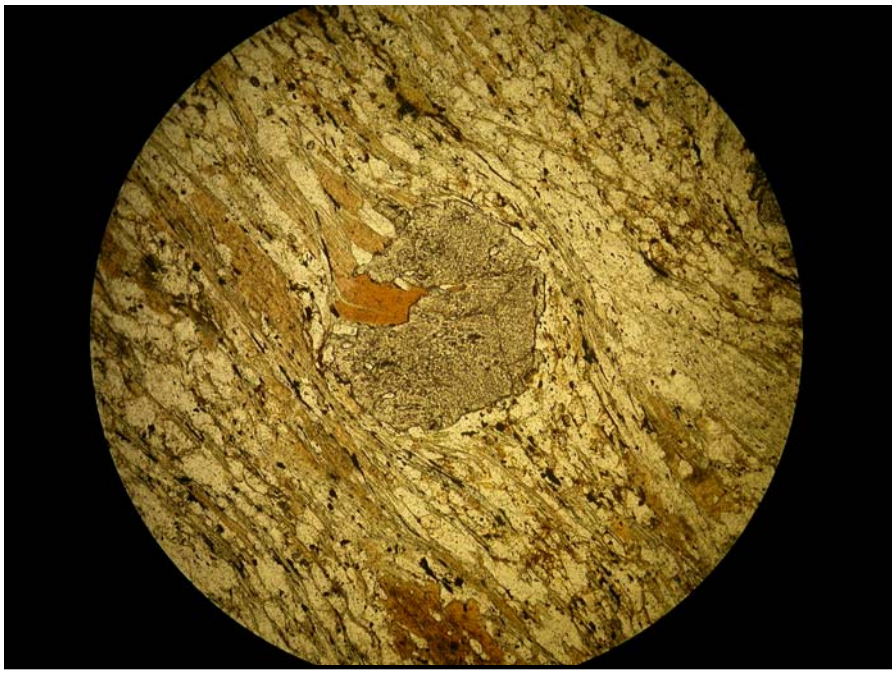

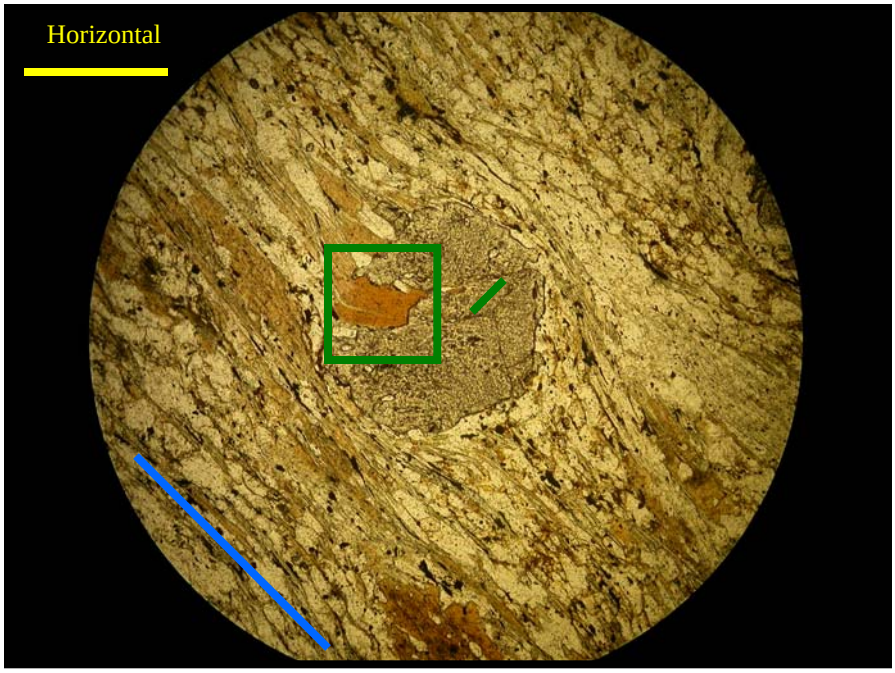
Horizontal

of S_e is not preserved by sericitized sillimanite mats. It is possible that compositional layering may be coincident with early upper amphibolite metamorphism (M_e) because M_e also predates S_m (Conley and Henika, 1973). This circumstantial evidence suggests that they could represent the same generation of early deformation (D_e).

The growth of the rims of garnets in the SRA is likely coeval with S_m because they engulf transitional orientations of S_m as S_m developed. Thus, the growth of the rims of garnets appears to be linked to main metamorphic (M_m) conditions, which differ in the SRA and the Lynchburg Group. Emplacement of the SRA along the Ridgeway fault is strongly suggested to post-date peak main metamorphism (M_m) because the Ridgeway fault emplaced higher-grade SRA rocks onto lower-grade Lynchburg Group metamorphic rocks. Yet, because the S_m orientation is consistent on each side of the Ridgeway fault, it appears that emplacement took advantage of the S_m schistosity.

D_m also appears to post-date the growth of the cores of garnets and to be synkinematic with the growth of garnet rims (*e.g.*, Yardley, 1989; Barker, 1998) because S_m defines strain caps and strain shadows and S_m is incorporated into the rims of garnets. Inclusion trails (S_i) in the cores of garnets in the Fork Mountain Formation appear to preserve an early tectonothermal foliation (S_e) that predates the main foliation (S_m) and likely represents an initial phase of a moderate- to high-grade metamorphic assemblage (M_e) in the SRA that precedes D_m and Ridgeway fault activity (*e.g.*, Bell, 1985; Yardley, 1989; Johnson and Vernon, 1995; Barker, 1998; Johnson, 1999a; Johnson, 1999b).

If each instance of compositional layering were interpreted as an early foliation (S_e), then S_e would be represented at mesoscale by compositional layering in main fold hinges and as isolated relict grains of mica in the matrix. S_e would also be represented at microscale by inclusion trails in the cores of garnets and perhaps by the inclusions in the rims of garnets that record transitional orientations. This relict fabric may represent an early tectonothermal event (D_e) that resulted in an early foliation (S_e) exclusive to the SRA.

The Ridgeway fault

Introduction

The SRA is bounded by the Ridgeway fault except on the SE and SW sides where it is cut by younger faults (Conley and Henika, 1973; Gates, 1987). The Ridgeway fault emplaces higher-grade metamorphic rocks of the SRA onto lower-grade metamorphic rocks of the Lynchburg Group. The Ridgeway fault is unexposed in the field area, but it is considered to be a fault because it juxtaposes rocks of differing types, with differing structural, metamorphic, and plutonic histories. Deformation in close proximity to the Ridgeway fault is characterized in detail at the large outcrop near the fault referred to as “The Wall” (Figure 4, inset) and at outcrops north of “The Wall” in the vicinities of Myers Creek (Loc11) and Rorer Creek (Loc12 and 17).

Observation of boudinage and shear sense

Quartz lenses are present in the medium-grained schist of the Fork Mountain Formation in close proximity to the Ridgeway fault. Quartz lenses range in dimension from microns to

decimeters. Some quartz lenses retain evidence of subgrain rotation (mortar texture) (Figure 26). Other quartz lenses are equant-grained with triple-point grain boundary junctions indicating static recrystallization. Commonly, quartz lenses exhibit elongate chocolate-tablet boudinage (Figure 32) with long and short chocolate-tablet axes that are suborthogonal. The orientations of long and short boudin axes are consistent across the large "Wall" outcrop (Figures 23 C and 4, inset). The short boudin axis is WNW-trending, parallel to the main stretching lineation (L_m) (Figures 23 C and 4, inset). The long axis is NNE-trending, parallel to the intersection lineation (L_i) (Figure 4, inset).

The quartz boudins also exhibit sigma asymmetries in WNW-ESE profile (Figure 27) that exhibit a top-(SRA)-to-the-WNW shear sense, subparallel to L_m (*e.g.*, Passchier and Trouw, 1996). Because L_m is folded by D_l it is presumed to result from D_m. In general, S-and-C fabric can not be confidently identified on the plane perpendicular to S_m and parallel to L_i. Evidence for strike-slip movement along the Ridgeway fault is not observed in the study area.

Interpretation of boudinage and shear sense

Chocolate-tablet quartz boudins suggest flattening, while shear sense exhibited on the WNW-ESE vertical plane suggests tectonic transport of the SRA toward the WNW during its emplacement onto the Lynchburg Group during D_m.

Figure 32: Chocolate-tablet quartz lens boudinage in the Fork Mountain Formation at Loc02. Intersection lineation (*i.e.*, the long dimension of chocolate-tablet boudinage) is oriented ~211, 17 (fuchsia). The quartz lens boudinage stretching main lineation is oriented ~098, 38 (orange). The plane of view is ~030 (left), 50 parallel to the main foliation.

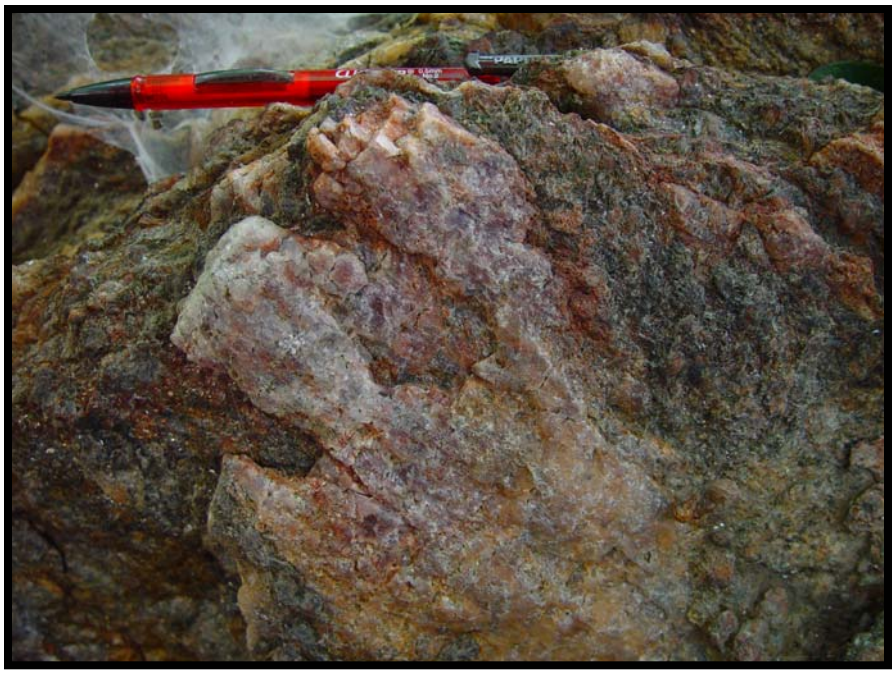

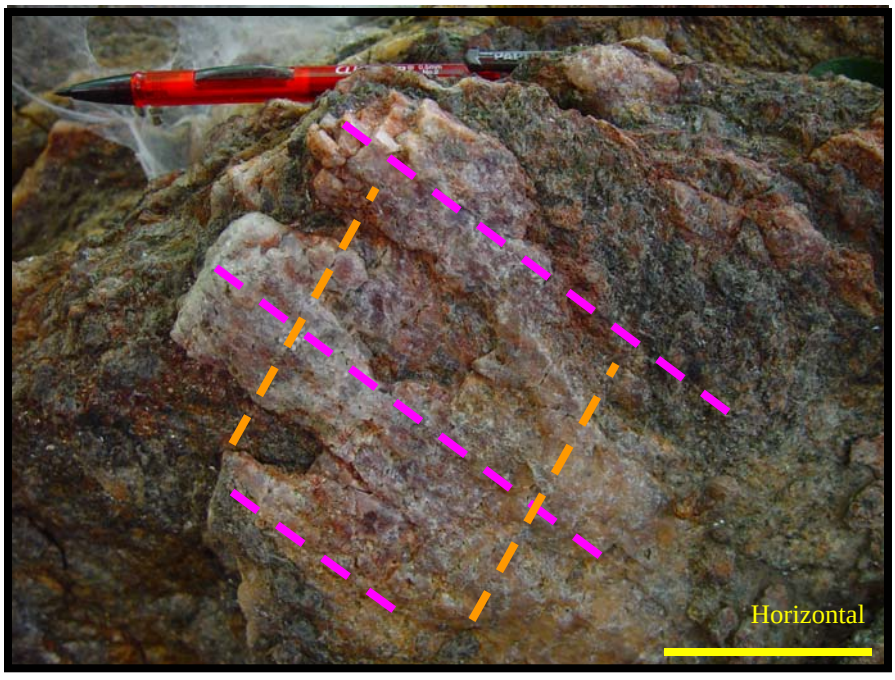
Horizontal

Observation of strain gradient and quartz influx

In close proximity to the Ridgeway fault, the Fork Mountain Formation exhibits grain size and quartz content similar to that observed in the Lynchburg Group, making it difficult to distinguish at mesoscale between the two rock types, particularly because there is little difference between the AFM projections (Thompson, 1957) of the schists of the Fork Mountain Formation and the Lynchburg Group within the study area. Distinction between Fork Mountain Formation and Lynchburg Group rocks is based on evidence for the upper amphibolite metamorphic assemblage, which is unobserved in the Lynchburg Group within the study area. The presence of fine-grained schists of the Fork Mountain Formation near the fault may reflect original stratigraphy in the otherwise lithodemic SRA. Alternatively, these rocks may indicate a gradient of grain-size reduction and quartz influx associated with Ridgeway fault activity.

Coarser grains of quartz are commonly present among finer grains of quartz as constituents of a seriate distribution of grain size in the schists of the Fork Mountain Formation (*e.g.*, Figure 22). These coarser grains of quartz commonly exhibit undulose extinction, which may represent the crystalline strain that induced the crystal plastic deformation. The presence of these coarser grains suggests that before Ridgeway fault activity, the fine-grained schists of the Fork Mountain Formation could have had the typical, general grain size observed throughout the rest of the formation. These coarse grains may be relict from the Fork Mountain Formation, which is generally coarser-grained than the Lynchburg

Group. The Fork Mountain Formation may have been subjected to grain-size reduction near the Ridgeway fault.

In the central domain (C-C'), quartz content of the Fork Mountain Formation increases gradually from ~10 to 70% (petrographically estimated) with increasing proximity to the Ridgeway fault trace (Figures 33 A and B, 3, and 4, inset). The ~60-70% quartz content of the finest-grained Fork Mountain Formation rocks near the Ridgeway fault at "The Wall" (Figure 25) is similar to the quartz content observed in the Lynchburg Group (Figure 33 B).

Petrographic estimates of quartz content are supported by whole rock geochemistry from Fork Mountain Formation samples in and near the study area (Carter, pers. com. 2006). These whole rock geochemistry data reflect Fork Mountain Formation quartz content ranging from ~45 (distant from the Ridgeway fault) to ~70% (near the Ridgeway fault).

The mean grain size and the distance between micaceous and chlorite-rich layers in the Fork Mountain Formation decrease gradually with increasing proximity to the Ridgeway fault across the central domain (Figures 33, 3, and 4, inset). The grain size of mica and chlorite in the Fork Mountain Formation decreases from ~1.26 to ~0.14 mm with increasing proximity to the Ridgeway fault (Figures 33 A, C, and D). The mean grain size of quartz in the matrix of the Fork Mountain Formation decreases from ~0.36 mm distant from the Ridgeway fault to ~0.036 mm closer to the fault. The distance between mica and chlorite-rich layers decreases from ~2.0 mm distant from the fault to ~0.7 mm nearer to the fault (Figures 33 A and B). Micaceous and chlorite-rich layers that are uneven at meso- and

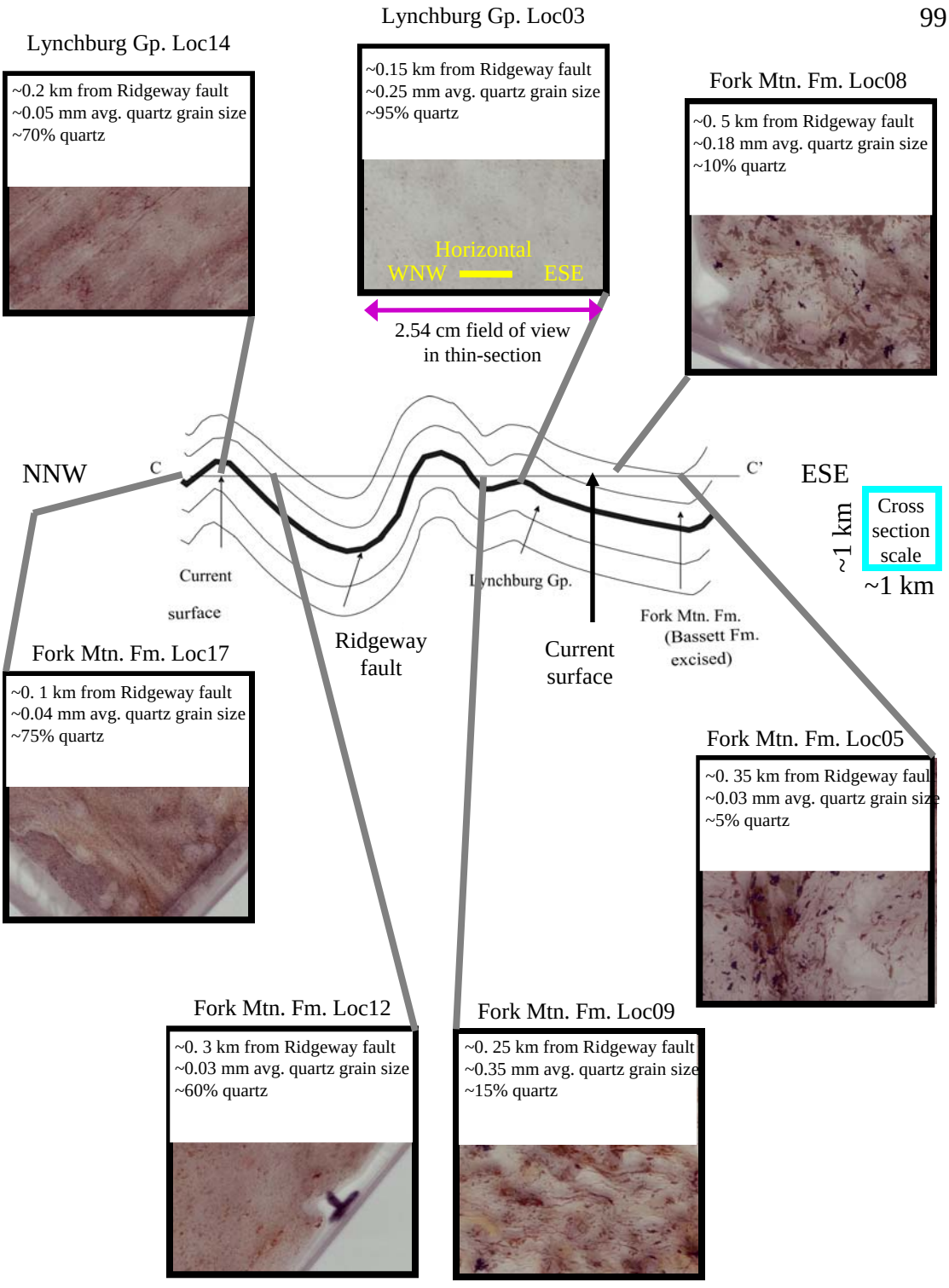

Figure 33 A: Gradient of quartz content, micro-fabric and grain size in central domain (Images are flatbed scans of thin-sections oriented on the page NNW (left)-ESE (right).)

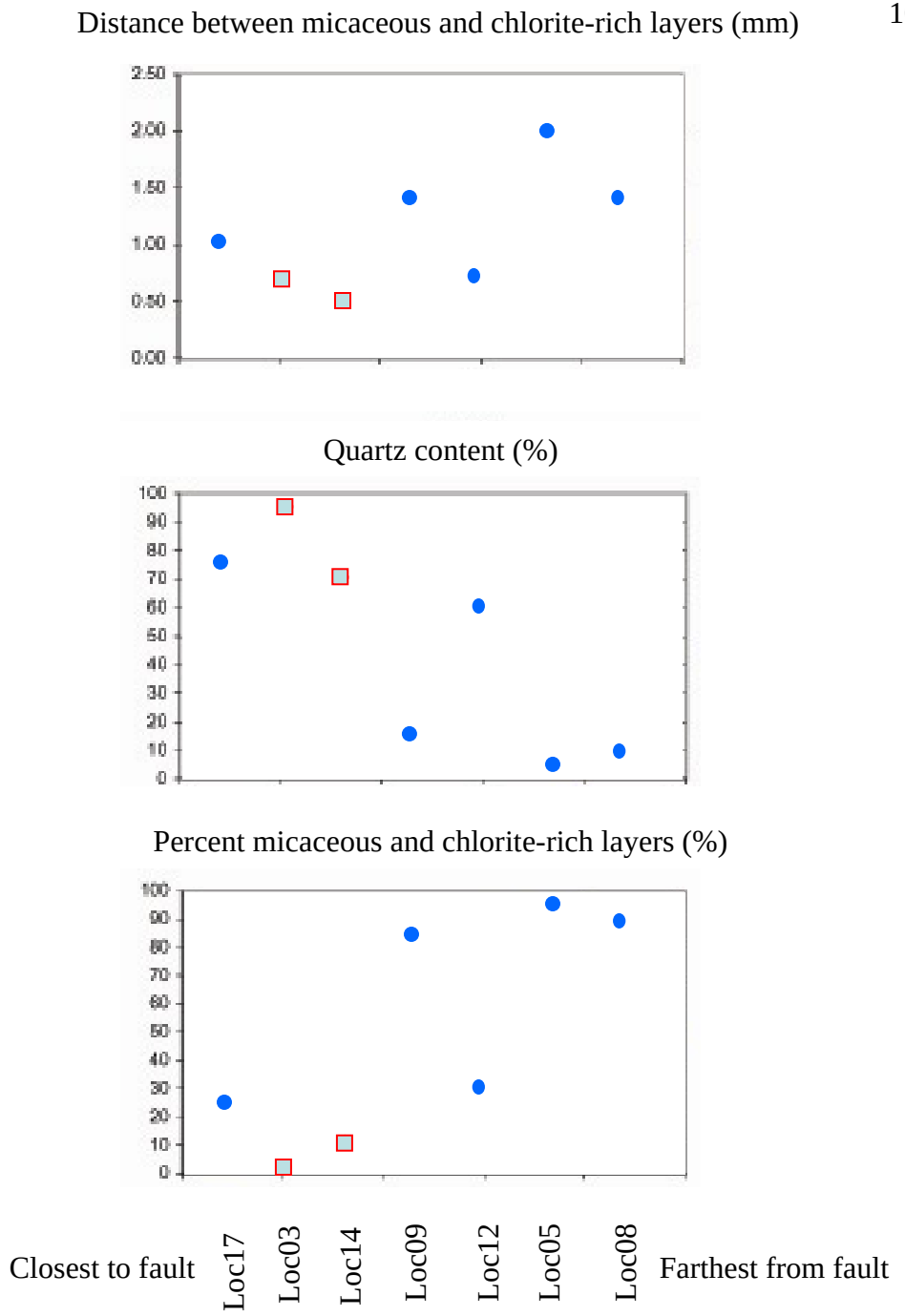

Figure 33 B: Gradient of quartz content, micro-fabric and grain size in central domain (data are petrographically estimated).

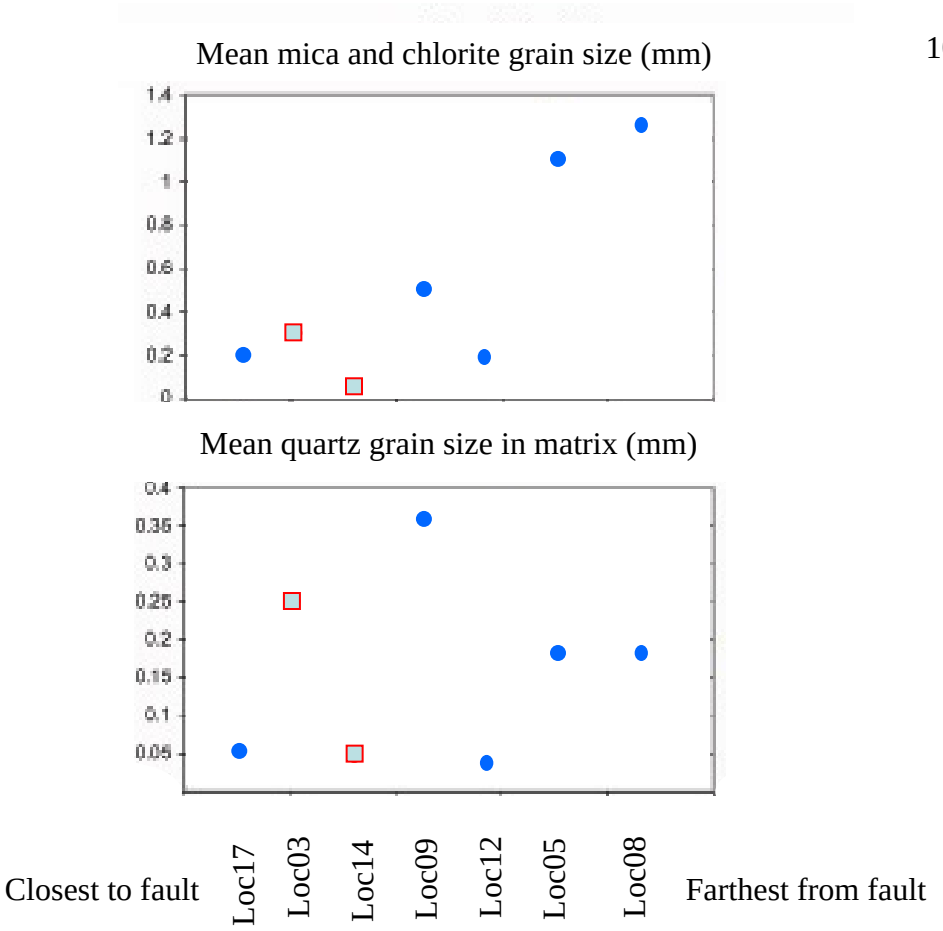

Figure33 C: Gradient of quartz content, micro-fabric and grain size in central domain (data are petrographically estimated).

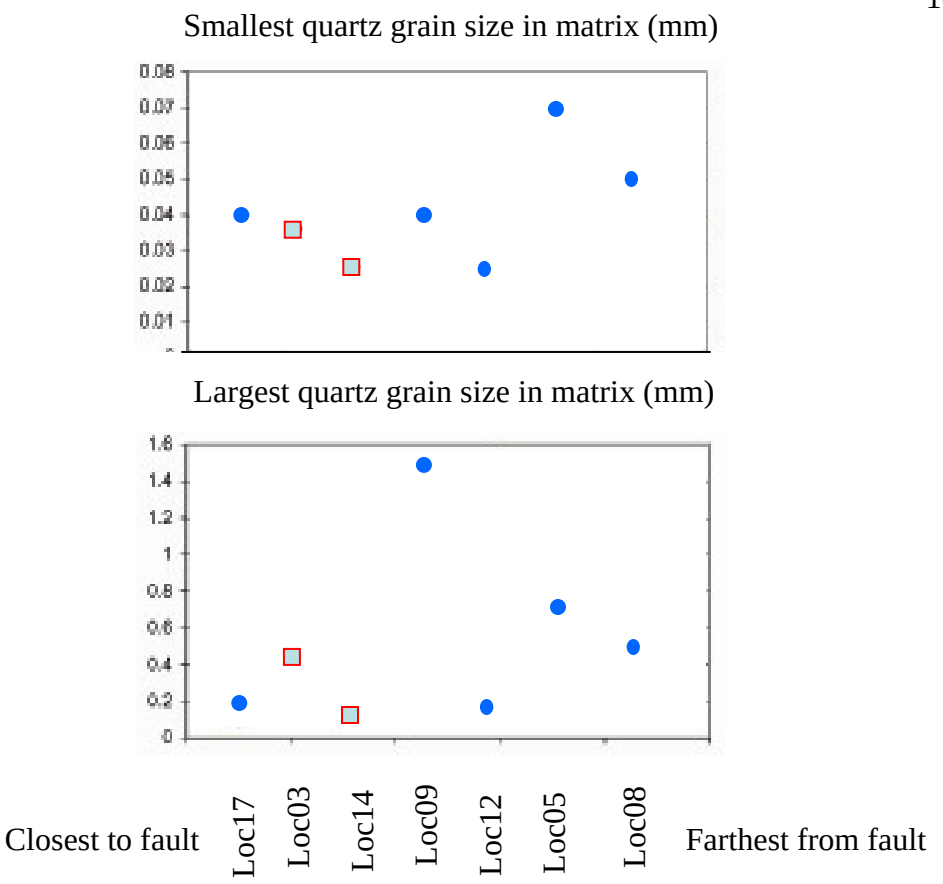

Figure 33 D: Gradient of quartz content, micro-fabric and grain size in central domain (data are petrographically estimated).

microscale away from the fault more closely approximate a plane closer to the Ridgeway fault. The smallest grain size of quartz in the seriate distribution of grain size is <0.05 mm across the central domain.

Quartz lenses are notably absent in the finer-grained, quartz-rich schists of the Fork Mountain Formation near the Ridgeway fault at "The Wall", which suggests that if quartz lenses had been present throughout the outcrop, they have since been obliterated by grain-size reduction. In contrast, the coarser, medium-grained, highly aluminous schists of the Fork Mountain Formation at "The Wall", also have elevated quartz content; however, this elevated quartz content is present in the form of quartz boudins that are isolated from the highly aluminous matrix.

Microscale evidence of crystal plastic deformation, such as grain boundary migration and subgrain rotation in quartz, are evident in the schists of the Fork Mountain Formation, particularly near the Ridgeway fault.

Interpretation of strain gradient and quartz influx

The cumulative evidence (*i.e.*, microscale evidence of crystal plastic deformation, relict coarse grains and a component of extremely small grain size, a gradient of increasing quartz content, decreasing grain size, and decreasing distance between micaceous and chlorite-rich layers as well as increasingly parallel micaceous and chlorite-rich layers) suggests that fine-grained schists of the Fork Mountain Formation near the Ridgeway fault are mylonitic. Because the initial grain size of the schist of the Lynchburg Group is generally fine in the

study area, it does not appear to display a range of grain size similar to that of the schists of the Fork Mountain Formation in the field area. The zone of influence of the most intense mylonitic fault activity is estimated to be <1 km based on the approximate locations in the structural profile of observations of L_m (Figure 9). The mylonitic damage zone of the Ridgeway fault likely obscures the contact between the SRA and the Lynchburg Group.

In the vicinity of the unexposed Ridgeway fault contact it is difficult to discern between the schists of the Fork Mountain Formation and the Lynchburg Group because of the apparent strain gradient and higher quartz concentration and the similarity of their AFM projections. Metamorphic grade and accompanying mineral assemblages (*e.g.*, garnet and sericitized sillimanite mats) observable only at microscale in the fine-grained rocks were therefore used to supplement mesoscale observations and thus to revise the mapped contact between the SRA and the Lynchburg Group (Figures 3 and 4).

Fluids in association with the Ridgeway fault appear to have introduced quartz into the micaceous schists of the Fork Mountain Formation. This quartz influx is observed as quartz lenses in the coarser, medium-grained rocks, but in the finer-grained schists of the Fork Mountain Formation the increase in quartz content is integrated with the fine-grained matrix. A sequence of events that may have led to an increase in quartz content follows. Siliceous fluid is introduced in advance of mylonitization (*i.e.*, before strain is accommodated by grain-size reduction). Subsequent mylonitization destroys any lens structures in the most intensely strained rocks, resulting in the finest-grained schists of the Fork Mountain Formation. Thus, these rocks may be devoid of quartz lenses because quartz

has been subjected to crystal plastic grain-size reduction. Coarser, medium-grained schists of the Fork Mountain Formation may have been less highly strained. This sequence of events is consistent with the shear-sense indicators observed in quartz lenses, evidence of crystal plastic deformation, cataclastic deformation of garnet, development of L_m, and redistribution of garnet fragments parallel to L_m in the discrete, finest-grained zones in schists of the Fork Mountain Formation across the study area (Figure 25).

The timing of the strain gradient and quartz influx is consistent with a general model of fluid pressure enabling initial fault activity and subsequent tectonic transport along the Ridgeway fault and parallel to L_m obliterating any quartz lenses that may have formed in the highly strained zones. Tectonic transport to the WNW is consistent with shear sense parallel to L_m. Tectonic transport is strongly suggested to have occurred after peak M_m because S_m comprises differing metamorphic mineral assemblages in the SRA and Lynchburg Group that have been juxtaposed by the emplacement of the higher-grade SRA rocks onto the lower-grade Lynchburg Group rocks. Ridgeway fault activity appears to have exploited the S_m surface because the relative orientation of S_m on either side of the fault appears undisturbed. Hence, Ridgeway fault activity likely occurred after the peak metamorphic event (M_m) whose mineral assemblages define S_m. Later deformation (D_l) appears to have occurred after substantial reduction of the geothermal gradient (*i.e.*, unroofing) and to be responsible for greenschist facies metamorphism. Reactivation of the Ridgeway fault may have occurred in advance of late folding (F_l), which likely ceased any further tectonic transport.

METAMORPHISM

Introduction

Analysis of metamorphic mineral assemblages is of use in interpreting the nature, number, conditions, and timing of metamorphic events and in determining their links to the structural record. Textural relations of metamorphic assemblages at meso- and microscale are examined, compared, and contrasted in detail in the schists of the Fork Mountain Formation and the Lynchburg Group. The SRA appears to have undergone three regional metamorphic events, while the Lynchburg Group appears to have experienced two, each of which is shared with the SRA. The regional, shared metamorphic events that accompanied the late deformation (D_l) and the main deformation (D_m) are referred to as M_l and M_m, respectively. The unshared event, restricted to the SRA, is referred to as the early metamorphism (M_e). M_e is presumed to have accompanied the early deformation (D_e) and may correspond with early structures of inclusion trails in garnet cores (S_i) and compositional layering that is folded by the main deformation D_m. These early structures appear to represent a relict early metamorphic foliation (S_e). As in the discussion of structural geology, the younger metamorphic events are progressively stripped away in order to recognize the more obscure record of the older metamorphic events; therefore, the metamorphic analysis progresses from the youngest to the oldest.

Late metamorphism (M_l)

Observation of late metamorphism (M_l)

The late metamorphic mineral assemblage (M_l) in the schists of the Fork Mountain Formation and Lynchburg Group appears to consist of: chlorite + muscovite ± biotite + quartz. M_l is difficult to discern with confidence because M_l weakly overprints M_m. This assemblage is consistent with the greenschist metamorphic facies previously reported for other portions of the SRA (Gates and Spear, 1991). Partial overprinting of biotite of M_m by chlorite of M_l appears to be ubiquitous in the schists of the Fork Mountain Formation and Lynchburg Group. However, M_l and M_m can only be reliably distinguished at hinge areas of late folds (F_l) where S_m, defined by M_m, lies perpendicular to S_l. For example at Loc01, biotite and muscovite define the moderately penetrative S_l that is parallel to the late axial surface; sericitized mats of sillimanite relict from M_e are partially aligned with S_l (Figure 15).

Interpretation of late metamorphism (M_l)

The presence of biotite suggests that M_l at least attained greenschist facies metamorphism. As indicated by the weak overprint of M_m by M_l, equilibrium is interpreted to be unattained between M_l and the minerals in the schists of the Fork Mountain Formation and Lynchburg Group on the whole. Thus, M_m remains the predominant equilibrium mineral assemblage in these rocks. This interpretation is further supported by the only moderate penetration of S_m.

Main metamorphism (M_m)

Observation of main metamorphism (M_m)

Discrete main metamorphic mineral assemblages (M_m) are present on both sides of the Ridgeway fault in the schists of the Fork Mountain Formation and Lynchburg Group.

The equilibrium metamorphic mineral assemblage (M_m) in the schists of the Fork Mountain Formation consists of: muscovite + biotite + porphyroblastic garnet (rims) + quartz + chloritoid + staurolite ± tourmaline ± epidote ± ilmenite ± magnetite ± monazite ± apatite.

The equilibrium metamorphic mineral assemblage (M_m) in the schists of the Lynchburg Group consists of: quartz + muscovite + biotite ± plagioclase feldspar ($An_{\sim 22\text{-}25}$ (Carter, 2006)) ± epidote ± ilmenite ± magnetite.

The predominant minerals that define the metamorphic grade of M_m include muscovite and biotite in the schists of the Lynchburg Group, and muscovite, biotite, porphyroblastic garnet (rims), chloritoid, and staurolite in the schists of the Fork Mountain Formation. Chloritoid and staurolite are observed to overprint minerals of M_e (*e.g.*, staurolite overprints sillimanite mats (Figure 34)), which defines sillimanite as a mineral of the preexisting early mineral assemblage (M_e). The predominant M_m minerals that define S_m in both the schists of the Fork Mountain Formation and the Lynchburg Group are muscovite, biotite, and elongate quartz. S_m is also defined by sericitized sillimanite in the schists of the Fork Mountain Formation (Figure 29).

Figure 34: Staurolite overprinting sericitized sillimanite mats in the Fork Mountain Formation at Loc08. The main foliation is subhorizontal (blue). The intersection lineation orientation is ~025, subhorizontal. Staurolite twins are marked by squares. The plane of view is ~000 (left), 05. Width of photomicrograph is ~1.1 mm. (cross-polarized light)

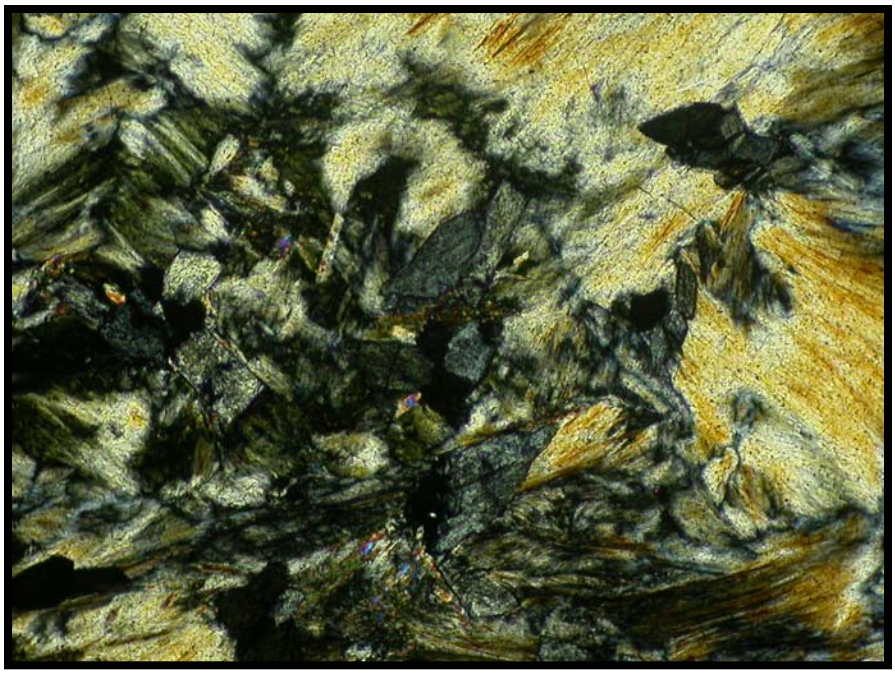

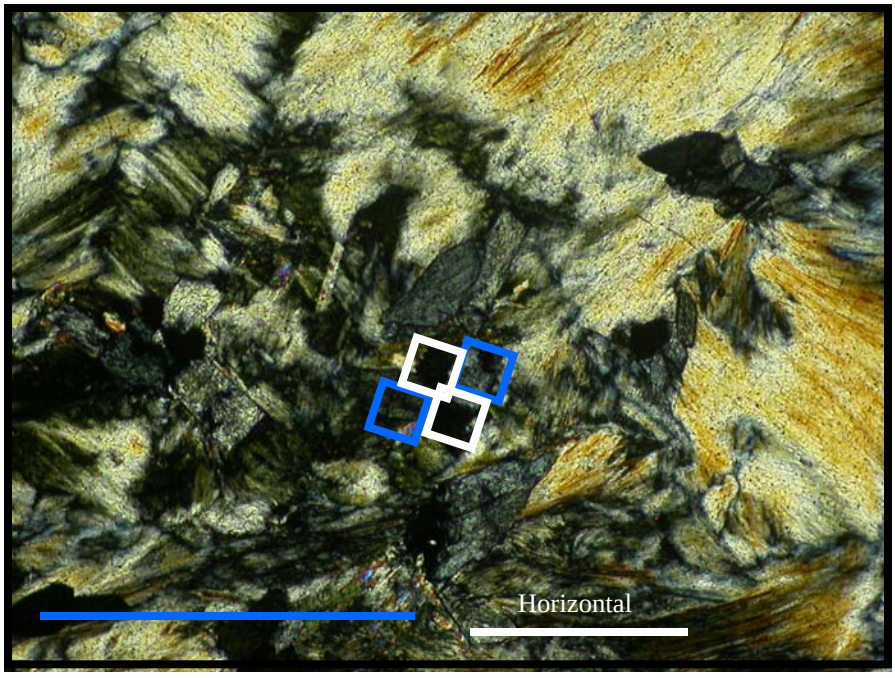
Horizontal

The rims of garnets are included in M_m of the schists of the Fork Mountain Formation because: 1) continuous sigmoidal inclusions of mineral grains that define S_m in the rock matrix are engulfed by the rims of garnets, suggesting simultaneous development during D_m (Figure 31), 2) planar inclusion trails (S_i), associated with D_e, are absent in the rims of garnets, suggesting that D_e preceded the growth of the rims of the garnets, and 3) inclusions of sillimanite fibrolite, associated with M_e, is overprinted by or entrapped in minerals of M_m, suggesting that sillimanite growth, thus M_e, predates these minerals. In particular, entrapment of sillimanite is observed between the core and rim of a garnet crystal (Gates and Speer, 1991), suggesting that M_e predates the rims of garnets. Inclusion trails in the cores of garnets, and thus the cores of garnets, are considered to correspond with M_e (*e.g.*, Yardley, 1989); rims of garnets are considered to represent M_m. The strain caps and strain shadows on many garnets comprising minerals that define S_m also suggest that garnet growth is synkinematic with M_m. Growth of the rims of garnets, both with and without strain caps and shadows, is evident in the schists of the Fork Mountain Formation. Those without strain caps may have grown late with respect to S_m, but because they generally have inclusion trails in their cores (S_i) that appear to be consistent with the S_i in the cores of garnets *with* strain caps and shadows, and because they are restricted to the SRA, it appears that the growth of the rims of garnets without strain caps and shadows are also restricted to M_m. Thus, the growth of the rims of garnets may be roughly of the same generation.

Interpretation of main metamorphism (M_m)

Two discrete metamorphic grades are present on either side of the Ridgeway fault in the schists of the Fork Mountain Formation and the Lynchburg Group. S_m is coplanar on either side of the Ridgeway fault, and M_m defines S_m on each side of the fault. Therefore, M_m in the SRA and the Lynchburg Group are both interpreted to represent the same main metamorphic (M_m) event. This interpretation strongly suggests that peak M_m occurred before emplacement of the higher-grade SRA onto the lower-grade Lynchburg Group metamorphic rocks along the Ridgeway fault. Because M_m consistently defines S_m, and S_m is coplanar on each side of the Ridgeway fault, it is reasoned that Ridgeway fault emplacement took advantage of the planar S_m. Otherwise, the parallel relation of S_m on either side of the fault would have likely been disturbed.

The consistent definition of S_m by M_m supports the interpretation that a single M_m metamorphic event was shared between the SRA and the Lynchburg Group (rather than discrete grades of metamorphism on opposite sides of the Ridgeway fault having resulted from separate events).

M_m is interpreted to have followed M_e based on the overprinting of minerals of M_e by minerals of M_m. Overprinting of M_e by M_m is characteristic of a reduction in temperature in the KMFASH system and indicates a shift of temperature conditions from M_e to M_m. The KMFASH system models chemical reactions in pelites based on the principal components of SiO_2, Al_2O_3, FeO, MgO, K_2O, and H_2O (*e.g.*, Yardley, 1989). The shift of temperature

conditions may have been facilitated by the influx of quartz-rich fluids, as suggested by a gradient of increased quartz content near the Ridgeway fault in fine-grained, mylonitic schists of the Fork Mountain Formation.

Early metamorphism (M_e)

Observation of early metamorphism (M_e)

The relict M_e equilibrium mineral assemblage in schists of the Fork Mountain Formation rocks consists of: muscovite + poikiloblastic biotite + quartz + poikiloblastic garnet (cores) + sillimanite mats ± plagioclase feldspar ($An_{\sim 22\text{-}25}$ (Carter, 2006)) ± ilmenite ± magnetite ± monazite ± apatite.

The predominant minerals that define the metamorphic grade of M_e in the schists of the Fork Mountain Formation include muscovite, biotite, garnet (cores), and sillimanite. The predominant minerals of M_e that define S_e in inclusion trails in garnet cores, and possibly in compositional layers, are muscovite, biotite, quartz, and sillimanite. Sillimanite is considered to represent M_e because it is overprinted by, and found as inclusions in, minerals of M_m.

Relict M_e is predominantly preserved as: 1) inclusion trails in the cores of garnets, which comprise aligned fine-grained (~0.05 mm) elongate quartz, muscovite, and biotite (Figure 29), 2) aligned fine-grained (~0.4 mm) poikiloblastic and ragged-edged biotite and muscovite overprinted by S_m (not associated with F_m hinges), 3) rare skeletal plagioclase feldspar, and 4) widespread sericitized sillimanite. Sericitized sillimanite mats are

transposed to lie parallel to S_m rather than to S_e, even where compositional layers (that may represent S_e) are folded by F_m (Figure 29).

Compositional layers are present in the schists of the Fork Mountain Formation but are observed only where they lie perpendicular to S_m in F_m hinges. Compositional layers (~3-4 mm thick) comprise quartz-rich layers that alternate with micaceous layers. Compositional layers may represent relict schistose to gneissic layers. The mineral assemblage that defines compositional layering is difficult to discern with confidence, but it may comprise biotite, muscovite, and quartz. The possible presence of biotite in compositional layering suggests that compositional layers are defined by a moderate- to high-grade metamorphic assemblage that at least attained greenschist facies.

Interpretation of early metamorphism (M_e)

M_e is interpreted to be sillimanite zone metamorphism. Sillimanite may have formed by the following reaction (Yardley, 1989): staurolite + muscovite + quartz -> garnet + biotite + sillimanite + water.

The overprinting of sillimanite mats by staurolite with crisp boundaries suggests the onset of the lower temperature conditions of M_m and perhaps the reversal of the above metamorphic reaction. M_e is thus interpreted to be a relict upper amphibolite facies metamorphic mineral assemblage that defines a relict early foliation (S_e). M_e is not in equilibrium and is broadly overprinted by M_m. Minerals unique to M_e, including plagioclase feldspar and sillimanite, appear to be in disequilibrium with M_m that overprints M_e.

The M_e assemblage is considered distinct from M_m in the schists of the Fork Mountain Formation because: 1) overprinting of M_e by minerals that define M_m (*e.g.*, mica, rims of garnets, staurolite, and chloritoid) (Figure 34), and 2) inclusions in cores of garnets (S_i) define M_e (Figure 29). The post-M_e timing of sericitization of sillimanite is unknown. Staurolite and chloritoid are characteristic of lower temperatures in the KMFASH system, in contrast to those defining M_e (Figure 35). Sericitization and chloritization of biotite, muscovite, sillimanite, and garnet further suggest that M_m is lower-grade than M_e. Overprinting of sillimanite by M_m is key to the identification of M_e as distinct from M_m. The presence of M_e suggests that relict compositional layering may be a metamorphic fabric rather than primary bedding (S_0) because M_e and compositional layering both coincidentally predate M_m, and there does not appear to be another mineral assemblage present in the schists of the Fork Mountain Formation from which S_i and compositional layers might have originated.

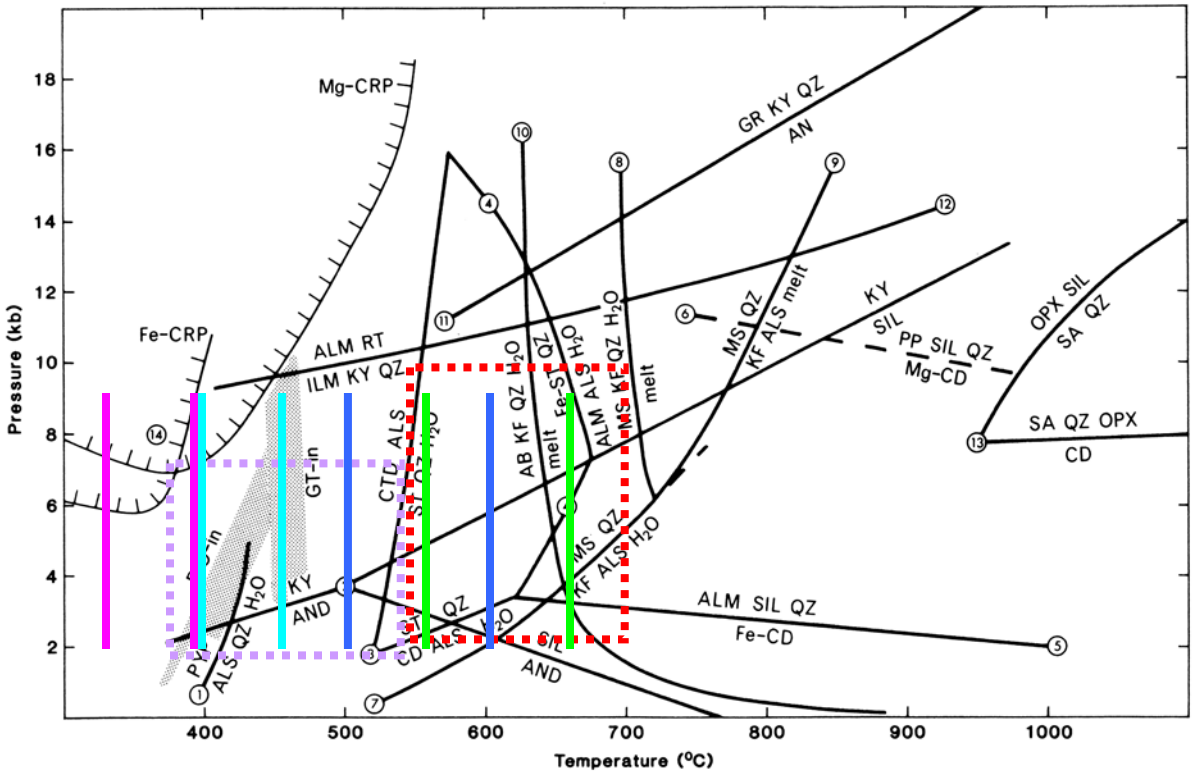

Ml	~350° C
Mm Fork Mountain Fm.	~500-600° C
Mm Lynchburg Gp.	~400-450° C
Me	~550-650° C
Amphibolite facies	
Greenschist facies	

Abbreviations used are: AB albite, ALM almandine, ALS Al-silicate, AN anorthite, AND andalusite, BIO biotite, CD cordierite, MS muscovite, OPX orthopyroxene, PP pyrope, PYP pyrophyllite, QZ quartz, RT rutile, SA sapphirine, SIL sillimanite, ST staurolite.

Figure 35: KMFASH petrogenetic grid showing metamorphic conditions. (Figure after Yardley, 1989)

Metamorphic conditions

Metamorphic conditions of the late metamorphic assemblage (M_l)

M_l conditions are consistent with biotite zone and lower greenschist facies metamorphism. However, these low temperature conditions are difficult to estimate with confidence because of the limited mineralogical record. The estimated temperature is ~350^o C, based on the fields of general metamorphic facies and KMFASH system (*e.g.*, Yardley, 1989) (Figure 35). Based on this temperature estimate the rocks would have been buried at a depth of ~11 km, assuming a geothermal gradient of ~30 ^{o}/km. The KMFASH system does not permit distinction of pressure with the given M_l mineral assemblage, but assuming a geo-pressure gradient of ~1 kbar/3 km the pressure would have been ~3-4 kbar.

Metamorphic conditions of the main metamorphic assemblage (M_m)

Higher-grade M_m SRA rocks are emplaced onto lower-grade M_m rocks of the Lynchburg Group. In the schists of the Fork Mountain Formation, the metamorphic grade of M_m is estimated to be staurolite zone and lower amphibolite facies metamorphism. In the schists of the Lynchburg Group, the metamorphic grade of M_m is estimated to be biotite zone and lower greenschist facies metamorphism. The temperature in the SRA is bracketed by the generalized fields of the metamorphic facies and by the presence of chloritoid and staurolite in the KMFASH system (*e.g.*, Yardley, 1989). The temperature estimate for M_m in the schists of the Fork Mountain Formation is ~500-600^o C; the temperature estimate for M_m in the schists of the Lynchburg Group is ~400-450^o C (Figure 35). It is appropriate that the

temperature estimate for the Lynchburg Group in the study area is lower than the estimates of other workers for parts of the Lynchburg Group that are structurally lower than the part currently exposed in the study area: 484-655±20 ^{o} C; (Wang, 1991); 484-655±20 ^{o} C (Gates, 1986). These rocks would have been buried during M_m at depths of ~13-15 km and ~16-20 km for the Lynchburg Group and the SRA respectively, based on these temperature estimates and assuming a geothermal gradient of ~30 ^{o}/km.

The KMFASH system does not permit further distinction of pressures with the given M_m mineral assemblages. Other workers have estimated pressures in the Lynchburg Group to be ~6.59 kbar (Wang, 1991) and ~5.75-6.59 kbar (Gates, 1986). These pressure estimates are broadly consistent with the above estimates of burial depth assuming a geo-pressure gradient of ~1 kbar/3 km (~18 km for Lynchburg Group rocks that are structurally lower than those in the study area). The observation of kyanite in area of the Altavista, VA led Gates and Speer (1991) to interpret an isobaric path from the conditions responsible for M_e to those responsible for M_m.

These estimates of depth of burial are consistent with the crustal depths necessary to achieve the ductile behavior observed in plagioclase and quartz as the transition zone between brittle/plastic crustal behavior is estimated to be ~12-15 km (*e.g.*, van der Pluijm and Marshak, 1997). The grain boundary migration exhibited by quartz in the study area supports the interpretation that metamorphic temperature conditions were in excess of the minimum necessary to produce crystal plastic deformation in quartz (>350 ^{o} C) (*e.g.*, Passchier and Trouw, 1996; van der Pluijm and Marshak, 1997).

Metamorphic conditions of the early metamorphic assemblage (M_e)

In the SRA, the conditions of metamorphism for the early metamorphic assemblage (M_e) are estimated to be sillimanite zone and upper amphibolite facies metamorphism (*e.g.*, Yardley, 1989). The temperature of M_e conditions are ~550-650^o C (Figure 35). These conditions are consistent with peak, middle-upper amphibolite facies metamorphism, characterized by sillimanite-bearing assemblages, as previously described for the region (Conley and Henika, 1973). These temperature estimates for the SRA are consistent with those of other workers: ~550-600^o C (Tracy and Beard, 2002; Beard and Tracy, 2002); 650^o C (Gates and Speer, 1991); 579±112 ^{o} C (Carter, 2006). Based on the temperature estimates, and assuming a geothermal gradient of ~30 ^{o}/km the rocks would have been buried within the crust at a depth of ~16-20 km.

The KMFASH system does not permit further distinction of pressures with the given M_e mineral assemblage. Other workers have estimated pressures in the Lynchburg Group to be 5.8 kbar (Gates and Speer, 1991) and 4.3±1.3 kbar (Carter, 2006). The depth of burial resulting from the pressure estimate of Gates and Speer (1991) (~18 km) is consistent with the above depth of burial, assuming a geo-pressure gradient of ~1 kbar/3 km. The depth of burial resulting from the pressure estimate of Carter (2006) suggests a shallower depth of burial (~12 km), assuming a geo-pressure gradient of ~1 kbar/3 km, and thus a geothermal gradient of a greater magnitude (~50 ^{o}/km) than the otherwise assumed gradient of ~30 ^{o}/km.

DISCUSSION AND CONCLUSIONS

Introduction

The SRA is the subject of investigation because of reported deformation, metamorphism, and intrusion (Conley and Henika, 1973), as well as a *c.* 530 Ma monazite age exclusive to rocks of the SRA (Hibbard *et al.,* 2003). Investigation of the early structures and metamorphism in the SRA should elucidate the kinematics of the early deformation that is unique to the SRA. Characterizing and associating the early deformation with the Early Cambrian monazite age would lend credence to one interpretation of the origin of the SRA. The rock types of the SRA and the underlying Lynchburg Group contrast in mineralogy as well as in structural, metamorphic, and intrusive histories (Conley and Henika, 1973). Hibbard *et al.* (2003) hypothesized that the Early Cambrian monazite age could represent the tectonothermal event responsible for the early upper amphibolite facies metamorphism and the structural record that is recognized in the SRA but not present in the Lynchburg Group (Conley and Henika, 1973). Hibbard *et al.* (2003) further hypothesized that the SRA was exotic with respect to Laurentia and was perhaps peri-Gondwanan, because an Early Cambrian tectonothermal event along the eastern margin of Laurentia conflicted with the documented drift environment (Hibbard and Samson, 1995; Hibbard *et al.*, 2005), and because other peri-Gondwanan accreted terranes in the southern Appalachians exhibit Early Cambrian tectonic events (*e.g.*, Hibbard and Samson, 1995; White and Barr, 1996; Dennis and Wright, 1997). However, detrital zircons in the SRA and the Lynchburg Group have similar signatures, which suggests that the SRA is peri-Laurentian (Carter *et al.*, 2006).

This study has focused on the nature and timing of deformation to delineate and contrast the histories of the SRA and Lynchburg Group in order to help elucidate the crustal affinity – Laurentian or Gondwanan – of the SRA.

Tectonic history of the SRA and the Lynchburg Group

The two latest orogenic deformational events (D_l and D_r) occurred after emplacement of the SRA onto the Lynchburg Group as evidenced by NE-trending elongate domes and basins, a moderately penetrative foliation, and a regionally penetrative NE-trending intersection lineation formed under relatively shallow (~6-9 km) crustal conditions of greenschist facies metamorphism. D_l and D_r likely reactivated the Ridgeway fault in advance of folding, as suggested by the absence of the Martinsville intrusive suite (MIS) in the Lynchburg Group and the shearing and truncation of the MIS by the Ridgeway fault (Henika, 1971; Rankin, 1975; Conley, 1985; Conley and Henika, 1995; Henika *et al.*, 1996). These latest deformations may be consistent with a WNW-directed transpressional tectonic setting attributed to *c.* 345-285 Ma by Gates (1987), but evidence for a strike-slip component of movement is unobserved at the Ridgeway fault in the study area. The Martinsville intrusive suite (*e.g.*, *c.* 430 and *c.* 445 Ma (Wilson, 2001)) likely intruded the SRA before late reactivation of the Ridgeway fault.

Tectonic transport of the SRA toward the WNW also occurred during the main deformation (D_m) and emplaced the SRA onto the Lynchburg Group along the low-angle Ridgeway thrust fault after the peak of the main metamorphic event (M_m). Peak M_m metamorphism

likely occurred *c.* 486 Ma as indicated by a monazite age from SRA rocks (Hibbard *et al.,* 2003). However, the Ordovician monazite age has not been confirmed in the Lynchburg Group because monazite has not been found in these rocks (Tracy, pers. com. 2005). Ridgeway fault activity emplaced lower amphibolite facies rocks that were deformed relatively deep in the crust (~9-15 km) onto greenschist facies rocks that were deformed at more moderate depths (~6-12 km). Both metamorphic grades are interpreted to represent M_m because they each define a penetrative fabric (S_m) that is correlated across the fault by virtue of its being coplanar and distinct from fabrics of subsequent and earlier events. M_m in the SRA is an alteration of an earlier metamorphic assemblage (M_e) that is restricted to the SRA. Ridgeway fault activity occurred under ductile conditions producing mylonite and exploiting S_m without reorienting it on either side of the Ridgeway fault. Ridgeway fault activity was likely coeval with an increase in quartz content near the Ridgeway fault.

The record of the early deformation (D_e), confined to the SRA, is preserved in the form of NE-trending planar inclusion trails in garnets (S_i), which appear to represent a relict early foliation (S_e). S_e may also be represented by compositional layering that predates D_m, is folded by F_m, and that is a component of a NE-trending intersection lineation (L_{i-1}) formed by the intersection of compositional layers with S_m. M_e, which presumably accompanied D_e, is evident in the relict upper amphibolite facies metamorphic assemblage. D_e is interpreted to correspond to the *c.* 530 Ma monazite age (Hibbard *et al.*, 2003), which suggests that the SRA does not originate from the eastern passive margin of Laurentia.

Conclusions and regional implications

The stripping away of each deformation in the course of this investigation supports the interpretation that the main foliation on each side of the fault shares a common origin, and that the Ridgeway fault was active during, as well as reactivated after, the main deformation. This study concludes that there is structural evidence for an early tectonothermal event in the SRA that pre-dates the main deformation. However, its state of preservation reveals only the approximate orientations of planar inclusion trails in garnets, the intersection lineation (compositional layering intersecting with S_m), and the approximate metamorphic conditions and depth of burial. Circumstantial evidence that the Early Cambrian monazite age, the early metamorphic assemblage, and the early foliation all precede the main deformation, and therefore may represent the same Early Cambrian event, supports the hypothesis that the SRA did not form immediately adjacent to the eastern Laurentian passive margin.

Future research

To further resolve the conflict of the affinity of the SRA, future research could strive to tie the early deformation to the monazite age rather than relying on circumstantial evidence. The placement of peri-Laurentian micro-continents could also be assessed (Cawood *et al.*, 2001) as it may be possible to have a peri-Laurentian source from which detrital zircons originate together with non-Laurentian tectonothermal activity (*e.g.*, Hibbard *et al.*, in press).

In this study, a mylonitic gradient is interpreted to exist in the fine-grained schists of Fork Mountain Formation rocks in close proximity to the Ridgeway fault that had previously been mapped as Lynchburg Group rocks (Marr, 1984; Henika, 1997, 2002). Further mapping and strain analysis studies could clarify this gradient and further distinguish it from possible interfingering of finer- with coarser-grained protolithic material. Further work could also locate the unexposed SRA-Lynchburg Group contact that is also the Ridgeway fault trace. Of particular interest regarding the Ridgeway fault is any evidence for reactivation.

Investigation of pegmatites could reveal the timing of their emplacement relative to Ridgeway fault activity and thus could further elucidate Ridgeway fault mobilization. There are not enough pegmatites in the study area to give a detailed account of their kinematic history. They are, however, weakly deformed but it is not clear which deformation is responsible.

Further work could catalog the orientations of the early foliation across the region as revealed in porphyroblastic inclusion trails (S_i) and compare the orientation to that of the main and late deformations. Such work could contribute to an understanding of the geometry and kinematics of the series of deformations. Chemical or geochronological analysis of S_i could confirm that S_i corresponds to other minerals in M_e. Metamorphic analysis could provide pressure and temperature paths for rocks on either side of the Ridgeway fault and more closely account for depth of burial and corresponding sequential events.

Further work in western Piedmont and eastern Blue Ridge paleogeography should continue to contribute to the placement of these deformations into the broad regional context and to the ultimate determination of the affinity of the SRA. If the SRA is confirmed to be exotic and the Ridgeway fault marks the eastern edge of Laurentia, it draws into question the affinity of other Piedmont terranes (Hibbard and Samson, 1995).

REFERENCES CITED

Achaibar, J., and Misra, K.C., 1984, Amphibolites of the Smith River allochthon, southwest Virginia, southern Appalachians (abs.): Geological Society of America Abstracts with Programs, v. 16, no. 3, p. 121.

Aleinikoff, J.N., Zartman, R.E., Walter, M., Rankin, D., Lyttle, P.T., and Burton, W.C., 1995, U-Pb ages of metarhyolites of the Catoctin and Mount Rogers Formations, Central and Southern Appalachians: Evidence for two pulses of Iapetan rifting: American Journal of Science, 295, 428-454.

Allmendinger, R.W., 2003, Stereonet for Windows V. 1.2. (http://www.geo.cornell.edu/geology/faculty/RWA/maintext.html)

Barker, A., 1998, Introduction to Metamorphic Textures and Microstructures, 2nd ed., Chapman and Hall, London, 264 p.

Beard, J.S., and Tracy, R.J., 2002, Spinels and other oxides in Mn-rich Rocks from the Hutter Mine, Pittsylvania Co., Virginia, USA: Implications for miscibility and solvus relations among jacobsite, galaxite, and magnetite: American Mineralogist, v. 87, p. 690-698.

Bell, T.H., 1985, Deformation partitioning and porphyroblastic rotation in metamorphic rocks: a radical reinterpretation: Journal of Metamorphic Geology, v. 3, p. 109-118.

Berquist, C.R., 1988, Geology and Mineral Resources of the Sandy Level and Callands Quadrangles, Virginia, Virginia Division of Mineral Resources, pub. 77.

Box, G.H., Allen, J.S., and Hibbard, J.P., 2006, Structural character of the Smith River allochthon in central and south-central Virginia (abs.): Geological Society of America Abstracts with Programs, v. 38, no. 3.

Carter, B.T., 2006, Geological Investigations in the Smith River allochthon and Lynchburg Group, southern Appalachians: Implications for the Neoproterozoic-Paleozoic evolution of the Laurentian margin, Ph.D. dissertation, North Carolina State University, Raleigh, North Carolina, 145 p.

Carter, B.T., Hibbard, J.P., Tubrett, M., Sylvester, P., 2006, Detrital zircon geochronology of the Smith River allochthon and Lynchburg Group, southern Appalachians: Implications for Neoproterozoic-Early Cambrian paleogeography, *in* McCausland, P., Murphy, B., and MacNiocaill, C., eds., Endings and Beginnings: Paleogeography of the Neoproterozoic-Cambrian Transitions: Precambrian Research, v. 147, p. 279-304.

Cawood, P.A., McCausland, P. and Dunning, G., 2001, Opening Iapetus: Constraints from Laurentian margin in Newfoundland: Geological Society of America Bulletin, v. 113, p. 443-453.

Coler, D.G., Samson, S.D., and Hibbard J.P., 2000a, The Chopawamsic and Milton terranes: Correlative Ordovician arc terranes built on ancient continental crust, southern Appalachians, Journal of Geology, v. 108, p. 321-338.

Coler, D.G., Wortman, G.L., Samson, S.D., Hibbard, J.P., and Stern, R., 2000b, U-Pb geochronologic, Nd isotopic, and geochemical evidence for the correlation of the Chopawamsic and Milton terranes, Piedmont zone, southern Appalachian orogen: Journal of Geology, v. 108, no. 4, p. 363-380.

Conley, J.F., 1978, Geology of the Piedmont of Virginia-interpretations and problems, *in* Contributions to Virginia geology - III, Virginia Division of Mineral Resources, pub. 7, p. 115-149.

Conley, J.F., 1981, Stratigraphic relationships between rocks of the Blue Ridge anticlinorium and the Smith River allochthon in the southwestern Virginia piedmont, *in* Conley, J.F., Marr, J.D., Jr., and Berquist, C.R., Jr., Stratigraphic relationships between rocks of the Blue Ridge anticlinorium and the Smith River allochthon in the southwestern Virginia piedmont, Virginia Division of Mineral Resources, 13th annual Virginia geological field conference, p. 1-28.

Conley, J.F., 1985, Geology of the southwestern Virginia Piedmont, Virginia Division of Mineral Resources, pub. 59, 33 p.

Conley, J.F., 1989, Geology of the Rocky Mount, Gladehill, Penhook, and Mountain Valley quadrangles, Virginia, Virginia Division of Mineral Resources, 15 p., one map.

Conley, J.F., and Henika, W.S., 1970, Geology of the Philpott Reservoir quadrangle, Virginia, Report of investigations 22, Virginia Division of Mineral Resources, 46 p.

Conley, J.F., and Henika, W.S., 1973, Geology of the Snow Creek and Martinsville East, Price and Spray quadrangles, Virginia, Report of investigations 33, Virginia Division of Mineral Resources, 71 p.

Conley, J.F., and Henika, W.S., 1995, Geology and mineral resources of Henry Co. and the city of Martinsville, Virginia, Virginia Division of Mineral Resources, pub. 137, map.

Conley, J.F., Piepul, R.G., Robinson, G.R., Jr., Lemon, E.M., Jr., and Berquist, C.R., Jr., 1989, Geologic map of the Penhook and Mountain Valley quadrangles, Virginia, Virginia Division of Mineral Resources, pub. 90B.

Conley, J.F., and Toewe, C.E., 1968, Geology of the Martinsville West quadrangle, Virginia, Report of investigations 16, Virginia Division of Mineral Resources, 44 p.

Dennis, A.J., and Wright, J.T., 1997, The Carolina terrane in northwestern South Carolina, USA: Late Precambrian-Cambrian deformation and metamorphism in a peri-Gondwanan oceanic arc: Tectonics, v. 16, p. 460-473.

Flinn, D., 1962, On folding during three-dimensional progressive deformation: Quarterly Journal of the Geological Society, v. 118, p. 385-433.

Furcron, A.S., 1969, Late Precambrian and early paleozoic erosion depositional sequences of northern and central Virginia: Georgia Geological Survey Bulletin 80, p. 57-88.

Gates, A.E., 1986, The tectonic evolution of the Altavista area, southwestern Virginia Piedmont, Ph.D. dissertation, Virginia Polytechnical Institute and State University, Blacksburg, Virginia, 256 p.

Gates, A.E., 1987, Transpressional dome formation in the southwestern Virginia Piedmont: American Journal of Science, v. 287, p. 927-949.

Gates, A.E., 1989, Reply: Transpressional dome formation in the southwestern Virginia Piedmont: American Journal of Science, v. 289, no. 6, p. 829-837.

Gates, A.E., 1997, Multiple reactivations of accreted terrane boundaries: An example from the Carolina terrane, Brookneal, Virginia, *in* Glover, L.G., and Gates, A.E., eds., Central and southern Appalachian sutures: Results of the EDGE Project and related studies: Geological Society of America Special Paper 314, p. 49-63.

Gates, A.E., and Speer, J.A., 1991, Allochemical retrograde metamorphism in shear zones: an example in metapelites, Virginia, USA: Journal of Metamorphic Geology, v. 9, p. 581-604.

Glover, L.G., III, 1989, Tectonics of the Virginia Blue Ridge and Piedmont: American Geophysical Union Field Trip Guidebook T363, 59 p.

Glover, L.G., III, Sheridan, R., Holbrook, W., Ewing, J., Talwani, M., Hawman, R., and Wang, P., 1997, Paleozoic collisions, Mesozoic rifting, and structure of the Middle Atlantic states continental margin: An 'EDGE' project report, *in* Glover, L.G., and Gates, A.E., eds., Central and southern Appalachian sutures: Results of the EDGE Project and related studies: Geological Society of America Special Paper 314, p. 107-135.

Greenberg, J.K., 1975, Tectonic implications of geophysical evidence in the Martinsville, Virginia area (abs.): Geological Society of America Abstracts with Programs, v. 7, no. 4, p. 493-494.

Hatcher, R.D., Jr., 1978, Tectonics of the western Piedmont and Blue Ridge, southern Appalachians: Review and speculation: American Journal of Science, v. 278, p. 276-304.

Henika, W.S., 1971, Geology of the Bassett quadrangle, Virginia, Report of investigations 26, Virginia Division of Mineral Resources.

Henika, W.S., 1997, Geologic map of the Roanoke 30 x 60 minute quadrangle, Virginia Division of Mineral Resources, pub. 148.

Henika, W.S., 2002, Geologic map of the Virginia portion of the Danville 30 x 60 minute quadrangle, Virginia Division of Mineral Resources, pub. 166.

Henika, W.S., Conley, J.F., and Sweet, P.C., 1996, Geology and mineral resources of Henry Co. and the city of Martinsville, Virginia, Virginia Division of Mineral Resources, pub. 137, 22 p.

Hibbard, J.P., Miller, B.V., Tracy R.J., and Carter, B.T., 2005, The Appalachian peri-Gondwanan realm: a paleogeographic perspective from the south: Geological Society, London, Special Publications, v. 246, p. 97-111.

Hibbard, J.P., and Samson, S., 1995, Orogenesis exotic to the Iapetan cycle in the southern Appalachians, *in* Hibbard, J.P., van Staal, C.R., and Cawood, P.A., eds., Current perspectives in the Appalachian-Caledonian orogen, Geological Association of Canada Special Paper 41, p. 191-205.

Hibbard, J.P., Shell, G., Bradley, P., Samson, S., and Wortman, G., 1998, The Hyco shear zone: implications for the Piedmont-Carolina zone boundary in North Carolina and southern Virginia: American Journal of Science, v. 298, p. 85-107.

Hibbard, J.P., Tracy, R.J., and Henika, W.S., 2003, Smith River allochthon: A southern Appalachian peri-Gondwanan terrane emplaced directly on Laurentia? Geology, v. 31, no. 3, p. 215-218.

Hibbard, J.P., van Staal, C.R., Rankin, D.W., and Williams, H., 2006, Lithotectonic map of the Appalachian Orogen, Canada-USA: Geological Survey of Canada, Map 2096A, Scale 1:1,500,000, 2 sheets.

Hibbard, J.P., van Staal, C.R., and Rankin, D.W., in press, A comparative analysis of pre-Late Ordovician crustal 'building blocks' of the northern and southern Appalachians: American Journal of Science.

Horton, J.W., Jr., Drake, A., and Rankin, D., 1989, Tectonostratigraphic terranes and their Paleozoic boundaries in the central and southern Appalachians, *in* Dallmeyer, D., ed.,

Terranes in the circum-Atlantic Paleozoic orogens: Geological Society of America Special Paper 230, p. 213-245.

Howard, D.S., 2001, Transposition structures on Glassy Mountain, Saluda 7.5-minute quadrangle, South Carolina, *in* Garihan, J.M., Ranson, W.A., and Clendenin, S.W., eds., Geology of the Inner Piedmont in the Caesars Head and Table Rock state parks area, northwestern South Carolina, Special Issue Devoted to the 2001 Field Trip of the Carolina Geological Society, South Carolina Geology, v. 43, p. 25-35, S.C. Department of Natural Resources.

Johnson, S.E., 1999a, Near-orthogonal foliation development in orogens; meaningless complexity, or reflection of fundamental dynamic processes? Journal of Structural Geology, v. 21, no. 8-9, p. 1183-1187.

Johnson, S.E., 1999b, Porphyroblast microstructures; a review of current and future trends: American Mineralogist, v. 84, no. 11-12, p. 1711-1726.

Johnson, S.E., and Vernon, R.H., 1995, Inferring the timing of porphyroblast growth in the absence of continuity between inclusion trails and matrix foliations; can it be reliably done? Journal of Structural Geology, v. 17, no. 8, p. 1203-1206.

Jonas, A.L., 1927, Geological reconnaissance in the Piedmont of Virginia: Geological Society of America Bulletin, v. 38, no. 4, p. 837-846.

Kohn, M.J., and Malloy, M.A., 2004, Formation of monazite *via* prograde metamorphic reactions among common silicates: Implications for age determinations: Geochimica et Cosmochimica Acta, v. 68, no. 1, p. 101-113.

Lanzirotti, A., and Hanson, G.N., 1997, An assessment of the utility of staurolite in U-Pb dating of metamorphism: Contributions to Mineralogy and Petrology, v. 129, p. 352-365.

Lewis, S.E., 1980, Geology of the Brevard Zone, Smith River allochthon, and Inner Piedmont in the Sauratown Mountains anticlinorium, northwestern North Carolina, Ph.D. dissertation, Chapel Hill, University of North Carolina, 128 p.

Lisle, R.J., 1985, Geological Strain Analysis: A Manual for the R_f-Φ Technique, Pergamon Press, Oxford, 99 p.

Marr, J.D., Jr., 1984, Geologic Map of the Pittsville and Chatham Quadrangles Virginia, Virginia Division of Mineral Resources, pub. 49.

Miller, B.V., Fetter, A.H., and Stewart, K.G., 2006, Plutonism in three orogenic pulses, Eastern Blue Ridge Province, southern Appalachians: Geological Society of America Bulletin, v. 118, no. 1/2, p. 171-184.

North American Commission on Stratigraphic Nomenclature, 2005, North American stratigraphic code: American Association of Petroleum Geologists Bulletin, v. 89, no. 11, p. 1547-1591.

Odom, A.L., and Russell, G.S., 1975, The time of regional metamorphism of the Inner Piedmont and Smith River allochthon: inferences from whole rock ages (abs.): Geological Society of America Abstracts with Programs, v. 7, no. 4, p. 522-523.

Passchier, C.W., and Trouw, R.A.J., 1996, Microtectonics, corrected 2nd printing, Springer-Verlag, 289 p.

Pavlides, L., Arth, J., Sutter, J., Stern, T., and Cortesini, H., 1994, Early Paleozoic alkalic and calc-alkalic plutonism and associated contact metamorphism, central Virginia Piedmont: U.S. Geological Survey Professional Paper 1529, 147 p.

Powell, C.M.A, 1979, A morphological classification of rock cleavage: Tectonophysics, v. 54, p. 25-43.

Ragland, P.C., 1991, Mesozoic igneous rocks, *in* Horton, J.W., Jr., and Zullo, V.A., eds., The Geology of the Carolinas, Carolina Geological Society Fifteenth Anniversary Volume, p. 171-190.

Ramsay, J.G., 1967, Folding and fracturing of rocks, McGraw Hill, New York, 568 p.

Ramsay, J.G., and Huber, M., 1983, The Techniques of Modern Structural Geology 1: Strain Analysis, Academic Press, 307 p.

Rankin, D.W., 1975, The continental margin of eastern North America in the southern Appalachians: the opening and closing of the proto-Atlantic Ocean: American Journal of Science, v. 275-A, p. 298-336.

Stewart, K.G., Adams, M.G., and Trupe, C.H., eds., 1997, Paleozoic structure, metamorphism, and tectonics of the Blue Ridge of Western North Carolina: Carolina Geological Society 1997, Field Trip Guidebook, 101 p.

Thompson, J.B., Jr., 1957, The graphical analysis of mineral assemblages in pelitic schists: American Mineralogist, v. 42, p. 842-858.

Tracy, R.J., and Beard, J.S., 2002, Manganoan kinoshitalite in Mn-rich marble and skarn from Virginia: American Mineralogist, v. 88, p. 740-747.

Tracy, R.J., Beard, J.S., and Henika, W.S., 2001, Electron microprobe U-Th-Pb geochronology of monazites in contact metamorphosed aluminous rocks of the Martinsville intrusive complex, Smith River allochthon, Virginia (abs.): Geological Society of America, Abstracts with Programs, v. 33, no. 2, p. A-8.

Trupe, C.H., Stewart, K.G., Adams, M.G., Waters, C.L., Miller, B.V., and Hewitt, L.K., 2003, The Burnsville fault: Evidence for the timing and kinematics of southern Appalachian Acadian dextral transform tectonics: Geological Society of America Bulletin, v. 115, n. 11, p. 1365–1376.

University of Sydney, School of Geosciences, 2006, Flinn diagram, New South Wales, Australia (http://www.geosci.usyd.edu.au).

U.S. Department of the Interior, 1966, 1982, Leesville Quadrangle, Virginia 7.5 minute topographic series, U.S. Department of the Interior, Geological Survey.

van der Pluijm, B., and Marshak, S., 1997, Earth Structure, An Introduction to Structural Geology and Tectonics, McGraw Hill, New York, 495 p.

Wang, P., 1991, Geology and tectonic significance of the Late Pre-Cambrian eastern Blue Ridge cover sequence in central Virginia, Ph.D. dissertation, Virginia Polytechnical Institute and State University, Blacksburg, Virginia, 156 p.

White, C.E., and Barr, S.M., 1996, Geology of the Brookville terrane, southern New Brunswick, Canada, *in* Nance, D., and Thompson, M., eds., Avalonian and related peri-Gondwanan terranes of the circum-North Atlantic: Geological Society of America Special Paper 304, p. 133-147.

Wilson, J.R., 2001, U/Pb Zircon Ages of Plutons from the Central Appalachians and GIS-Based assessment of Plutons with Comments on Their Regional Tectonic Significance, MS thesis, Virginia Polytechnical Institute and State University, Blacksburg, Virginia, 114 p.

Wortman, G., Samson, S., and Hibbard, J.P., 1998, Precise U-Pb zircon timing constraints on the kinematic development of the Hyco shear zone: implications for the central Piedmont shear zone, southern Appalachian orogen: American Journal of Science, v. 298, p. 108-130.

Yardley, W.D., 1989, An introduction to metamorphic petrology, Longman Scientific and Technical, New York, 248 p.

APPENDICES

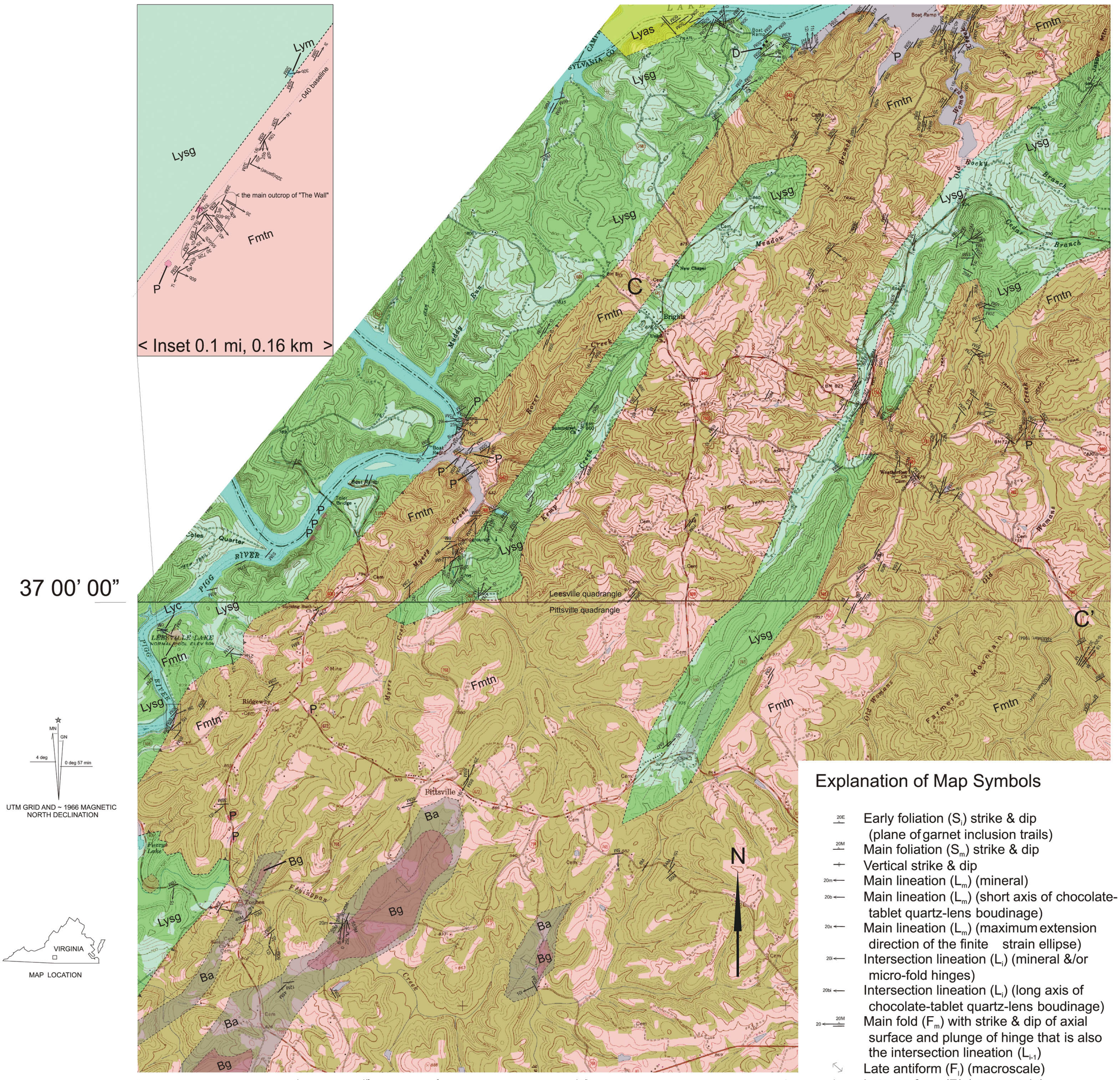

Explanation of Map Symbols

- Early foliation (S_i) strike & dip (plane of garnet inclusion trails)
- Main foliation (S_m) strike & dip
- Vertical strike & dip
- Main lineation (L_m) (mineral)
- Main lineation (L_m) (short axis of chocolate-tablet quartz-lens boudinage)
- Main lineation (L_m) (maximum extension direction of the finite strain ellipse)
- Intersection lineation (L_i) (mineral &/or micro-fold hinges)
- Intersection lineation (L_i) (long axis of chocolate-tablet quartz-lens boudinage)
- Main fold (F_m) with strike & dip of axial surface and plunge of hinge that is also the intersection lineation (L_{i-1})
- Late antiform (F_l) (macroscale)
- Late synform (F_l) (macroscale)
- Late antiform (F_l) overturned (macroscale)
- Late synform (F_l) overturned (macroscale)
- Late fold (F_l) (mesoscale)
- Later fold (F_r) (mesoscale)
- Late & later fold interference (mesoscale)
- Late antiform (F_l) (mesoscale)
- Ridgeway fault, contact (concealed) (sawteeth on thrust sheet)
- Contact (concealed)
- Normal fault (mesoscale)

Cross-section:

- Early foliation (S_i)
- Main folds (F_m)

C — Schematic Geologic Cross Section, no vertical exaggeration — C'

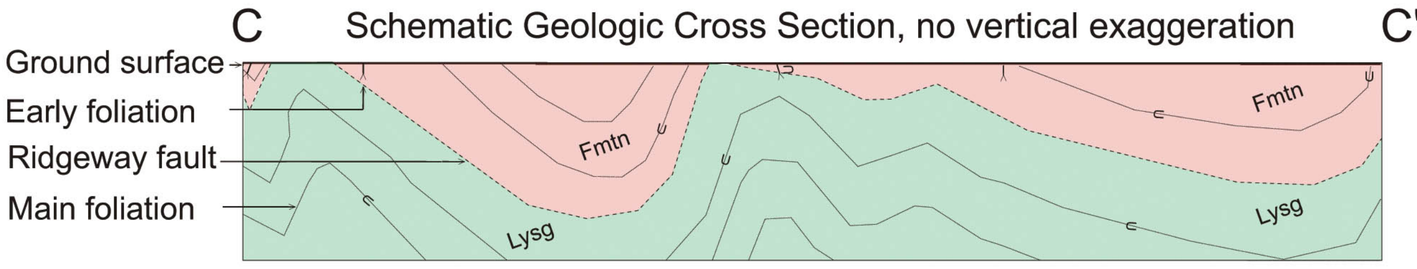

Unit Descriptions

Smith River allochthon:

Fork Mountain Formation

Fmtn — Medium gray, reddish-brown weathering, fine- to coarse-grained, muscovite-biotite-chlorite schist with sericitized sillimanite and porphyroblasts of garnet

Bassett Formation

Ba — Bassett amphibolite: dark gray, fine-grained, foliated amphibolite

Bg — Bassett gneiss: gray, fine- to medium-grained, equigranular, biotite gneiss

Lynchburg Group:

Lysg — Light to dark gray, brown weathering, fine- to medium-grained, muscovite-biotite-chlorite gneiss and schist

Lyas — Dark greenish-gray, fine-grained, actinolite schist

Lym — Light gray, fine-grained, foliated marble

Lyc — Light gray, coarse-grained, foliated metaconglomerate

Other:

P — White to light gray, coarse-grained, granoblastic, weakly foliated pegmatite

Dark gray, fine- to medium-grained, phaneritic diabase

Appendix 1: Geologic map of the area of Pittsville, Virginia, scale 1:24,000 including portions of Leesville and Pittsville USGS 7.5' quadrangles
Geology by Gordon Box 2004-2006.

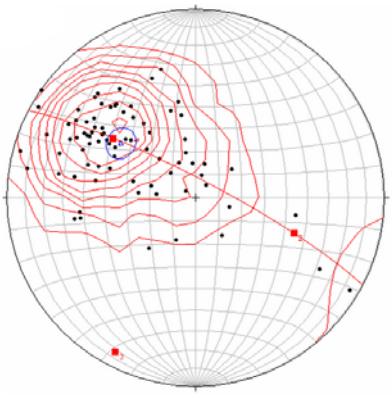

n = 84
Kamb contour interval
(c) = 2 sigma
Pole to best-fit great circle
(a) = 208, 08

A-SRA and Lynchburg Group

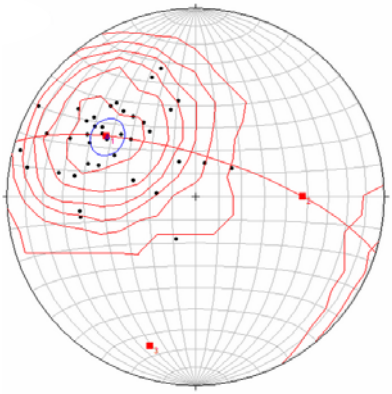

n = 40
c = 2
a = 197, 18

B-SRA

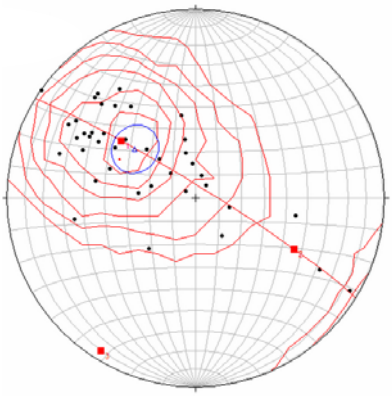

n = 44
c = 2
a = 212, 05

C-Lynchburg Group

Appendix 2 A, B, C: Equal area, lower hemisphere, stereoplot of poles to planes of the main foliation in the northern transect.

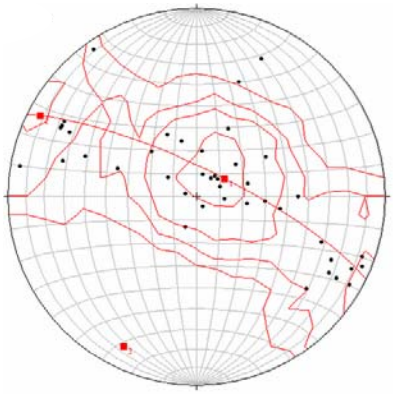

n = 43
Kamb contour interval
(c) = 2 sigma
Pole to best-fit great circle
(a) = 206, 13

A-SRA and Lynchburg Group

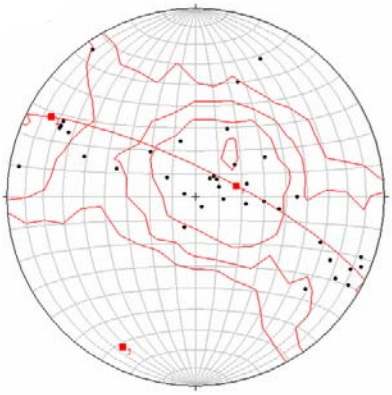

n = 38
c = 2
a = 206, 12

B-SRA

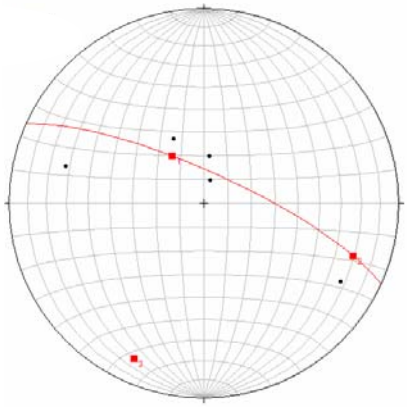

n = 5
a = 204, 13

C-Lynchburg Group

Appendix 3 A, B, C: Equal area, lower hemisphere, stereoplot of poles to planes of the main foliation in the central transect (central domain inclusive).

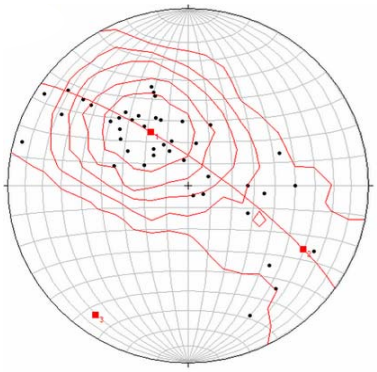

n = 43
Kamb contour interval
(c) = 2 sigma
Pole to best-fit great circle
(a) = 215, 11

A-SRA and Lynchburg Group

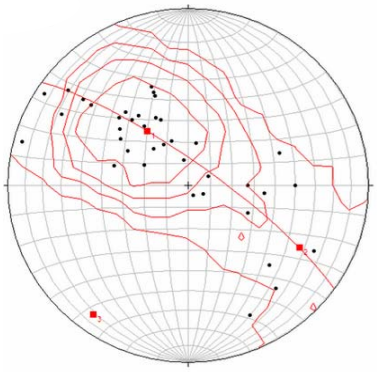

n = 38
c = 2
a = 216, 11

B-SRA

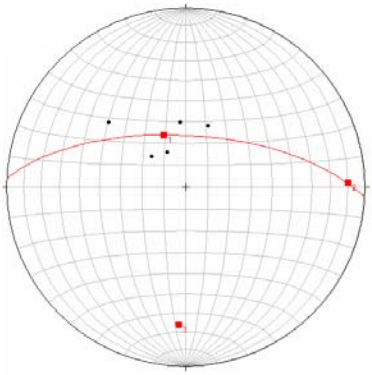

n = 5
a = 183, 24

C-Lynchburg Gp

Appendix 4 A, B, C: Equal area, lower hemisphere, stereoplot of poles to planes of the main foliation in the southern transect.

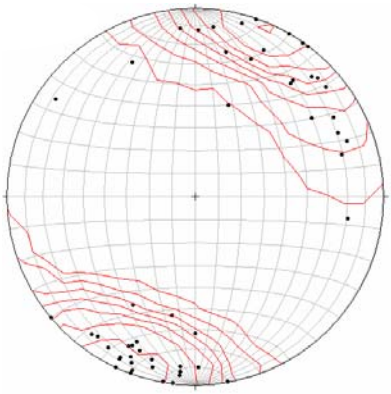

n = 56
Kamb contour interval
(c) = 2 sigma
Rose outer circle = 23%

A-SRA and Lynchburg Group

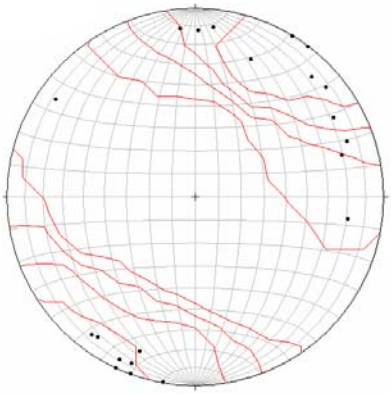

n = 23
c = 2
Rose outer circle = 26%

B-SRA

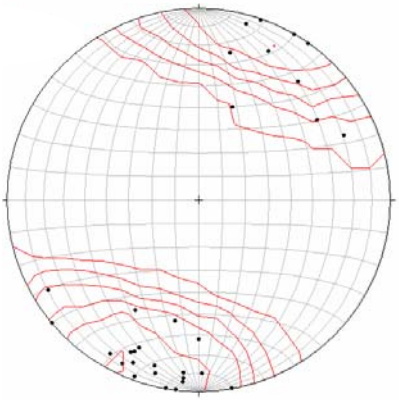

n = 31
c = 2
Rose outer circle = 19%

C-Lynchburg Group

Appendix 5 A, B, C: Equal area, lower hemisphere, stereoplot of the intersection lineation in northern transect.

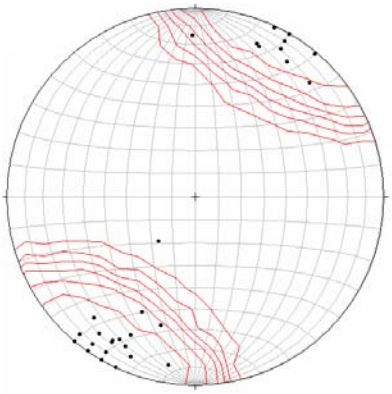

SRA and Lynchburg Group

n = 34
Kamb contour interval
(c) = 2 sigma
Rose outer circle = 29%

Appendix 6: Equal area, lower hemisphere, stereoplot of the intersection lineation in central transect (SRA).

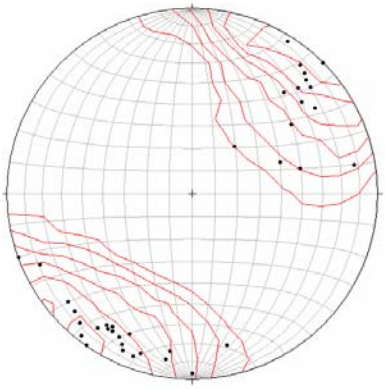

n = 37
Kamb contour interval
(c) = 2 sigma
Rose outer circle = 22%

A-SRA and Lynchburg Group

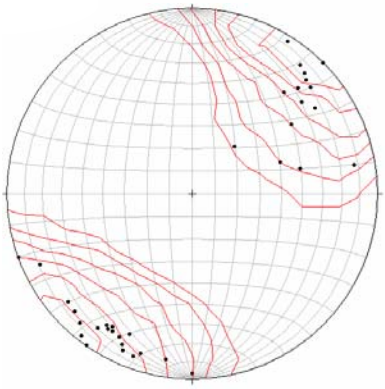

n = 35
c = 2
Rose outer circle = 23%

B-SRA

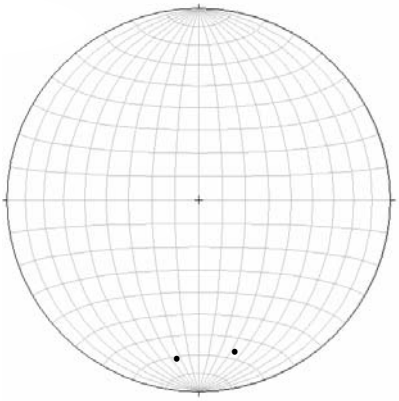

n = 2
Rose outer circle = 50%

C-Lynchburg Group

Appendix 7 A, B, C: Equal area, lower hemisphere, stereoplot of the intersection lineation in southern transect.